

## ABSTRACT

Title of Dissertation: STATISTICAL ANALYSIS AND EVALUATION OF  
THE ADVANCED BIOMASS AND NATURAL GAS  
CO-COMBUSTION PERFORMANCE

Xuejun Qian, D.Eng., May 2019

Dissertation Chair: Seong W. Lee, Ph.D.  
Department of Industrial and Systems Engineering

Increasing electricity demand and high emissions from fossil fuels combustion have created severe environmental problems and adverse impacts on human health. Biomass is considered as a promising energy resource to replace fossil fuels due to the large availability, clean, and relatively low cost. Poultry litter is a biomass and animal waste from poultry farms. However, excess production and land application also caused problems. Poultry litter and natural gas co-combustion were studied as one of the alternative solutions. Combustion efficiency and emissions in the lab-scale advanced swirling fluidized bed combustor (SFBC) system have been evaluated in previous studies. However, performance of energy production (electricity and hot water) were not evaluated yet. The main research objectives of this study are to: (1) study fuel properties and predict higher heating value (HHV) of biomass fuels (i.e., poultry litter) from proximate analysis

data, (2) conduct statistical analysis and evaluate electricity generation during poultry litter and natural gas co-combustion process, and (3) evaluate the heat generation during co-combustion process by using the lab-scale shell and tube heat exchanger (STHE) prototype.

Fuel properties, include HHV, proximate and ultimate analysis compositions were analyzed. Proximate analysis-based regression models were developed, compared, and validated to predict the HHV of poultry litter with lower estimation errors. The best-fit regression model has the highest  $R^2$  value (91.62%), lowest average absolute error (5.98%) and average biased error (0.35%). Then, the Stirling engine was successfully integrated into the lab-scale SFBC system to produce electricity (about 1 kW) from co-combustion process. Results also indicated that lower emissions (e.g., CO, NO<sub>x</sub>, SO<sub>2</sub>) and particulate matter (0.002 lb/MMBtu) were lower than the Maryland emission threshold. After that, the innovative lab-scale STHE system was designed, fabricated, and tested along with lab-scale SFBC system. Results proved that the lab-scale STHE is able to produce hot water (up to 139 °F) and provide space heating of mobile mini-trailer (from 55°F to 85°F) within 3 hours during co-combustion process. This study showed the possibility of electricity and hot water generation with acceptable emissions from the poultry litter and natural gas co-combustion process in the small-scale biomass conversion system. In the long term, results from this research will provide a sustainable and net-zero pathway and solution to convert poultry litter into on-farm energy with minimal emissions, and ultimately provide additional energy cost savings for the poultry farms.

STATISTICAL ANALYSIS AND EVALUATION OF THE ADVANCED BIOMASS  
AND NATURAL GAS CO-COMBUSTION PERFORMANCE

by

Xuejun Qian

A Dissertation Submitted in Partial Fulfillment  
of the Requirements for the Degree  
Doctor of Engineering

MORGAN STATE UNIVERSITY

May 2019

STATISTICAL ANALYSIS AND EVALUATION OF THE ADVANCED BIOMASS  
AND NATURAL GAS CO-COMBUSTION PERFORMANCE

By

Xuejun Qian

has been approved

March 2019

DISSERTATION COMMITTEE APPROVAL:

\_\_\_\_\_, Chair  
Seong W. Lee, Ph.D.

\_\_\_\_\_  
Guangming Chen, Ph.D.

\_\_\_\_\_  
Richard A. Pitts, Jr., Ph.D.

\_\_\_\_\_  
James G. Hunter, Jr., Ph.D.

## Acknowledgements

It truly feels like a miracle that this dissertation exists, and I don't think it would be done without the so many people who have encouraged, helped and inspired me. Especially, I can't finish this study without God's guidance and help.

First, I would like to thank my supervisor and mentor, Dr. Seong W. Lee for guiding me into the world of research, providing financial support during my graduate studies, and sharing his life experience and technical knowledge with me. Thank you very much again for the many helpful discussions, suggestions, encouragement, and teaching me how to scientifically conduct research projects, interpret results, and summarize key points until the dissertation completion. You are really encouraging, amazing and inspiring me to build my career on the academic area with wide research interests.

Thank you to Dr. Guangming Chen, Dr. James G. Hunter, Jr. and Dr. Richard A. Pitts, Jr. who agreed to serve as one of the committee members for my doctoral dissertation and study. Your valuable comments and questions from proposal presentation, helped me a lot to conduct research and write whole dissertation. Thank you to Dr. Hunter who give me a clear suggestion on the framework of the dissertation, raise questions and provide ideas to continue my future studies. And thank you to Dr. Chen, who provide a suggestion on experimental design and statistical analysis that we can collaborate and publish papers together. And Dr. Pitts, who shared his vision and experience as well as comments on dissertation formatting that I can organize the dissertation in professional way.

Thank you to my lab members, friends and brothers in the Center for Advanced Energy Systems and Environmental Control Technologies (CAESECT), Jingwen, Prem, Raghul, Yulai, Moses, Marc and Sam. Without your help, I can't to conduct the

experiment, collect results and analyze the results by myself. Thank you for helping me relaxing when I was stressed, hanging out with me for delicious foods, and spending some happy times together at Morgan State University.

I really appreciate the financial help from Mr. Simpson and Ms. Hatcher at the School of Graduate Studies who provided assistantship and travel grants to attend conferences and publish our findings on the peer-reviewed journals.

Last but not least, I would like to thank my lovely family members, my farther (Donghua Qian), my mother (Dezi Yu), my sister (Yingshi Qian), and my girlfriend (Jingwen Xue). You have always believed in me and I would never have come this far without your constant love, care, trust, support and encouragement. I truly appreciate all the patience you had with me going through the years of fulfilling my milestones.

## Table of Contents

<b>ACKNOWLEDGEMENTS .....</b>	<b>III</b>
<b>LIST OF FIGURES.....</b>	<b>VIII</b>
<b>LIST OF TABLES.....</b>	<b>XI</b>
<b>CHAPTER 1. INTRODUCTION .....</b>	<b>1</b>
<b>1.1 Electricity Demand and Production.....</b>	<b>1</b>
<b>1.2 Fossil Fuels and Associated Problems.....</b>	<b>4</b>
<b>1.3 Renewable Energy Resources as Alternatives.....</b>	<b>5</b>
<b>1.3.1 Renewable Energy Resources and Biomass .....</b>	<b>5</b>
<b>1.3.2 CO<sub>2</sub> Neutral Effect of Biomass .....</b>	<b>6</b>
<b>1.3.3 Potential Contribution of Biomass to Energy Demand .....</b>	<b>7</b>
<b>1.4 Biomass Conversion Process.....</b>	<b>8</b>
<b>1.5 Motivation of Study .....</b>	<b>11</b>
<b>1.5.1 Poultry Litter Production and Associated Problems.....</b>	<b>11</b>
<b>1.5.2 Alternative Poultry Litter Disposal Methods .....</b>	<b>13</b>
<b>1.5.3 Combustion of Poultry Litter with Natural Gas .....</b>	<b>15</b>
<b>1.6 Research Objectives of Study .....</b>	<b>17</b>
<b>CHAPTER 2. LITERATURE REVIEW .....</b>	<b>18</b>
<b>2.1 Fuel Properties .....</b>	<b>18</b>
<b>2.1.1 Ultimate Analysis .....</b>	<b>19</b>
<b>2.1.2 Proximate Analysis .....</b>	<b>21</b>
<b>2.1.3 Higher Heating Value (HHV) .....</b>	<b>25</b>
<b>2.1.4 Mathematical Models to Predict HHV .....</b>	<b>26</b>
<b>2.2 Emissions during Biomass Combustion Process.....</b>	<b>29</b>
<b>2.2.1 Carbon Monoxide (CO) Formation .....</b>	<b>29</b>
<b>2.2.2 Nitrogen Oxides (NO<sub>x</sub>) Formation .....</b>	<b>30</b>
<b>2.2.3 Sulfur Oxides (SO<sub>2</sub>) Formation .....</b>	<b>33</b>
<b>2.2.4 Particulate Matter (PM) Formation.....</b>	<b>33</b>
<b>2.3 Effect of Operating Conditions on Emissions .....</b>	<b>36</b>
<b>2.3.1 Effect of Secondary Air (SA) on Emissions .....</b>	<b>36</b>

2.3.2 Effect of Excess Air (EA) on Emissions .....	38
2.3.3 Effect of Mixing Ratio on Emissions .....	39
2.4 Stirling Engine.....	41
2.5 Shell and Tube Heat Exchanger (STHE).....	44

### **CHAPTER 3. FUEL PROPERTY CHARACTERISTICS AND HHV PREDICTION 52**

3.1 Materials and Methods.....	52
3.1.1 Data Collection, Selection and Normalization .....	52
3.1.2 Regression Methods and Proposed HHV Models.....	54
3.1.3 Evaluation and Validation of New Regression Models .....	58
3.2 Results and Discussion.....	60
3.2.1 Fuel Properties of PW samples .....	60
3.2.2 Effects of Proximate and Ultimate Analysis Composition on HHV .....	62
3.2.3 Derivation of the New Regression Models .....	66

### **CHAPTER 4. EVALUATION OF ELECTRICITY IN THE STIRLING ENGINE-BASED BIOMASS CONVERSION SYSTEM...74**

4.1 Materials and Methods.....	74
4.1.1 Apparatus and Experiment Setup .....	74
4.1.2 Materials .....	77
4.1.3 Statistical Methods.....	77
4.2 Results and Discussion.....	78
4.2.1 Electricity Outputs.....	78
4.2.2 Temperature Profiles.....	80
4.2.3 Emissions Performance .....	82

### **CHAPTER 5. EVALUATION OF HEAT GENERATION BY USING THE LAB-SCALE SHELL AND TUBE HEAT EXCHANGER .....90**

5.1 Methodologies.....	90
5.1.1 Design Phase .....	90
5.1.2 Fabrication Phase.....	94
5.1.3 Testing and Evaluation of the Lab-scale STHE System.....	97
5.3 Results and Discussion.....	99

### **CHAPTER 6. CONCLUSIONS, RECOMMENDATIONS AND FUTURE WORKS.....106**

**6.1 Conclusions and Concluding Remarks ..... 106**

**REFERENCES .....112**

## List of Figures

Figure 1.1: World Net Electricity Generation (U.S. EIA, 2016a) .....	2
Figure 1.2: Electricity Consumption by Sectors in 2013 (U.S. EIA, 2014) .....	3
Figure 1.3: Sources of U. S. Electricity Generation in 2017 (U.S. EIA, 2016b).....	3
Figure 1.4: Photosynthesis Process (Houshfar, 2012) .....	7
Figure 1.5: Carbon Cycle (Saidur et al., 2011) .....	7
Figure 1.6: Summary Biomass Conversion Technology and End Products .....	9
Figure 2.1: Produced Ash Fractions in the Biomass Combustion Unit .....	24
Figure 2.2: Simplified Fuel-N Conversion (Nussbaumer 2003).....	32
Figure 2.3: Methods and Instruments for PM Characterization (Amaral et al., 2015).....	35
Figure 2.4: Energy Efficiency Advantage of CHP than Traditional Energy Supply .....	43
Figure 2.5: Coupling of SE with MCHP System (Damirchi et al., 2016) .....	44
Figure 2.6 Schematic Diagram of the STHE (Zhang et al., 2012).....	46
Figure 2.7: Types of Baffles (a) Segmental, (b) Double Segmental, (c) Helical.....	47
Figure 2.8: Sketch of the Twisted Oval Tube .....	48
Figure 2.9: Flow Pattern of the Tube Side and Shell Side.....	49
Figure 2.10: Secondary Flow on the Tube Side.....	49
Figure 3.1: Relationships between HHV and (a) FC; (b) VM; (c) Ash .....	64
Figure 3.2: Scatter Plot of HHV and Ultimate Analysis Elements.....	65
Figure 3.3: Comparison between Predicted and Experimental HHV Results .....	70
Figure 3.4: Summary of AAE and ABE of New Developed Models .....	71
Figure 3.5: Comparison of Estimation Errors between Existing Proximate-based Models (E1–E17) and New Regression Models (N1, N15) .....	72

Figure 4.1: Schematics of the SEBC System and Instrumentations .....	75
Figure 4.2: Power out Vs. Head Temperature at Various Water Flow Rates .....	79
Figure 4.3: Axial Temperature Profiles at Various Combustor Heights .....	82
Figure 4.4: Total Air Flow Rate Vs. CO Emissions .....	83
Figure 4.5: Effect of EA on CO, NO <sub>x</sub> and SO <sub>2</sub> Emissions .....	84
Figure 4.6: Effect of SA/TA on CO emissions .....	85
Figure 4.7: Effect of Mixing Ratio on CO, NO <sub>x</sub> and SO <sub>2</sub> Emissions .....	87
Figure 4.8: SO <sub>2</sub> Emissions Vs. PA & Feeding Rates.....	88
Figure 5.1: 2D Design of Shell and Tube .....	91
Figure 5.2: 2D Design of Baffle .....	91
Figure 5.3: 2D Design of Rectangular and Cycle Flanges.....	92
Figure 5.4: Preliminary 3D Modeling of the STHE System.....	93
Figure 5.5: 2D Design of Lab-scale STHE.....	94
Figure 5.6: Raw Materials for SHTE Components.....	95
Figure 5.7: Flanges and Shell of the STHE System.....	95
Figure 5.8: Components of the Lab-scale STHE System .....	96
Figure 5.9: Parts and Twisted Tubes of the Lab-scale STHE System .....	96
Figure 5.10: Tools of Soft Soldering (Left) and Hard Soldering (Right) .....	97
Figure 5.11: Twisted Tube-based Lab-scale STHE without Shell and Side View .....	97
Figure 5.12: Experimental Setup of the Lab-scale STHE System Evaluation .....	98
Figure 5.13: Hot Water Temperature of the Lab-scale STHE System .....	100
Figure 5.14: Heat Capture Efficiency of the Lab-scale STHE System.....	101
Figure 5.15: Temperature of Heat Exchanger Outlets Vs. Radiator Outlets .....	102

Figure 5.16: Closed Loop of the Lab-scale Heating Module.....	103
Figure 5.17: Comparison of Concurrent and Countercurrent .....	103

## List of Tables

Table 1.1: Cost Comparison of Biomass and Fossil Fuels .....	8
Table 2.1: Biomass Analysis Methods (Vargas-Mareno et al., 2012) .....	19
Table 2.2: Analysis of Biomass and Bituminous Coal (Khan et al., 2009) .....	22
Table 2.3: Ash Analysis of Biomass and Bituminous Coal (Mass Basis, wt%).....	25
Table 2.4: HHV and LHV of Biomass Fuels (Koppejan & Van Loo, 2012) .....	26
Table 2.5: Existing Proximate Analysis-based Models for the HHV Prediction .....	28
Table 2.6: Investigations of Twisted Tubes Under Various Conditions.....	51
Table 3.1 Summary of FC, VM, A and HHV in Dry-basis (Qian et al., 2018).....	54
Table 3.2: Data for Multiple Linear Regression .....	55
Table 3.3: List of Proposed Regression Models .....	57
Table 3.4: Descriptive Statics of Fuel Properties for Poultry Litter Samples.....	60
Table 3.5: Summary of New Regression Models for PW Samples .....	66
Table 4.1: Proximate and Ultimate Analysis of Poultry Litter .....	77
Table 4.2: Factors and Individual Levels for Mixed Level Factorial ( $2^1 \times 3^3$ ) Design.....	78
Table 4.3: Summary of Temperature Distribution in Combustion Chamber .....	80
Table 4.4 Summary of ANOVA Table for T1 (H =431.8 mm).....	81
Table 5.1: Emissions from Combustion Process .....	104
Table 5.2 Summary of Energy Production and Associated Emissions.....	104
Table 5.3 German and U.S. EPA Standards for Municipal Solid Wastes .....	105

## **Chapter 1. Introduction**

In Chapter 1, a brief introduction on the current electricity demand and production, fossil fuels and associated problems, renewable energy resources, biomass co-combustion process were covered first. Then, the motivation and research objective of this study is introduced. In Chapter 2, literature reviews were summarized to provide a solid background and unique approach to achieve the research objectives of this study in the following chapters. In Chapter 3, the methodology to characterize the fuel properties and predict the higher heating value (HHV) were introduced. The detailed steps and results on sample collection, regression model development and model validation of HHV were also introduced. In Chapter 4, methodologies and results on the evaluation of performance (e.g., electricity and emissions) during poultry litter and natural gas co-combustion process in the Stirling engine-based biomass conversion system were summarized. In Chapter 5, the heat generation during poultry litter and natural gas co-combustion were evaluated by using the lab-scale shell and tube heat exchanger (STHE). In Chapter 6, the major findings, conclusion and recommendations for this study were covered.

### **1.1 Electricity Demand and Production**

According to data published by United Nations, the population of the world in 2013 was 7.2 billion. The population is expected an increase of 1 billion until 2025 and may reach 9.6 billion by the year 2050 (Tripathi et al., 2016). As the population of the world increase, the demand for energy, oil, gas and electricity are increasing as well. Based on the International Energy Outlook 2016 by the U.S. Energy Information Administration (EIA), the world net electricity generation are expected to increase from 21.6 trillion

kilowatt hours (kWh) in 2012 to 25.8 trillion kWh in 2020 and expect to reach 36.5 trillion kWh in 2040 as shown in Figure 1.1 (U.S. EIA, 2016a).

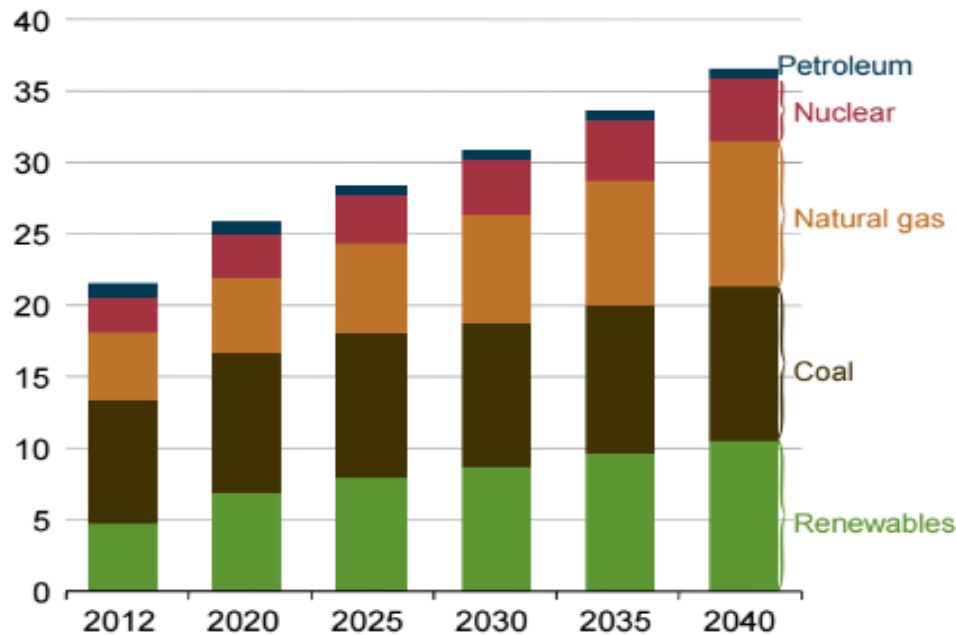


**Figure 1.1: World Net Electricity Generation (U.S. EIA, 2016a)**

As shown in Figure 1.2, electricity is demanded by various sectors, including industrial, commercial and residential (U.S. EIA, 2014). The major end use of electricity includes lighting, space heating and cooling, ventilation, refrigeration and electronics, and water heating. According to the global energy statistical yearbook 2018, China, U.S., India, Russia, Japan, Germany, South Korea, Brazil, Canada, Iran, France and Indonesia are top 12 energy consumption countries (World Energy Statistics, 2018). Among them, U.S. is the world's second largest energy consumer as well as producer, behind only China. The energy consumption of U. S. is close to 2, 201 Million Tonnes of Oil Equivalent (Mtoe). As shown in Figure 1.3, major amounts of electricity are generated from various energy resources, including coal, natural gas, renewables, nuclear and petroleum (U.S. EIA, 2016b). In 2017, net generation of electricity in the U. S. was about 4.01 trillion kilowatt-hours (kWh). About two thirds (about 65%) was generated using fossil fuels: coal (30%),

natural gas (32%), and petroleum (1%) while more than one thirds from nuclear (20%) and renewables (17%) (US EIA, 2016b).

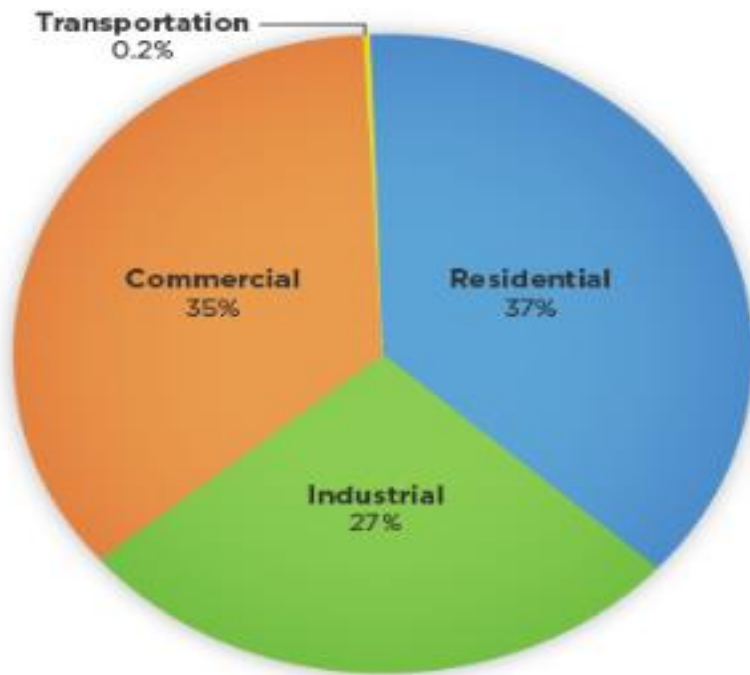


**Figure 1.2: Electricity Consumption by Sectors in 2013 (U.S. EIA, 2014)**

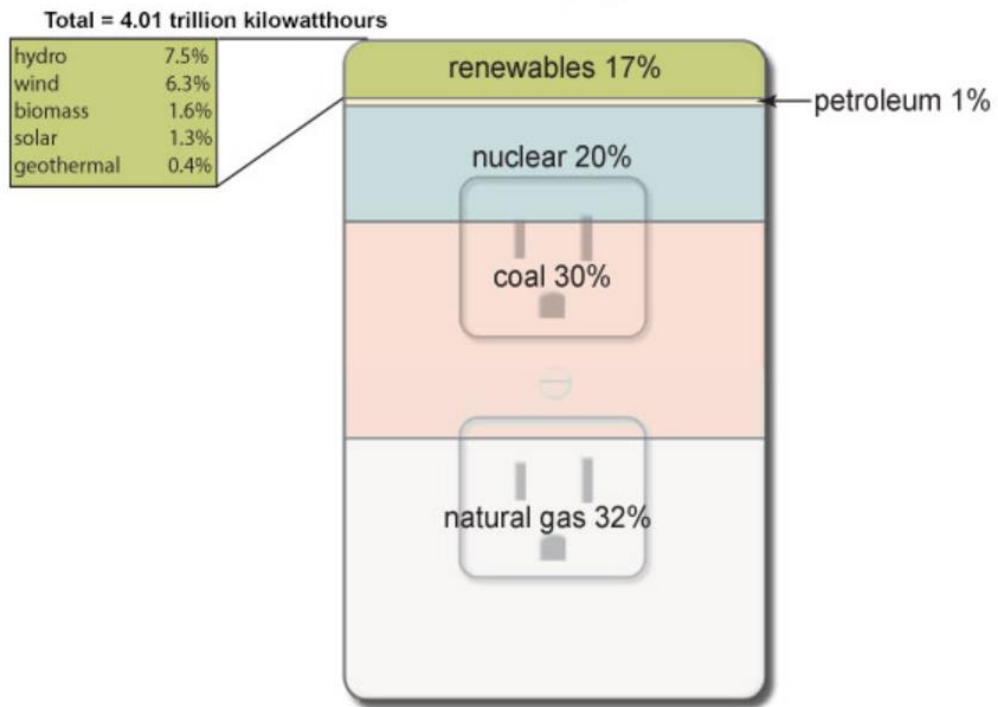


**Figure 1.3: Sources of U. S. Electricity Generation in 2017 (U.S. EIA, 2016b)**

## 1.2 Fossil Fuels and Associated Problems

Most of the world's energy generation and consumption is fulfilled by fossil fuels (e.g., natural gas, coal) because of fossil fuels are easily accessible and available resource for energy production (Patel et al., 2016). However, fossil fuels are limited and to fulfill the world's increasing energy demand for a very long time (Biswas et al., 2014). It is anticipated that these sources may depleted within next 40-50 years (Saidur et al., 2011). In addition, energy production from fossil fuels combustion in the power plants have serious consequences on atmospheric pollutions and greenhouse gas (GHG) emissions. During the combustion process, the thermal power plants emit carbon ( $\text{CO}_2$ ), carbon monoxide (CO), nitrogen oxides ( $\text{NO}_x$ ), sulfur dioxide ( $\text{SO}_2$ ) and air-borne inorganic particles, such as fly ash, carbonaceous material (soot), suspended particulate matter (Verma et al., 2017; Mittal et al., 2012).

In the case of the U.S., electricity production from burning fossil fuels emits 30% of the total GHG in 2014 (US EPA, 2014). These emissions include a majority of  $\text{CO}_2$  and small amounts of nitrous oxide ( $\text{N}_2\text{O}$ ) and methane ( $\text{CH}_4$ ). These GHG trap heat and make our planet warmer than the before, ultimately create global warming, which is one of the major concerns among researchers, politicians, and the public in general. Recently, the United Nations Intergovernmental Panel on Climate Change (IPCC) announced that continued GHG emissions from fossil fuel conversion will ultimately increase the global average temperature between 1.4 and 5.8 °C over the period from 1990 to 2100 and accelerate the global warming speed and climate change (Mahmoud et al., 2009). Moreover, high amounts of N and S in the coal increase the emission of  $\text{NO}_x$  and  $\text{SO}_2$ . There are about 67% of  $\text{NO}_x$  emissions from coal combustion process (Zhou et al., 2010).

Both  $\text{NO}_x$  and  $\text{SO}_2$  are major contributors to acid rain (Hu et al., 200; Beer, 2000). Emission of pollutants causes a variety of adverse impacts such as premature mortality, morbidity, crop losses, risks to biodiversity and acidification of soil and surface water (Amann et al., 2013).

## **1.3 Renewable Energy Resources as Alternatives**

### **1.3.1 Renewable Energy Resources and Biomass**

Many countries, particularly among the Organization for Economic Cooperation and Development (OECD), have enacted environmental policies and regulations intended to reduce GHG from power plants by decreasing the fossil fuels (i.e., coal) utilization. In 2015, President Obama and the Environmental Protection Agency (EPA) announced the Clean Power Plan (CPP) – a historic and important step in carbon pollution reduction from power plants that takes real action on climate change (US EPA, 2016). Energy resource depletion, environmental damages, strict regulations and policies have shifted energy production from fossil fuels towards utilizing a variety of renewable energy resources (RES). RES, such as hydropower, solar, wind, biomass and geothermal are environmentally friendly and sustainable way to produce energy (Saaki et al., 2009; Saidur et al., 2011). RES are the fastest-growing energy resources for electricity generation, with increase of 2.9% per year from 2012 to 2040 (U.S. EIA, 2016a).

Biomass is one of most important RES and widespread in nature. Biomass is a carbon-based fuel, which mainly contain C, H and O with lower N and S content than conventional coal. Thus, replacement of fossil fuels by biomass can significantly contribute to reduce the  $\text{SO}_2$  and  $\text{NO}_x$  emissions during conversion process (Savolainen et al., 2003). Biomass is considered to have a potential to be used as a promising alternative energy

resource due to environmental benefit, national energy policy, rising energy price and efforts to address the current climate change (Tripathi et al., 2016; Dong et al., 2009).

Biomass is a complex biological organic matter derived from living or recently living organism (e.g., plant, animal) and available naturally (Tripathi et al., 2016). Biomass is also a general term which includes plant biomass (or phytomass) and terrestrial animal biomass (or zoomass). Plants convert sun's energy (or radiant energy) into chemical energy by photosynthesis process and stored in the form of terrestrial and aquatic vegetation. This vegetation was consumed by animals as food and converted into animal excreta. Thus, the excreta from animals can be used as an energy resource (Saidur et al., 2011). Plant and animal biomass materials include wood from forests, crops, seaweed, material left over from agricultural and forestry processes (e.g., wood residues, forestry residues, temperate and tropical crop residue), and organic industrial, human and animal wastes. In addition, waste materials, such as sewage, municipal solid waste, corn waste, palm waste, wooden chips (wood chips), sugarcane, wooden pellet, reuse derived fuel (RDF or animal waste, poultry litter) also considered as biomass resources (Saidur et al., 2011; Koh and Hoi, 2003, Sami et al., 2001).

### **1.3.2 CO<sub>2</sub> Neutral Effect of Biomass**

The photosynthesis reaction of plants can be illustrated in Figure 1.4 and following equation (Houshfar, 2012). During the photosynthesis reaction, plants absorb and convert CO<sub>2</sub> into O<sub>2</sub> during growth state from the atmosphere (Saidur et al., 2011).



If plants are used as energy resource during the combustion process, the similar amount of CO<sub>2</sub> is released during the conversion process (Demirbas et al. 2009). As shown

in Figure 1.5, there is no net addition of CO<sub>2</sub> during photosynthesis process and combustion process. This is known as the carbon cycle or zero carbon emission (Saidur et al., 2011). Thus, biomass can be regarded as a carbon sink and have CO<sub>2</sub> neutral effect.

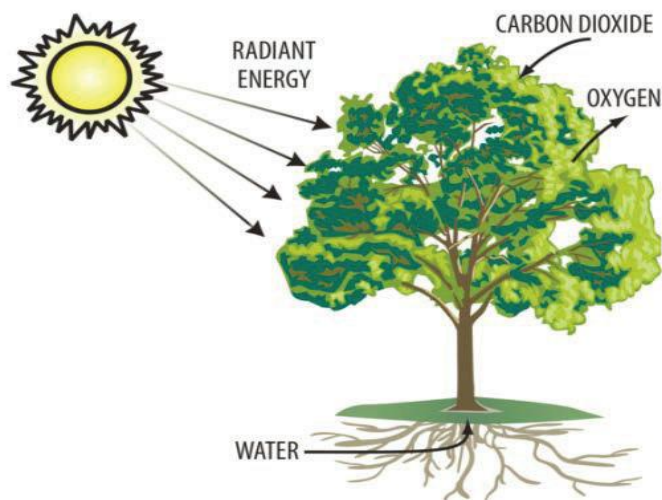


**Figure 1.4: Photosynthesis Process (Houshfar, 2012)**

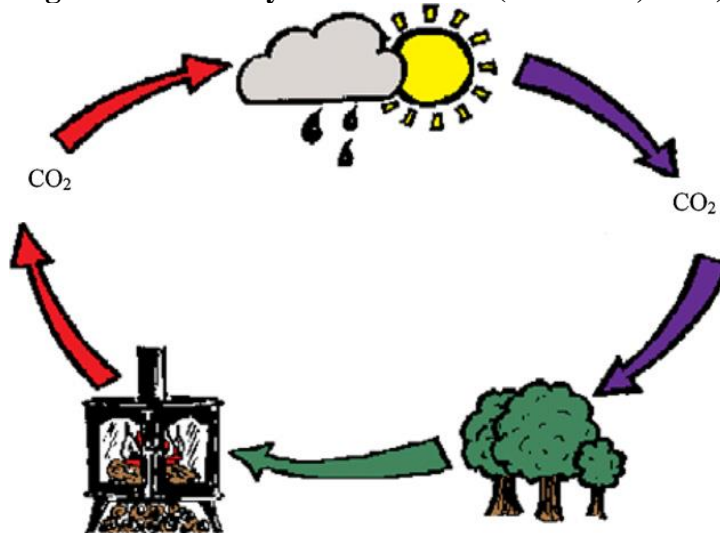


**Figure 1.5: Carbon Cycle (Saidur et al., 2011)**

### 1.3.3 Potential Contribution of Biomass to Energy Demand

Two U.S. EPA scenarios indicated that the contribution of biomass to total energy supply was in the range of 13-16% (Berndes et al., 2003). A study of potential contribution of biomass to the sustainable energy development indicated that bioenergy provides roughly 35% of energy demand in developing countries and 13% of energy demand in

worldwide (Demibas, 2006, Balat, 2006; Balat & Bozbas, 2006). Recent studies indicated that the contribution of biomass resources increased to 38% of energy in developing countries and 14% of global energy (Patel et al., 2012).

The biomass contribution to the global energy is increasing and uncertain by two most crucial parameters, including land availability and yield levels. Moreover, recent study also showed that all countries in the European Union (EU) are marking efforts to reach share of energy from renewable resources up to 20% by 2020. Among all these renewable sources, the expected share of biomass is about 45.1% by 2020 (Proskurina et al., 2016). Biomass is one of the earliest energy resources in rural areas because it is often the only accessible and affordable energy source (Demirbas, 2004). Some of biomass resources are available at relatively cheap prices. Table 1.1 shows the typical price to produce energy from biomass and conventional fossil fuels in July 2017 (Biomass Energy Center, 2017). From comparison, energy production cost (pence/kWh) from biomass (i.e., wood chips) are cheaper than other resources (e.g., natural gas, liquefied petroleum gas).

**Table 1.1: Cost Comparison of Biomass and Fossil Fuels**

Fuel Type	Energy Density by Volume, kWh/m <sup>3</sup>	Price Per Unit	Pence Per kWh
Wood chips (at 30% MC <sup>1</sup> )	694-868	£110/t	3.1
Natural Gas	9.8	4.9 pence per kWh	4.9
LPG	6,600	43 pence per liter	6.5

Note: <sup>1</sup>Moisture Content

## 1.4 Biomass Conversion Process

As shown in the Figure 1.6, the biomass energy sources are classified in five categories, include woody biomass, agricultural biomass, aquatic biomass, animal and

human waste, and industrial waste (Tripathi et al., 2016). There are several methods available to convert biomass into useful energy. The foremost among them is thermal conversion process which include combustion, gasification and pyrolysis. Thermochemical conversion technology and end products can be varied by type and quantity of available biomass feedstock, environmental standards, economic factors and other factors. The biochemical process includes fermentation, anaerobic digestion and esterification where microorganism is required, and high moisture content biomass is used (Saidur et al., 2011). Even though biochemical conversion is relatively cheap and environmentally friendly than thermochemical conversion, but the rate of hydrogen and yield is quite low. Thus, the foremost and popular thermochemical conversion technologies, combustion, pyrolysis and gasification are widely used (Saidur et al., 2011; Tripathi et al., 2016). The major end products from conversion technology are heat, power, bio-oil, gases (i.e., H<sub>2</sub>), fuels (e.g., alcohol, diesel), liquid fuels and bio-char.

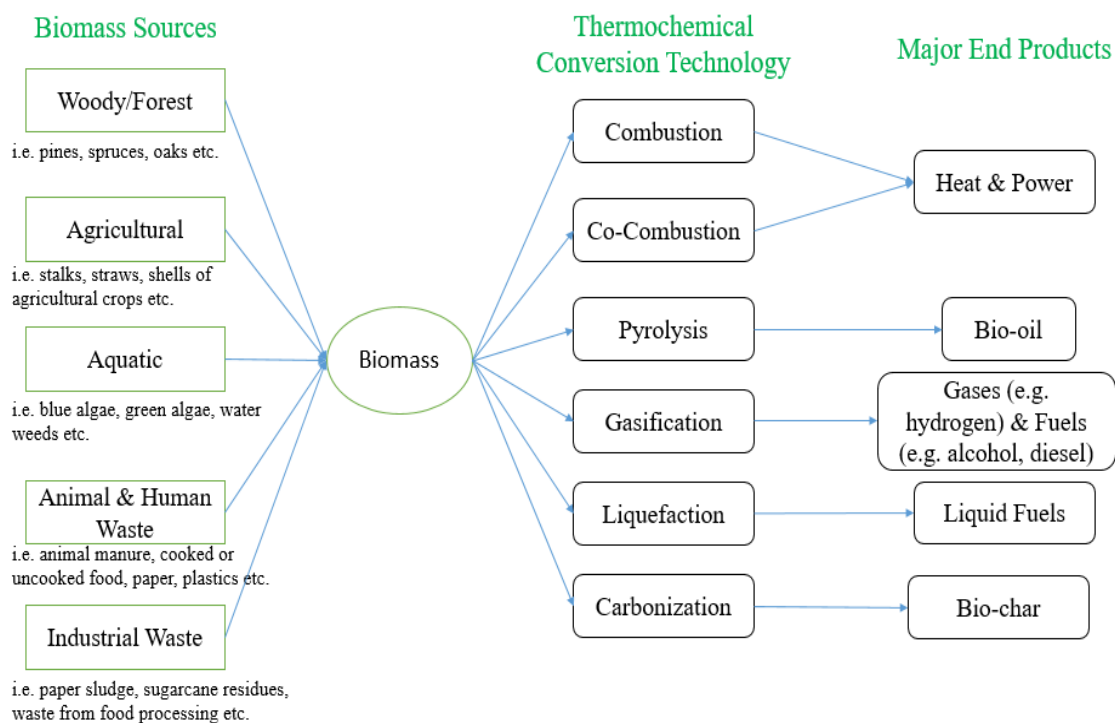


**Figure 1.6: Summary Biomass Conversion Technology and End Products**

Biomass combustion is the simplest thermochemical conversion technology (Patel et al., 2016). Combustion is a process in which the chemical energy stored in the biomass is obtained in the form of heat by its direct burning in the presence of oxygen (Tripathi et al., 2016). Generated heat can be further used to produce steam for making electricity (Saidur et al., 2011). Biomass combustion method is also the most widely applied conversion method that provides heat and electricity for industries, homes and farm facilities (Demirbas, 2005; Fournel et al., 2015). However, high moisture content and lower heating value of biomass may cause ash-related problems.

Co-combustion (or co-firing) of biomass with fossil fuels were usually suggested to alleviate fouling (Demirbas, 2005; Kazagic et al., 2009). Recently, biomass co-combustion is regarded as one of the attractive options for biomass utilization in the power generation industry, due to low cost options for electricity generation and low GHG emissions (Loeffler et al., 2014, Agbor et al., 2014). In the process, the primary fossil fuel (i.e., coal) is partially substituted or simultaneously blended by biomass in a reactor to produce useful energy (Patel et al., 2016). The amount of biomass fuel that is co-fired is called the co-combustion level or rate of co-combustion. Depending on the system capacity and efficiency, the co-combustion level varies between 5 and 20 by weight (5-20 wt.%) (Sebastián et al., 2011). Biomass co-combustion in the existing coal-fired boilers draws upon widely-available and presents an immediate opportunity for electricity generation from biomass in an efficient and cleaner way (Demirbas, 2004; Baxter, 2005). Co-combustion of biomass with coal (about 10% wt. biomass with 90% fossil fuels) for electricity production from biomass has been found to be a promising method in the nearest

future due to the CO<sub>2</sub> neutrality, mature, simplest, low cost and high conversion efficiency (Saidur et al., 2011; Tripathi et al., 201).

## **1.5 Motivation of Study**

### **1.5.1 Poultry Litter Production and Associated Problems**

Biomass can include woody fuels, herbaceous crops or grasses, dedicated energy crops and manures (McKendry, 2002a). Poultry litter is one such manure and large quantities of poultry litter were produced during poultry production process. Poultry litter consists of a mixture of bedding materials (e.g., wood shavings, sawdust, pine bark, wood chips, rice hulls, peanut hulls, ground corncobs, chopped straw), excreta (or feces, urine, manure), spilled waste feed (or food) and feathers (Lynch et al., 2013a; Palma & Martin, 2013). Major consideration of bedding materials is cost and availability. In addition, bedding materials need to be a very absorbent and have a reasonable drying time as well as no toxic to poultry or poultry growers.

The rate of poultry litter production can be affected by many factors, so the estimation of litter production in published literature varies widely (Coufal et al., 2006). Chastain et al. (2001) stated that the broiler farms produced 850-1,140 kg of litter per 1,000 broilers and litter production depending on bedding practices and frequency of litter removal. Patterson et al. (1998) reported the different litter production for various bird size. Farms growing smaller birds produced litter at a rate of 1.07 tons per 1,000 broilers, and larger birds produced litter at a rate of 1.65 tons per 1,000 broilers. Depend on house cleaning out period, Chamblee and Todd (2002) estimated broiler litter production in Mississippi to be 1.6 tons per 1,000 broilers if the houses were cleaned out completely on

an annual basis, and a rate of 1 ton per 1,000 broilers if houses were cleaned out completely at the end of 2 years. The Natural Resource, Agriculture, and Engineering Service (NRAES, 1999) reported whole litter production from broilers to be 1.25 ton per 1,000 birds. Based on several sources, Malone (1992) estimated average litter production to be 1.0 dry metric ton per 1,000 broilers per flock with a range of 0.7 to 2.0 metric tons. Perera et al. (2010) assumed that the amount of litter generated annually by broilers was equal 1.2 tons per 1,000 birds per year. Lynch et al. (2013b) used 1.4 ton of litter per 1000 birds in the calculation for U.S. litter production estimation.

Using a litter production of 995 kg of litter per 1,000 birds, a broiler house that holds 23,400 birds per flock and produces 5.5 flocks per year (6-7 week/flock, 5-6 flock/year) will produce about 128 t/yr of poultry litter (about 282,000 lb/yr; Chastain et al., 2012). Excludes states producing less than 500,000 broilers, the total poultry litter production from top poultry production states in U.S. were estimated about 10.8 million tons in 2008 and 10.3 million tons in 2009 (Perera et al., 2010). In most cases, the poultry litter is spread on cropland as an organic fertilizer due to its rich nutrients of nitrogen, phosphorous, potassium, sulfur and calcium (Henihan et al., 2003; Li et al., 2008). However, over-application of poultry litter to the soil can results in enrichment of water-soluble nutrient and eutrophication of water sources. When eutrophication occurs, algae present within the water reproduce excessively under aerobic metabolism, effectively using large quantities of the water's dissolved oxygen, creating dead zones and destroying the aquatic ecology (Jia & Anthony, 2011; Whitely et al., 2006).

In addition, the abundances of poultry litter can lead to nitrate leaching, high biological oxygen demand (BOD), ammonia toxicity, high chlorine concentrations,

pathogen contamination, air pollution, emission of greenhouse gases, nuisances (e.g., flies, odors), crop toxicity (due to high concentrations of ammonia, nitrite, nitrate and soluble salts), fish death, health impacts of human and animals (Li et al., 2008; Lynch et al., 2013b). The land application of poultry litter is no longer desirable, due to environmental concerns, health impacts and legislative constraints (Abelha et al., 2003; Whitely et al., 2006; Li et al., 2008; Jia and Anthony, 2011; Lynch et al., 2013; Palma & Martin, 2013).

### **1.5.2 Alternative Poultry Litter Disposal Methods**

Due to excess production and associated problems of land application, it has stimulated interest into cleaner and efficient disposal options for poultry litter. Kelleher et al. (2002) introduced an excellent review of alternative poultry litter disposal methods, include composting (or aerobic digestion), anaerobic digestion and combustion. Gasification is another main alternative disposal method of poultry litter (Topal et al., 2012). Among four main alternative disposal methods of poultry litter, one of the most widely used methods is combustion. Direct combustion of poultry litter is able to provide a cost-effective, environmentally benign disposal route for the litter while providing for both space heating of poultry houses and large-scale schemes involving power generation or combined heat and power (CHP; Kelleher et al., 2002; Li et al., 2008; Topal et al., 2012). However, there can be problems on maintaining steady and complete combustion of poultry litter due to the high moisture and ash contents, as well as low heating value of the poultry litter (Kelleher et al., 2002; Whitely et al., 2006; Li et al., 2008; Lynch et al., 2013). The calorific value of poultry litter decreases with increasing moisture content, air dried samples having a typical value of 13.5 MJ/kg, which is about half of coal (Abelha et al.,

2003). Therefore, the co-combustion of poultry litter with fossil fuel is considered as a better means to process poultry litter into useful energy (Li et al., 2008; Topal et al., 2012).

In the last two decades, co-combustion of poultry litter with coal was considered as a better alternative to process poultry wastes and produce useful energy along with minimum emissions. Abelha et al. (2003) investigated the combustion of chicken litter alone and co-combustion with peat by 50% on weight basis. Results indicated that secondary air (SA/PA=0.4) in two stages reduced nitrogen oxide (NO<sub>x</sub>) (about 160-220 ppm) in freeboard and reduced carbon monoxide (CO) emission (about 1,450-5,820 ppm). Henihan et al. (2003) performed gaseous emissions modeling of fluidized bed co-combustion of 50% w/w chicken litter with peat. Atmospheric dispersion model predicted ground-level concentrations (e.g. CO and volatile organic compound) decreased with the appropriate ratio between primary air (or fluidizing air) and secondary air (PA/SA) and would be below air quality standards. Li et al. (2008) investigated effect of co-combustion of chicken litter with coal on emission in a laboratory-scale fluidized bed combustor at chicken litter mass fraction of 10%, 25% and 50%. The experimental results indicated that the increasing of chicken litter mass fraction reduced sulfur dioxide (SO<sub>2</sub>) emissions, but increased CO emissions. Jia and Anthony (2011) evaluated combustion characteristics of co-firing poultry-derived fuel (PDF) with coal in a pilot-scale circulating fluidized bed combustor. It was found that co-combustion of PDF/coal emitted about 20% higher NO<sub>x</sub> emissions (in range of 265-280ppm) than 100% coal. But, the emission of polycyclic aromatic hydrocarbons (PAHs) and polychlorinated dibenzodioxins/furans (PCDD/Fs) were comparable to 100% coal firing and very a low concentration of all metals were detected in the flue gas. Topal et al. (2012) determined some important emissions during

the co-combustion of poultry wastes with coal in a special bottom-feed combustion system under various excess air (EA) ratio (1.3-2.7) and percentage of poultry wastes/coal (0/100, 25/75, 50/50, 75/25). Combustion of poultry wastes with rice husk (PWR) and poultry wastes with sawdust (PWS) indicated that the effect of EA ratio had a remarkable effect on CO and CH<sub>4</sub> while its effect on NO<sub>x</sub> and SO<sub>2</sub> were ignorable.

### **1.5.3 Combustion of Poultry Litter with Natural Gas**

Compared to with coal resource, natural gas (NG) is increasingly seen as ‘bridge fuel’ for transitions to renewable and/or near-zero emission energy resources and comprised about a quarter of U.S. energy use (Paltsev et al., 2011; Zhang et al., 2014). The shift from coal into NG in recent decades due to very small amounts of CO<sub>2</sub>, NO<sub>x</sub>, SO<sub>2</sub>, CO, other reactive hydrocarbons and virtually no particulate matter were emitted during the combustion process (Liang et al., 2012). Recently, Zhang et. al (2014) also indicated that NG power plant can produce half of century-intergraded warming than coal plant in the long-term consideration with appropriate power plant efficiency and lower CH<sub>4</sub> leakage. Even though, the high capital cost of NG power plant, Skeer and Wang (2006) concluded that NG could significantly reduce the CO<sub>2</sub> emissions. Moreover, introduction of carbon charge at \$22/tonne or more, the NG-fired power will be cheaper than coal-fired power in the electricity generation process. In 2017, about 32% and 30% of net electricity generation were came from natural gas and coal, respectively (US EIA, 2016b). There is increasing trend of using natural gas as energy resources in the U.S. as well as other countries. Despite the advantages and increasing trend of NG usages, there were limited studies conducted on the co-combustion of poultry litter and natural gas in the FBC.

In the previous studies by former research students, the co-combustion performance of poultry wastes and natural gas in the advanced swirling fluidized bed combustor (SFBC) mainly investigated the effect of three different wastes (poultry litter, poultry manure, sawdust), excess air ratio (0-40%) and secondary/total air ratio (0-50%) on the carbon combustion efficiency (Zhu et al., 2005). In addition, combustion characteristics such as temperature distribution, heat recovery efficiency and major gaseous pollutants emissions were also discussed. The result indicated that excess air and secondary air play important roles in achieving high combustion efficiency and achieving stable combustion. The carbon combustion efficiency was increased 8-10% when the excess air is increased to 25% with secondary air being 20% at low injection height. The NO<sub>x</sub> emission was very low, though the materials contain high levels of nitrogen.

Furthermore, the previous research aimed to explore a feed-forward back-propagation artificial neural network (BPANN) approach to predict combustion efficiency of chicken litter in an advanced SFBC (Zhu et al., 2007). The response surface of combustion efficiency along with five operational conditions, moisture content, excess air, litter ratio, secondary air and its injection height was accordingly predicted. Results indicated that the Levenberg-Marquardt training algorithm is much faster than the gradient decent for same mean squared error. The relative high combustion efficiency (over 84%) was achieved within the operational ranges: moisture (11-14%), litter ratio (0.05-0.1), excess air (0.22-0.45), secondary air (0.18-0.27). A series of validation experiments indicated that the ANN approach provided an easy and accurate prediction for combustion efficiency. However, previous studies only focused on the effect of operating conditions

emissions and combustion efficiency. There is limited study on energy generation (e.g., electricity, hot water) during the poultry litter and natural gas co-combustion process.

## **1.6 Research Objectives of Study**

This project is anticipated to further develop a lab-scale advanced swirling fluidized bed combustor (SFBC) system into a clean and efficient small-scale biomass conversion system that able to convert biomass (i.e., poultry litter) into useful energy (e.g. electricity and hot water) with minimal emissions. The main research objectives of this study are to: (1) study fuel properties of poultry litter and predict of higher heating value (HHV) of biomass (or poultry litter) wastes from proximate analysis, (2) conduct statistical analysis & evaluation of performance (e.g., emissions and electricity) for the Stirling engine-based biomass conversion system, (3) investigate heat generation during poultry litter combustion process by using the lab-scale Shell and Heat Tube Exchanger (STHE) prototype. For electricity generation, the Stirling engine was integrated into the lab-scale SFBC system to form the Stirling engine-based biomass conversion system that produce electricity from poultry litter and natural gas co-combustion process. The heat generation was achieved by using the lab-scale STHE to produce hot water from the residual heat in the hot flue gas.

## **Chapter 2. Literature Review**

In the first part of Chapter 2, the literature reviews of the fuel properties, ultimate analysis, proximate analysis, higher heating value (HHV) and HHV prediction models were summarized. In the second part, emissions (e.g., CO, NO<sub>x</sub>, SO<sub>2</sub>) during the biomass combustion process and formation process of emissions were discussed. In the third part, the effect of operation conditions including secondary air (SA), excess air (EA), and mixing ratio (MR) on emissions on emissions in the different combustion systems were deeply studied and analyzed. Then, the energy generation components, Stirling engine and shell and tube heat exchanger (STHE) were reviewed in the last two parts.

### **2.1 Fuel Properties**

The characteristics of the biomass fuels are not only influenced by the origin of the biomass, but also by the entire supply system preceding any conversion step. Fuel properties are often used to determine the technologies for the energy conversion process. Depending on fuel properties, a biomass fuel can be excluded for specific combustion options due to the technical challenges and environmental reasons (Khan et al., 2009). The most important fuel properties which give the first impression of a certain fuel are given by proximate analysis, ultimate analysis and heating value (Khan et al., 2009). Table 2.1 shows the examples of the methods to analyze the proximate and ultimate composition of biomass samples according to the American Standard Testing Methods (ASTM) and European Committee for Standardization (CEN, according to its French designation) criteria (Vargas-Moreno et al., 2012).

**Table 2.1: Biomass Analysis Methods (Vargas-Mareno et al., 2012)**

<b>Proximate Analysis</b>	
Moisture Content	UNE-EN 14774-1:2010
	ASTM E871-82 (2006)
Ash	UNE-EN 14775:2010
	ASTM D1102-84 (2007)
	ASTM E830-87 (2004)
Volatile Content	UNE-EN 15148:2010
	ASTM E872-82 (2006)
	ASTM E897-88 (2004)
Fixed Carbon	By difference
<b>Ultimate Analysis</b>	
Carbon (C)	UNE-CEN/TS 15104:2008 EX
	ASEM E777-08
Hydrogen (H)	UNE-CEN/TS 15104:2008 EX
	ASEM E777-08
Nitrogen (N)	UNE-CEN/TS 15104:2008 EX
	ASEM E778-08
Sulphur (S)	ASTM E775-87 (2008) e1
Oxygen (O)	By difference
Chlorine (Cl)	ASTM E776-87 (2009)
Sample preparation for analysis	UNE-CEN TS 14870:2008 EX

### 2.1.1 Ultimate Analysis

The elemental composition from ultimate analysis is one of the most important fuel properties for biomass fuels. It is usually complex, with six major elements in organic phase (C, H, O, N, S, and Cl) and ten (10) in the inorganic phase (Si, Al, Ti, Fe, Ca, Mg, Na, K, S, and P). The percentages of N, S and Cl provide an idea of the impact of the use a biomass fuel while the concentration of C, H and O allow to estimate theoretical air required for complete combustion and determine the heating value of fuel (Vargas-Moreno et al., 2012; Patel & Gami, 2012). The latter inorganic compositions are important in the characterization and utilization of ash as byproduct. The elemental compositions of biomass are also necessary to analyze the overall process of thermochemical conversion methods and helps to predict flue gas flow rate, air requirement, and flue gas compositions in the combustion process (Nhuchhen, 2016).

C, H, and O are the three main components of biomass fuels. C and H are oxidized during the combustion process by exothermic reaction (formation of  $\text{CO}_2$  and  $\text{H}_2\text{O}$ ). C is the basic element of organic chemistry and is used by all known living organisms. H also plays an important role in all fuel combustion systems. The originally bound O released through the thermal decomposition of biomass fuels covers a part of the overall oxygen need for the combustion process. Thus, the greater  $(\text{H}+\text{C})/\text{O}$  ratio, the greater heating value of a fuel (Vargas-Moreno et al., 2012). Typical dry-basis weight percentages of biomass for C, H and O are 30% - 65%, 5% to 6%, and 30% to 45%, respectively (Koppejan & Van Loo, 2012). Vassilev et al. (2010) found a different range of biomass samples that C content in the range 42-71%, H content in the range of 3%-11%, and O content in the range of 16 wt%-49 wt% (dry ash free, DAF; Vassilev et al., 2010). Lower C content in biomass fuels than coal is present in partly oxidized forms, which explains the heating value of biomass fuels are lower than coal samples (Koppejan & Van Loo, 2012).

N is a micronutrient for plants and critical to their growth. Fuel-N is converted to nitric oxide ( $\text{NO}$ >90%) and nitrous oxide ( $\text{NO}_2$ <10%) through a series of elementary reaction steps called the fuel  $\text{NO}_x$  mechanism (Gardiner, 2000). One of the greatest environmental impacts of biomass combustion and co-combustion is nitrogen oxides ( $\text{NO}_x$ ) production. Thus, analysis of the N concentration in the biomass fuel is particularly important in terms of environmental protection. Normally, N values fluctuate between 0.1% to 12% (Vassilev et al., 2010). Previous studies found that  $\text{NO}_x$  formation during biomass combustion process mainly results from the fuel-N content at temperature between 800°C and 1100°C (Leckner & Karlsson, 1993; Koppejan & Van Loo, 2012). S forms the gaseous compounds (e.g. sulfur dioxide ( $\text{SO}_2$ ), sulfur trioxide ( $\text{SO}_3$ )), salt ( $\text{K}_2\text{SO}_4$ ),

hydrogen sulfide ( $\text{H}_2\text{S}$ ), and alkali sulphates during the biomass combustion process. The efficiency of sulfur fixation in the ash depends on the concentration of alkaline earths (i.e., Ca) in the ash as well as dust precipitation technology. However, biomass is usually poor in S (around 0.01 wt% to 2.3 wt%, DAF; Vassilev et al., 2010). Sulphur oxides ( $\text{SO}_x$ ) are a result of complete oxidation of fuel-S content. It is mainly  $\text{SO}_2$  (>95%) and some  $\text{SO}_3$  (<5%) may be formed at lower temperatures (Koppejan & Van Loo, 2012).

Regarding its behavior in different combustion related problems, Cl is another important element for the biomass fuels. The Cl in biomass exerts its effect through its salts (e.g., KCl, NaCl), chlorine ( $\text{Cl}_2$ ), and the hydrochloric acid (HCl) generated during combustion. In addition, high percentage of silica (Si) together with K and Cl also cause severe ash deposition problem at high or moderate combustion temperature (Khan et al., 2009). Corrosive effects of  $\text{Cl}_2$  and its compounds may have a negative impact on the walls of metallic furnaces as well as influence the acidic emissions and particles (Vargas-Moreno et al., 2012; Koppejan & Van Loo, 2012). Cl generally between 0.01 wt% and 0.9 wt% in DAF and differs from one type of biomass to another (Vassilev et al., 2010).

### **2.1.2 Proximate Analysis**

Besides elemental composition from ultimate analysis, the design and operation of more efficient biomass combustion systems rely substantially on several important fuel characteristics, namely heating value, moisture, ash content (Sheng & Azevedo, 2005; Yin, 2011). Proximate analysis provide the composition in terms of fixed carbon (FC), volatile matter (VM), moisture and ash. As shown in the Table 2.2, proximate and ultimate analysis of some biofuels and bituminous coal (in mass basis) vary in wide ranges. Compared with coal, biomass show a high reactivity due to their high volatile matter content and a much

lower C and high O content which are responsible for their low heating values (Khan et al., 2009). In addition, biomass also have lower fixed carbon and higher moisture content than coal.

**Table 2.2: Analysis of Biomass and Bituminous Coal (Khan et al., 2009)**

Fuel	Proximate Analysis (%)				Ultimate Analysis (%)					
	M	VM	FC	ASH	C	H	O <sup>d</sup>	N	S	Cl
<b>Wood Pellets (Pine)</b>	4.9	80.4	14.5	0.2	45.5	6.6	47.7	LLD	LLD	LLD
<b>Demolition Wood Pellets</b>	9.1	69.6	19.7	1.7	45.7	6.3	36.2	0.9	LLD	0.1
<b>Pepper Plant Residue</b>	6.5	60.5	19.5	13.5	33.8	4.0	39.1	2.5	0.5	0.1
<b>Greenhouse Residue</b>	2.5	61.0	5.50	31.0	47.1	7.4	10.9	1.0	LLD	0.1
<b>Wheat Straw</b>	13.9	77.9	21.5	6.8	56.7	6.7	48.8	1.0	0.2	N.R
<b>Sunflower Pellets</b>	11.2	65.2	19.5	4.1	44.1	5.17	34.6	0.5	0.1	0.1
<b>Olive Cake Pellets</b>	11.9	64.2	15.7	8.2	42.1	4.99	31.0	1.3	0.1	0.3
<b>Sewage Sludge</b>	6.9	44.6	7.0	41.5	52.0	6.3	32.1	6.3	3.1	N.R.
<b>Bituminous Coal</b>	4.9	32.3	48.1	14.7	65.7	5.6	7.7	1.2	0.5	LLD

Note: LLD – below the lower detection limit, N.R. – Not reported.

Moisture content is one of the most fuel properties during biomass combustion process and normally determined by using oven at 110°C. The moisture content of biomass can vary considerably, depending on the type of biomass and biomass storage method, in a wide range from 10% to 70% (Khan et al., 2009). The moisture content influences the combustion behavior, adiabatic temperature of combustion and volume of flue gas produced per energy unit (Koppejan & Van Loo, 2012). High moisture content of biomass fuels can cause ignition issues and reduce the maximum possible combustion temperature (the adiabatic combustion temperature), which in turn hinders the combustion of the reaction products and consequently affects the quality of combustion (Khan et al., 2009). High amount of moisture may also pose problem of fuel sizing, conveying and feeding

(Patel and Gami, 2012). Thus, biomass combustion needs a longer residence time for drying and reduce moisture content before gasification and charcoal combustion take place (Koppejan & Van Loo, 2012; Khan et al., 2009). Therefore, the biomass combustion requires large and long combustion chamber that ensures an enough residence time of the flue gas in the combustion chambers for a complete combustion and lower emissions.

Biomass generally has a very high volatile matter (VM) content than coals, and usually varies between 70 wt% and 86 wt% (d.b.) (Koppejan & Van Loo, 2012). VM are further subdivided into gases such as light hydrocarbons, carbon monoxide (CO), carbon dioxide (CO<sub>2</sub>), hydrogen (H<sub>2</sub>), moisture, and tars (Khan et al., 2009). In comparison with coals (anthracite less than 10% and bituminous between 5% to 6%), biomass has higher VM (a typical value of 75%; Khan et al., 2009). Due to their high volatile fraction, biomass fuels are easier to ignite even at low temperatures and the majority part of biomass is vaporized before homogeneous gas phase combustion reactions take place; the remaining char then undergoes heterogeneous combustion reactions. Therefore, the amount of VM strongly influences the thermal decomposition and combustion behavior of solid fuels (Koppejan & Van Loo, 2012). The quick release of a large fraction of volatiles makes biomass fuels necessary to have longer high temperature zones in order to achieve complete combustion at high efficiency and to ensure low pollutant emissions (Khan et al., 2009).

Ash is the inorganic un-combustible part of fuel which is left after complete combustion, containing the bulk of the mineral fraction of the original biomass. The most commonly applied techniques for the determination of the ash content and composition of coals and other solid fuels in the laboratory involve heating the fuel slowly in the air to constant mass at a temperature of 815 °C. As shown in Figure 2.1, ash is produced in the

form of bottom ash, cyclone fly-ash, and filter fly-ash in the combustion unit, multi-cyclone, and filter fly-ash precipitator, respectively (Koppejan & Van Loo, 2012). Ash-related two major combustion problems, (1) agglomeration, fouling, and slagging, and (2) corrosion.

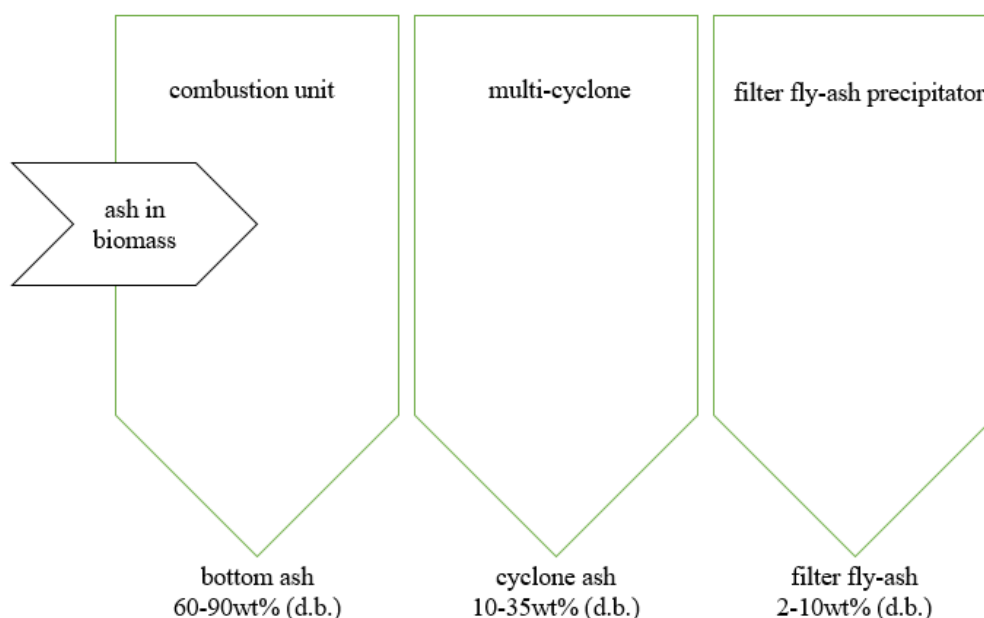


**Figure 2.1: Produced Ash Fractions in the Biomass Combustion Unit**

The resultant ash residue is normally weighted to provide an estimate of the ash content of the fuel. The major inherent ash forming elements in biomass include Si, Al, Ti, Fe, Ca, Mg, Na, K, S, and P (Khan et al., 2009). Thus, ash residue was analyzed for the ten major elements present in biomass ashes (e. g.,  $\text{SiO}_2$ ,  $\text{Al}_2\text{O}_3$ ,  $\text{Fe}_2\text{O}_3$ ,  $\text{CaO}$ ,  $\text{MgO}$ ,  $\text{TiO}_2$ ,  $\text{Na}_2\text{O}$ ,  $\text{K}_2\text{O}$ ,  $\text{P}_2\text{O}_5$  and  $\text{SO}_3$ ) (Koppejan & Van Loo, 2012). Table 2.3 shows the ash analysis of some selected biofuels and bituminous coal. The ash content varies from one biofuel to another. It can be from <1% (wood, demolition wood) to up to 30–40% (green house residue) (Khan et al., 2009). Koppejan & Van Loo (2012) found that the ash content varies from around 0.5 wt% (d.b.) for some kinds of clean woody biomass up to 12.0 wt% (d.b.) for some straw and cereal assortment.

**Table 2.3: Ash Analysis of Biomass and Bituminous Coal (Mass Basis, wt%)**

Fuel	SiO <sub>2</sub>	Al <sub>2</sub> O <sub>3</sub>	Fe <sub>2</sub> O <sub>3</sub>	Mn	MgO	CaO	Na <sub>2</sub> O	K <sub>2</sub> O	TiO <sub>2</sub>	P <sub>2</sub> O <sub>5</sub>	SO <sub>3</sub>
Wood Pellets	4.3	1.3	1.5	5.9	8.5	55.9	0.6	16.8	0.1	3.9	1.3
Demolition Wood Pellets	20.4	3.5	2.2	0.3	7.5	27.5	4.8	10.5	2.5	11.1	LLD
Pepper Plant Residue	12.6	4.9	2.0	0.2	7.4	32.2	0.9	24.6	0.5	5.2	LLD
Greenhouse Residue	28.4	3.9	18.4	0.3	5.7	25.8	0.8	9.7	0.8	3.8	LLD
Sunflower Pellets	2.9	0.6	0.8	0.1	21.6	21.6	0.24	22.8	0.1	15.2	14.0
Olive Cake Pellets	12.8	2.9	3.0	0.1	4.9	17.5	3.9	47.9	0.2	6.0	1.1
Wheat Straw	53.1	3.6	1.2	N.R	3.0	17.7	4.5	30.0	N.R	4.1	N.R
Sewage Sludge	38.3	0.8	12.5	N.R	2.8	9.1	2.2	2.2	0.8	15.4	1.1
Bituminous Coal	59.7	20.3	7.0	<0.01	1.9	1.8	1.0	2.3	0.9	0.1	1.3

Note: LLD – below the lower detection limit, N.R. – Not reported.

### 2.1.3 Higher Heating Value (HHV)

The heating value (or calorific value) defines the energy content of fuel and is one of the most important fuel properties for achieving energy balance, engineering analysis, design calculations, and numerical simulations of thermal conversion systems (Yin, 2011; Nhuchhen and Salam, 2012). The heating value is usually measured by the higher heating value (HHV) or lower heating value (LHV). HHV, also known as the gross calorific value or gross energy, refers to the heat released by the complete combustion of fuel with the assumption of water originally present in the fuel and any generated water are present in a condensed state (Sheng and Azevedo, 2005; Ghugare et al., 2014). For instance, all carbon converted to CO<sub>2</sub>, and all hydrogen converted to water (H<sub>2</sub>O). The HHV is given for standard condition (101.3 kPa, 25 °C) of all products and includes the condensation enthalpy of water (Friedl et al., 2005). LHV, also known as the net calorific or heating

value, assumes that the water is present in a vapor state at the end of combustion and is determined by subtracting the latent heat of water vaporization from the HHV (Vargas-Moreno et al., 2012). While the HHV is generally used in the U. S., the LHV is more common in European countries (Friedl et al., 2005). Table 2.4 shows the examples of the HHV and LHV for biomass fuels.

**Table 2.4: HHV and LHV of Biomass Fuels (Koppejan & Van Loo, 2012)**

Fuel Types (MJ/kg, d.b.)	Wood pellets	Sawdust	Straw	Olive Residue
HHV (or GCV)	19.8	19.8	18.7	21.5
LHV (or NCV)	16.4	8.0	14.5	6.1

Experimentally, an adiabatic bomb calorimeter is used to measure the enthalpy change between reactants and products (Cordero et al., 2001; Sheng et al., 2005). For instance, an IKA C5003 bomb calorimeter was used in accordance with the Spanish Association for Standardization, UNE standard 164001EX to measure the HHV of poultry waste samples (Quiroga et al., 2010). Results indicated that the HHV of samples from nine different farms vary between 12,052 and 13, 882 kJ/kg. Experimentally, Cotana et al. (2014) measured the HHV of two poultry waste samples from different farming practices by using a LECO AC350 calorimeter, in compliance with UNI9017 standard. However, bomb calorimeters may not always be accessible to all laboratories. In addition, the experimental method based on various standards is complicated, cost intensive and time consuming as it requires a trained chemist and sophisticated equipment (Majumder et al., 2008).

#### **2.1.4 Mathematical Models to Predict HHV**

Therefore, numerous mathematical models have been developed to predict the HHV of energy resources from results collected from ultimate analysis (or elemental analysis), proximate analysis, chemical analysis, and structural analysis (Vargas-Moreno,

2012). Ultimate and proximate analyses provide basic fuel characterizations and are the most commonly used analyses to predict the HHV. Sheng and Azevedo (2005) found that mathematical models based on ultimate analysis are more accurate than models derived from proximate and chemical analyses because ultimate analysis quantifies elemental contents and provides a more detailed chemical composition of fuels. Yin et al. (2010) also suggested that ultimate analysis-based models are more accurate than proximate analysis. But ultimate analysis also requires expensive element analyzers as well as special experimental arrangements with skillful analysts (Majumder et al., 2008).

Hence, proximate-based models have developed into an important tool for estimating the HHV of energy resources over time. Proximate analysis is rapid, economical, easy, and can be run by any competent scientist, researcher, or engineer using common laboratory equipment with standard test methods (Demirbas, 2009; Vargas-Moreno, 2012). Common laboratory equipment namely includes a balance, simple oven (for determination of M content), and furnace (for determination of VM and ASH contents) (Parikh et al., 2005; Özyuğuran et al., 2017). Proximate analysis of coal using a simple muffle furnace, which is comparatively cheaper than bomb calorimeter and can be performed by a moderately trained chemist (Majumder et al., 2008). As shown in Table 2.5, seventeen proximate-based models that have been proposed and applied for estimating the HHV for a variety of solid fuels were collected from literature reviews and evaluated (Qian et al., 2018). Unfortunately, most proximate-based models used a wide range of data points and fuel types, which is not very accurate and applicable for other fuel types (Nhuchhen et al., 2017). Özyuğuran and Yaman (2017) also found that the values of the coefficient of determination,  $R^2$  were not very close to one (about 81–83%) because several

different biomass species were accounted for in the samples. In response to the need of more accurate HHV predictions, several researchers have developed models for each subclass of fuels, such as herbaceous, woody, and agriculture residues. However, few researchers have centered their studies on subclass of fuels from poultry raising process (i.e., poultry waste). In addition, Lynch et al. (2013) compared experimental results (18.0 GJ/t) of the HHV with calculated results (15.7 GJ/t) from existing proximate-based model. The relatively high percentage error indicates unsuitability of existing proximate-based models when utilizing a fuel such as poultry waste.

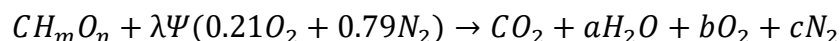
**Table 2.5: Existing Proximate Analysis-based Models for the HHV Prediction**

Existing Models	HHV (MJ/kg) *	Raw Materials
E1	$HHV = -10.81408 + 0.3133 (VM + FC)$	Lignocellulosic Residues
E2	$HHV = 76.56 - 1.3 (VM + A) + 7.3 \times 10^{-3} (VM + A)^2$	Coal
E3	$HHV = 0.196 (FC) + 14.119$	Biomass
E4	$HHV = 0.3543 FC + 0.1708 VM$	Lignocellulosics & Charcoals
E5	$HHV = -0.066 (FC)^2 + 0.5866 (FC) + 8.752$	Shell of biomass
E6	$HHV = 0.356047 VM - 0.118035 FC - 5.600613$	Municipal solid waste
E7	$HHV = 19.914 - 0.2324 A$	Biomass fuels
E8	$HHV = 0.3536 (FC) + 0.1559 (VM) - 0.0078 A$	Solid fuels
E9	$HHV = 0.25575 VM + 0.28388 FC - 2.38638$	Sewage sludge
E10	$HHV = 18.96016 - 0.22527 A$	Straw
E11	$HHV = -0.1882 (VM) + 32.94$	Vegetable oil and tallow
E12	$HHV = 0.1905 VM + 0.2521 FC$	Biomass
E13	$HHV = -2.057 - 0.092 A + 0.279 VM$	Greenhouse crop residues
E14	$HHV = 20.7999 - 0.3214 VM/FC + 0.0051 (VM/FC)^2 - 11.2277 A/VM + 4.4953 (A/VM)^2 - 0.7223 (A/VM)^3 + 0.038 (A/VM)^4 + 0.0076 FC/A$	Biomass
E15	$HHV = 1.83 \times 10^4 - 3.98 A^2 - 112.10 A$	Spanish biofuels
E16	$HHV = 0.1846 VM + 0.3525 FC$	Torrefied biomass
E17	$HHV = 10.982 + 0.1136 VM - 0.2848 A$	Biomass

\* HHV = Higher Heating Value; FC = Fixed Carbon; VM = Volatile Matter; A = Ash.

## 2.2 Emissions during Biomass Combustion Process

The products from the biomass combustion are formed from the reaction  $O_2$  of in the oxidant (or air) and fuel elements. Mainly, the carbon is oxidized into  $CO_2$  and hydrogen is oxidized to  $H_2O$ . The combustion of a typical biomass fuel with air can be written as:



where  $\lambda$  is the EA ratio and  $\Psi$  is the stoichiometric coefficient, calculated based on the full burnout condition ( $\lambda=1$  and  $b=0$ ). Theoretically, the main products, such as  $CO_2$ ,  $H_2O$ ,  $O_2$  and  $N_2$  are released during the complete biomass combustion process.

However, biomass combustion process is a complex phenomenon which involves simultaneous coupled heat and mass transfer with chemical reactions and fluid flow. The emission rate of various pollutants during biomass combustion depends on fuel properties, combustor design and operating conditions (Saidur et al., 2011). Besides main products from complete combustion, there are other emissions (e.g.,  $CO$ ,  $NO_x$ ,  $SO_2$ ) and inorganic species (e.g. alkali chlorides, sulfates, carbonates and silicates; Jenkins et al., 1998). With sufficient air input, unburned pollutants (such as  $HC$ , tar, polycyclic aromatic hydrocarbons (PAH),  $C_xH_y$ ) are expected at insignificant levels. Meanwhile,  $HCl$  emissions are considered to be negligible due to small  $Cl$  contents in the biomass fuels (Werther et al., 2000).  $CO$  and  $NO_x$  are the major pollutants and  $SO_2$  is minor pollutants emitted during biomass combustion (Permchart and Kouprianov, 2004).

### 2.2.1 Carbon Monoxide (CO) Formation

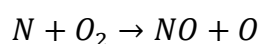
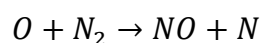
$CO$  emission is due to incomplete combustion of fuels during the combustion process which is affected by different parameters, such as EA ratio, residence time,

chamber temperature and other gaseous species. Small EA ratio ( $<1$ ) or too little  $O_2$  into the combustion zone may result large CO formation while large EA ratio may decrease the overall system efficiency by heat loss from the waste flue gas. Enough residence time is needed for complete combustion, otherwise increasing CO formation (Laryea-Goldsmith, 2010). Temperature is another important parameter to convert intermediate CO into  $CO_2$ . Results show that zones with low temperatures favor formation of CO, while at higher temperatures the reactions proceed faster toward complete oxidation CO into  $CO_2$ . In addition, other gaseous species may affect CO formation. For example, HCl in the flue gas has a direct relation with the CO emission level, affected by the presence of radicals and catalytic reactions in presence of gaseous species (Wei et al., 2004). Combined  $NO_x$  and HCl result in a higher CO emission due to a considerable decrease in CO oxidation in the presence of these gases (Roesler et al., 1995). Likewise, it also has been shown that  $SO_2$  in the presence of NO prevents CO oxidation by reducing the concentration of free radicals (Glarborg et al., 1996).

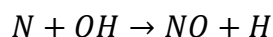
### **2.2.2 Nitrogen Oxides ( $NO_x$ ) Formation**

Nitrogen oxides ( $NO_x$ ) is a collective term of NO and  $NO_2$ .  $NO_x$  emission has both a negative effect on the climate (e.g., ozone formation, acid rain, vegetation damage, smog formation during the reaction with organic compounds) and human health (i.e., to respiratory system, when reacting with ammonia and other compounds to form small particles which can penetrate deeply into sensitive parts of the lungs; Tariq & Purvis, 1996). Three major types of  $NO_x$  formation mechanisms, include thermal mechanism (Zeldovich), prompt mechanism (Fenimore) and fuel-N mechanism (Fuel-N conversion; Laryea-Goldsmith, 2010).

Thermal NO<sub>x</sub>: Thermal or Zeldovich mechanism is predominant at temperatures higher than 1500 °C (Wüning and Wüning, 1997). According to literatures, thermal NO<sub>x</sub> formation in different biomass combustion systems starts at temperatures above 1400 °C (Salzmann & Nussbaumer 2001; Mahmoudi et al., 2010). Ozturk notes that thermal NO<sub>x</sub> is formed rapidly and dominates at temperatures over 1300 °C (1573 K; Ozturk, 2010). Thermal NO formation occurs primarily via three principal reactions that are fast at high temperatures (Miller, 1989). The set of chemical reactions for this highly temperature dependent mechanism can be written as:

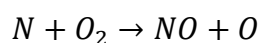
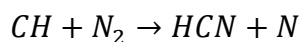


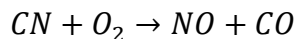
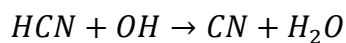
With fuel rich conditions and an EA ratio is close to one, the third reaction is also important because it combines the first two reactions.



In previous studies, most biomass combustion and co-combustion takes place within the temperature range of 800-1000°C (McKendry, 2002b). Thus, the relatively low and unfavorable temperature conditions reduce thermal NO<sub>x</sub> emissions during the biomass combustion and co-combustion process.

Prompt NO<sub>x</sub>: Prompt NO<sub>x</sub> (mainly prompt-NO) involves a series of reactions that dominates the formation of NO at lower temperature. Prompt NO<sub>x</sub> formation mechanism was first identified by Fenimore (Fenimore, 1971). The chemical reactions are very complex, but a simple reaction chain can be introduced as below (Miller, 1989):





Contributions from the prompt mechanism are mainly found in fuel rich conditions and depend on the hydrocarbon (CH) radical concentrations. The prompt mechanism is slower than thermal NO, its contribution to total NO<sub>x</sub> is often small. Due to fuel lean conditions, relatively long residence times and less CH radical production during biomass combustion, prompt NO<sub>x</sub> contribution is very low.

Fuel-N mechanism: Fuel-N mechanism refers to NO<sub>x</sub> formation from fuel that contains nitrogen compounds. Fuel-N mechanism are simplified and illustrated in the Figure 2.2 (Nussbaumer et al, 2003).

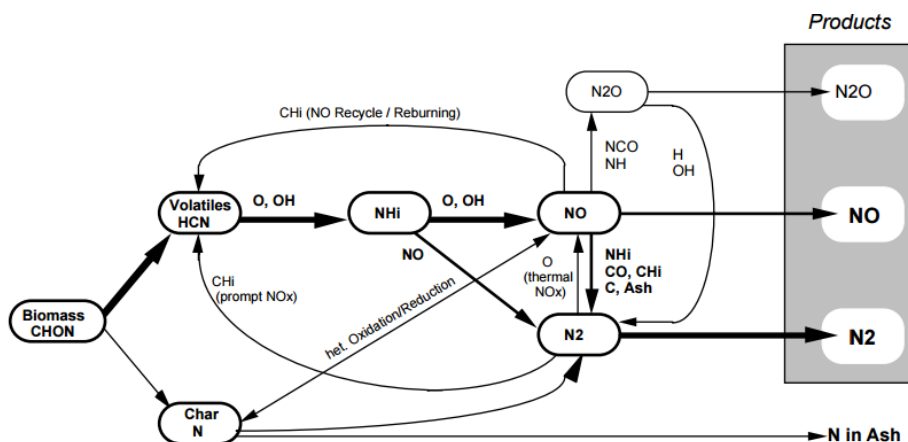


**Figure 2.2: Simplified Fuel-N Conversion (Nussbaumer 2003)**

In the pulverized coal combustion, more than 80–90% of NO<sub>x</sub> emission is coming from fuel-N mechanism while the remaining emissions are the results of the thermal NO<sub>x</sub> mechanism (Glarborg et al., 2003). In biomass combustion and co-combustion systems, fuel-N conversion is even more dominant due to its relatively low temperature conditions.

During biomass combustion and co-combustion, the major part of  $\text{NO}_x$  is coming from fuel-N mechanism and a minor share of  $\text{NO}_x$  is coming from thermal  $\text{NO}_x$  while the prompt mechanism can be neglected.

### **2.2.3 Sulfur Oxides ( $\text{SO}_2$ ) Formation**

Sulfur oxides ( $\text{SO}_x$ ) is a product of complete oxidation of fuel sulfur. It is mainly  $\text{SO}_2$  (>95%) and some  $\text{SO}_3$  (<5%) may be formed at a lower temperature. The fuel sulfur will convert to  $\text{SO}_x$  while a significant fraction in the ashes and a minor fraction of salt ( $\text{K}_2\text{SO}_4$ ). Nikolaisen et al. (1998) found that 57-65% sulfur from straw combustion was released into the flue gas as  $\text{SO}_2$  while remainder was bound in the ashes (Nikolaisen et al., 1998). Further test and evaluation of material balances have shown that 40-90% of the total S input by biomass fuel is bound in the ashes and the rest is emitted with the flue gas as  $\text{SO}_2$  and a minor extent as  $\text{SO}_3$  (Koppejan & Van Loo, 2012).

### **2.2.4 Particulate Matter (PM) Formation**

Particulate matter (PM) is defined as a mixture of solid particles and liquid droplets which can be found in the air. Complete combustion process of biomass may produce  $\text{CO}_2$ ,  $\text{H}_2\text{O}$ , heat, and fly-ash. Fly-ash consists of coarse fly-ashes (e.g., particle with a diameter larger than 1 micrometers ( $\mu\text{m}$ ), and entrainment of ash and fuel particles from fuel bed) and aerosols (e.g., particles with a diameter less than  $1\mu\text{m}$ , and reaction of easily volatile elements at low temperature by nucleation and condensation processes) (Koppejan & Van Loo, 2012). However, incomplete combustion processes of biomass are unavoidable due to lack of air or unfavorable conditions (i.e., temperature too low) and may form particulate matter (PM). Three main types of PM are: carbonaceous solid material (denoted as soot), condensable organic compounds (denoted as tar), and inorganic particles (denoted as ash)

during biomass combustion process (Nussbaumer, 2017; Koppejan & Van Loo, 2012). PM can be classified and analyzed with the following parameters:

- Size (or aerodynamic diameter): Inhalable particles with an aerodynamic diameter smaller than 10  $\mu\text{m}$  ( $\text{PM}_{10}$ ), respirable fraction referred to fine particles smaller than 2.5  $\mu\text{m}$  ( $\text{PM}_{2.5}$ ), and coarse PM with diameter between  $\text{PM}_{10}$  and  $\text{PM}_{2.5}$ . Furthermore, particles smaller than 1.0  $\mu\text{m}$  ( $\text{PM}_{1.0}$ ) are denoted as ultrafine particles (UFP) while particles smaller than 0.1 (100 nanometers) are denoted as nanoparticles (Nussbaumer, 2017). Total Suspended Particles (TPS) with particle diameters smaller than 100  $\mu\text{m}$  (European Environment Agency).
- Mass concentration: mass of particles per unit volume of flue gas (i.e.,  $\text{mg}/\text{Nm}^3$ )
- Number concentration: number of particles per unit volume of flue gas (i.e.,  $\text{particles}/\text{cm}^3$ )
- Mass size distribution: mass concentration distributed over particle size
- Number size distribution: number concentration distributed over particle size
- Chemical concentration: element (e.g., K, Na, Cl, S, Mg, Ca etc.)
- Emission factor (EF): mass of PM emitted per mass of fuel consumed ( $\text{g}/\text{kg}$ ) or per energy output ( $\text{g}/\text{kJ}$ )

In addition, physical characteristics, such as surface area, density, and morphology also were used to study the PM formation and effect (Bølling et al., 2009). Emission cycles (e.g., daily, weekly, seasonal, annual) were also considered to evaluate the influence of PM on the air quality and set the emission standards. As shown in Figure 2.3, Amaral et al. (2015) presented an overview of instruments available on the market for measuring PM in terms of concentration (mass, number and surface area) and size distribution. For mass and

size distribution, low pressure cascade impactors (e.g., Andersen Impactor, Dekati Low-Pressure Impactor) are frequently used (Obaidullah et al., 2012). The chemical analysis can be done off-line by using a sample collection from a filter (or a cascade impactor). Chemical analysis can be conducted by the following instruments, such as Energy Dispersive X-ray Spectroscopy (EDX), Inductively Coupled Plasma-Mass Spectrometry (ICP-MS), Scanning Electron Microscopy (SEM), and Time of Flight-Secondary Ion Mass Spectrometry (TOF-SIMS; Obaidullah et al., 2012).

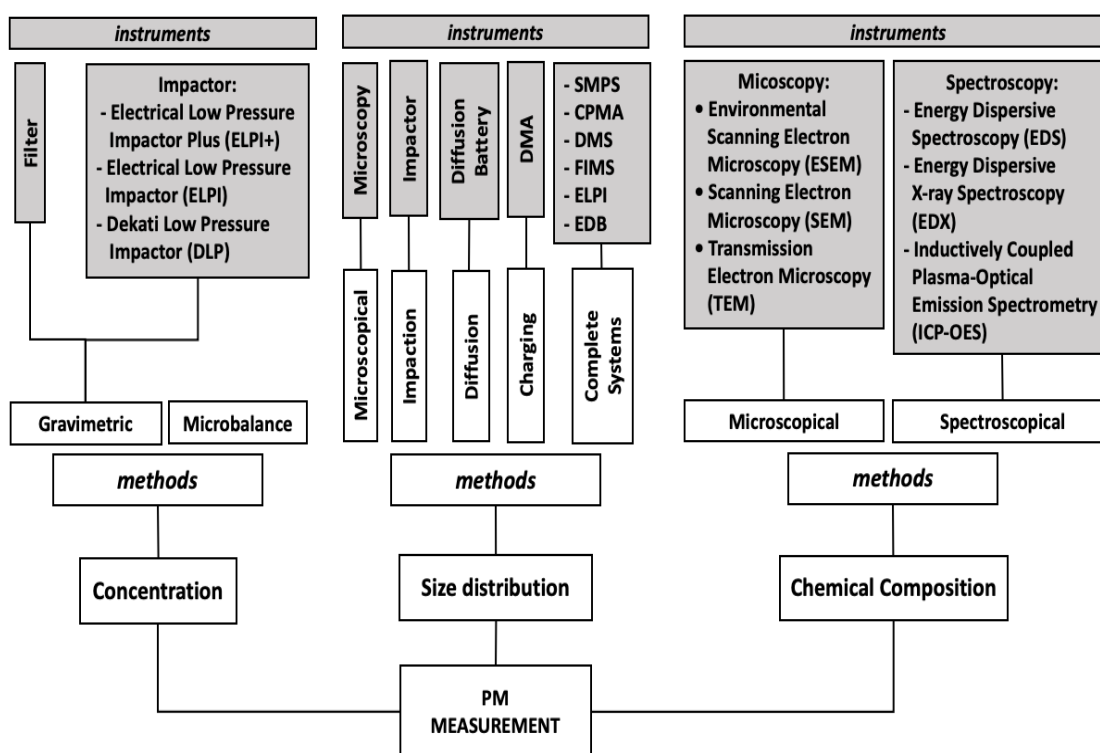


**Figure 2.3: Methods and Instruments for PM Characterization (Amaral et al., 2015)**

There is worldwide concern about PM emissions from biomass combustion. The majority of the particles is fine PM (e.g.,  $PM_{2.5}$ ,  $PM_{1.0}$ ) and emitted directly to ambient air from the combustion devices (Obaidullah et al., 2012). Many different studies (e.g. epidemiologic studies, in vivo and vitro exposure studies) showed strong evidence that exposure to ambient PM is related to a wide range of adverse health outcomes (Vicente &

Alves, 2018). An increased risk in mortality from cardiovascular and respiratory illnesses, exacerbation of existing allergic symptoms (i.e., asthma), aggravation of skin diseases (i.e., atopic dermatitis), decline in lung function, and an increase in blood pressure (Vicente & Alves, 2018; Nussbaumer, 2017). In addition, people who have a prior history of heart and lung diseases, especially children, are vulnerable to PM exposure (US EPA). In addition to health risks and impacts, PM emissions also reduce performance of combustion equipment (i.e., deposition on surface) and cause atmospheric changes (e.g. absorbing and scattering of solar radiation, condensation nuclei causing cloud formation). It is important to investigate and understand the PM during biomass combustion to improve the air quality and to reduce the risk of human health in the long term.

## **2.3 Effect of Operating Conditions on Emissions**

Effect of operating conditions, such as secondary air (SA), excess air (EA), and mixing ratio (MR) on combustion performance were widely studied to improve combustion efficiency and reduce emissions during the biomass combustion process. Effect of SA, EA and MR on emissions were reviewed and summarized in the following subsections. It was found that the optimal operating conditions were changed by the fuel types, air injection methods, and types of combustion system.

### **2.3.1 Effect of Secondary Air (SA) on Emissions**

Staged-combustion is applied with consecutive secondary air (SA) injection in the combustion chamber and primary air (PA) injection in the fuel bed. SA injection enables the good mixing of combustion air with combustible gases formed by devolatilization and achieving the complete burnout to encourage the formation of  $N_2$  rather than  $NO_x$  emissions (Nussbaumer, 2003). There are several studies in the literatures to investigate

the effect of SA ratios on combustion efficiency and emissions during the combustion and co-combustion of solid fuels in fluidized bed combustor (FBC).

Piao et al. (2000) studied the combustion behavior of two kinds of refuse derived fuel (RDF) in a bubbling FBC. Results indicated that increasing SA injection decreased both CO and NO emissions for both types of RDFs.

Suksankraisorn et al. (2004) investigated the effect of SA on emissions and combustion characteristics for the co-combustion of municipal solid waste (MSW) and Thai lignite in a laboratory scale bubbling FBC. Results showed that NO emissions dropped as SA ratio increased because the bed became the reduction zone and the freeboard became the oxidizing zone during staged-combustion.

Xie et al. (2007) performed an experiment to see the influence of air staging on emissions in a bench-scale circulating FBC for co-combustion of coal and rice husk. Result reported that air-staging decreased NO emission.

Kuprianov et al. (2011) studied the effect of air staging and moisture on the emissions for risk husk combustion in a swirling FBC. With elevated SA/PA ratio, the NO emission exhibited a slight reduction while CO emission increased, and more volatiles carried over from the bottom causing the elevation in the  $C_xH_y$  emissions.

Varol et al. (2014b) performed co-combustion of lignite and woodchips in a circulating FBC to investigate the effect of SA ratio on the flue gas emissions. Result indicated that increasing SA ratio increased CO and  $SO_2$  emissions but decreased NO emissions.

When SA was introduced into the combustor in staged-combustion of biomass, the amount of PA was reduced, and more reducing atmosphere is dominated in the dense

phase. Therefore, the decrease  $\text{NO}_x$  observed might be explained by the formation of reducing atmosphere (or oxygen) at the lower parts of the combustor. However, the effect of SA on CO was not very clearly. SA ratio in the range of 10–15% was shown to be the best for CO emission. With further increase in SA ratio, CO emissions got worse because increased SA ratio caused temperature decreases at cyclone outlet (Suksankraisorn et al., 2004; Kuprianov et al., 2011; Duan et al., 2013; Varol et al., 2014b).

### **2.3.2 Effect of Excess Air (EA) on Emissions**

Theoretically, the combustion is said to be stoichiometric when fuel and oxygen from the air are in perfect balance. However, stoichiometric (or perfect) combustion is not feasible in the real-world practice. The theoretical amount of air would provide insufficient oxygen and some of the carbon in the fuel would be converted into CO emissions and leads to smoke production. To ensure complete combustion of fuel, combustion chambers must be supplied with excess air (EA). EA ratio describes the ratio between locally available and stoichiometric amount of combustion air (Nussbaumer, 2003). There are several literatures to investigate the effect of EA ratios on combustion performance and emissions.

- Permchart et al. (2004) investigated the effect of EA on the emissions for various biomass fuels in a single FBC. Results indicated that the CO emission for distinct fuels were rapidly diminished with an increase in EA (up to 50-60%). But, a weak dependence on EA was found in the region of 60-100%.
- Suksankraisorn et al. (2004) conducted the co-combustion study of high moisture municipal solid waste and high sulfur Thai lignite in a laboratory scale bubbling FBC. Results indicated CO reduction when the EA ratio is relatively low (60% and below) and CO increment when the EA is relatively high (80% and above).

- Eiamas-Ard et al. (2008) investigated the impact of EA injection on the combustion characteristics of rice husk in a dual-staging vortex-combustor. Experiment results indicated that both CO and NO emission are slightly increased with the rise of EA.
- Duan et al. (2013) studied effect EA ratio on emission characteristics of high volatile content rice husk combustion in a vortexing FBC. Result indicated that the increasing of EA ratio from 0.33 to 1.00, increased NO emission due to the increased freeboard temperature and reduced possibility of NO reduction with CO (by chemical reaction:  $2\text{NO}+2\text{CO}\rightarrow 2\text{CO}_2+\text{N}_2$ ).
- Varol et al. (2014b) studied the effect of EA ratio on the flue gas emissions of co-combustion of Bursa-Orhaneli lignite and woodchips in CFBC. In case of EA between 1.20 and 1.35, CO and NO emissions were under the limits but SO<sub>2</sub> emission was above the limit.

From literatures, researchers suggested various EA ratio ranges for the different fuels due to the complexity of fuel properties and combustion systems. Large EA may decrease the combustion temperature as well as combustion efficiency because EA carrying extra heat energy in the exhaust flue gases. If there is a lack of EA, high level of particulates and CO emissions and resulting in increased exhaust emissions (Baskar and Senthikumar, 2016). However, there is possibility to reduce CO and NO emissions by optimal EA ratios.

### **2.3.3 Effect of Mixing Ratio on Emissions**

Mixing ratio (MR) of biomass fuel and fossil fuel during the co-combustion process is one of important factors on the emission performance. Mixing ratio is normally calculated by either heating value or weight differences. Several studies have been

conducted to identify the effect of MR on combustion efficiency and emissions during the combustion and co-combustion of solid fuels in FBC.

- Li et al. (2008) investigated the effect of chicken litter fraction on the pollutant emissions during co-combustion with coal in a laboratory-scale FBC. Results indicated that the introduction of high volatile chicken litter causes CO increment while SO<sub>2</sub> and NO emissions reduction as a result of fuel-S dilution and larger amount of volatile matter suppressed NO formation.
- Munir et al. (2011) performed co-combustion tests of pulverized Russian coal with different biomasses in 20 kW down-fired combustor. Addition of biomass shares (5%, 10% and 15% by thermal content) had a positive impact on carbon burnout and NO reduction under optimal conditions.
- Jia and Anthony (2011) evaluated the combustion characteristics of co-firing poultry-derived fuel (PDF) with coal in pilot-scale circulating FBC. PDF addition actually lowered fuel-N to NO<sub>x</sub> conversion because the organic N fraction in the PDF operates similarly to the de-NO<sub>x</sub> effect of adding NH<sub>3</sub> or urea to a circulating FBC environment.
- Sun et al. (2013) conducted co-combustion of bituminous coal and sawdust pellets in a 0.2 MW circulating FBC to study the influence of biomass share (0-25 wt. %) on the gaseous emissions. Results indicated that higher biomass shares at dense zone created a reducing atmosphere and inhibited the generation of NO, N<sub>2</sub>O and SO<sub>2</sub>, which also generated great amounts of CO emission and low temperature condition.
- Varol et al. (2014a) studied effect of weight ratio (10%, 30% and 50% wt. of woodchips in Bursa-Orhaneli lignite) on the flue gas emissions in a circulating FBC. Test results

indicated that the addition of woodchips increased CO emission, but reduced char formation and NO emissions.

Addition of biomass in the coal during co-combustion process decrease  $\text{NO}_x$  emissions and increase CO emission. The presence of CO promoted the NO reduction rate because of char catalyzes NO reduction. In addition, the lower temperature ( $<800\text{ }^\circ\text{C}$ ) during biomass co-combustion avoided decomposition of  $\text{CaSO}_4$ , which is advantageous to retention reaction of  $\text{SO}_2$ .

## **2.4 Stirling Engine**

In the conventional power plant, hot flue gases generated in the fossil fuel combustion process are used to produce steam. Subsequently, the steam is used to turn the steam turbine and generator to produce electricity. However, the conventional thermoelectric power plant is responsible for large emissions as well as the largest water withdrawals and third largest water consumption sector after irrigation and industrial sectors in the U.S. (Yang and Dziegielewski, 2007). Large amounts of water are used in power plants for generating electricity with steam-driven turbine generators and cooling the power-generating equipment (Martín et al., 2017).

In contrast to large amounts of water usage by steam-driven turbines found in conventional power plants, the Stirling engine (SE) used pressurized working fluids (i.e., helium) and small amounts of water to convert residual heat energy into combined heat and electricity (CHP) simultaneously (Thombare & Verma, 2008). Stirling engine (SE) is an external heat engine which converts heat energy into mechanical work via a closed regenerative thermodynamic cycle that has same theoretical thermal efficiency of the Carnot cycle. SE experiences cyclic compression and expansion of working fluid (e.g., air,

nitrogen, hydrogen, helium) in a cold and hot cylinder, separately. SE experiences periodical compression and expansion at different temperature levels to convert thermal energy into mechanical work. The external heat sources can be flammable biomass (e.g. agricultural wastes), solar, biogas, mid-high temperature waste flues gases (García et al., 2014). The external heat input is transferred from outside to working fluid at a high temperature (typically 700-750 °C) (Swaminathan, 2013). SE was observed to have the following advantages: smoothness, reliability, flexible external heat source, and high thermodynamic efficiency (Miccio, 2013).

Generating electricity and useful heat from the same power plant is called “CHP” in Europe and “Cogeneration” in North America. CHP is one of the most efficient and clean approach to generate energy from a single fuel source. As shown in Figure 2.4, instead of producing electricity from power plant and separately producing heat from boiler (~50% Efficiency), the CHP system offer electricity and heat simultaneously (~75% Efficiency) and improve the energy efficiency about 20%. In recent year, small-scale CHP have found in domestic and office applications to rapidly vary their electrical load and control the thermal outputs (Maghanki et al., 2013). Small-scale has a relatively lower power output (usually less than 5 kWe) and also referred to as the domestic CHP (dCHP) or Micro CHP (MCHP). The portability and simplicity of MCHP allowed them for installation in millions of homes, particularly where there is a huge market for heating fuel. In such domestic applications, the MCHP serves as the central heating unit providing heat, hot water and additionally electrical power requirements (Barelli et al., 2012). Currently, the use of biomass-based CHP for district heating of commercial buildings are still increasing and it has also been expanding rapidly in countries. The CHP technology was

recognized as one of the methods for achieving the primary energy saving goals of the European Union. CHP represents over 30% generating capacity in European countries such as Denmark, Finland and the Netherlands. However, over 82.7GW of CHP capacity represents approximately 8% of U.S. generating capacity and exists at over 4,400 industrial and commercial facilities across the U.S. (DOE, 2014). While CHP has been in use in the U.S. for more than 100 years, it remains an underutilized resource today. In U.S., it is critical important to develop a clean and efficient CHP system by using biomass as fuel source.

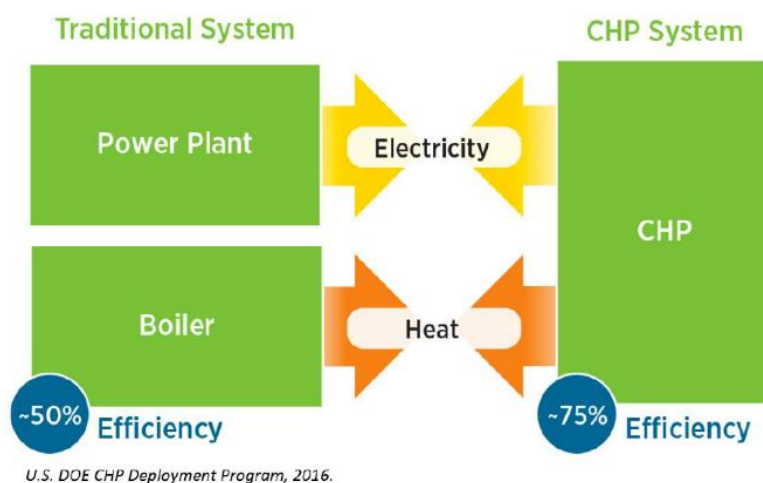


**Figure 2.4: Energy Efficiency Advantage of CHP than Traditional Energy Supply**

SE is capable of being manufactured in a low-power range of 1-10 kWe that is suitable for residential use. As a result, SE has attracted increasing attention as an alternative option for micro-CHP systems (Corria et al., 2006; Miccio, 2013). Recently, SE has been integrated into FBC (Lombardi et al., 2015; Miccio, 2013), wood pellet burners (Cardozo et al., 2014), and combustion chambers (Damirchi et al., 2016) to produce heat along with power for residential usage. As shown in Figure 2.5, a biomass-based MCHP system using a Gamma type SE and conventional combustion chamber was designed and manufactured. Stirling engine performance depends on the various factors, such as thermal

properties of working flow, temperature difference between hot and cold sections, charger pressure of working fluid and regenerator, heater and colder performance (Damirchi et al., 2016). Thereby, the significant operating conditions, the heat source temperature (370-560 °C), pressure of working liquid helium (1-12 bar) and different types of biomass (e.g., sugarcane bagasse, wood, wheat straw, poplar wood and sawdust) were used to investigate the performance of engine. Experimental results indicated that the most power was obtained from sawdust (46 W) and low power for wood (21 W) with internal thermal efficiency of engine was 16 % (Arashnia et al., 2015; Damirchi et al., 2015; Damirchi et al., 2016). However, the feasibility of SE has been barely studied in the swirling FBC to study the feasibility of producing electricity and effect of SE on the emissions.

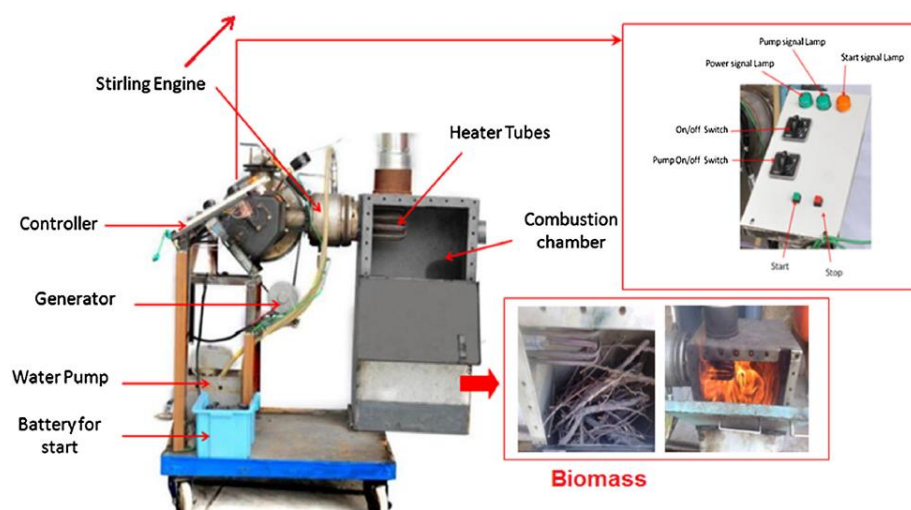


**Figure 2.5: Coupling of SE with MCHP System (Damirchi et al., 2016)**

## 2.5 Shell and Tube Heat Exchanger (STHE)

Heat exchangers are used for transferring thermal energy between two or more fluids, or solid particulates and a fluid, at different temperature and in thermal contact (Bichkar et al., 2018). Heat exchangers are widely used in many industrial applications, such as power plant, petroleum/oil refining, refrigeration system, chemical engineering,

food processing, and nuclear power plant. Different types of heat exchanger are used worldwide that differ from each other because of their specific requirements, such as double pipe, shell and tube, plate fin, plate and shell, pillow plate, etc. are a few types of heat exchangers used on an industrial scale (Salahuddin et al., 2015). Shell and tube heat exchanger (STHE) are the one of the most common types exchangers widely used in the industrial processes (Salahuddin et al., 2015; Zhang et al., 2009; Duan et al., 2016). According to Master et al. (2003) and Master et al. (2006), more than 35-30% of heat exchanger are the STHE type due to their robust geometry construction, easy maintenance and possible upgrades (Zhang et al., 2009; Duan et al., 2016). In addition, STHEs are used in all sorts of industries because they have much lower production cost, are easily cleaned and are considered more flexible adaptability compared with other heat exchanger.

The most common types of STHE are: U-type, straight tube (one pass tube-side), straight tube (two pass tube-side). In some other studies, STHEs can be also divided into three categories according to the type of flow: longitudinal, transverse, and helical (Salahuddin et al., 2015). As shown in Figure 2.6, a STHE mainly consist of a shell (vessel with different sizes, normally large vessel) and a bundle of tubes inside shell. In STHE, two fluids of different temperature flow through the heat exchanger without mixing with each other. One working fluid runs through the tubes (the tube side), and other working fluid flows between outside tubes and shell (the shell side). Heat is transferred from one fluid to the other through the tube walls, either from tube side to shell side or vice versa. The temperature of the two fluids will tend to equalize. The fluids can either be liquids or gases on either the shell or tube side (Dubey et al., 2014).

For efficient heat transfer process, the STHE system should have following characteristics, high heat transfer coefficient, low pressure drops, low or no fouling phenomena, low possibility of vibration. The major factors affecting the performance of STHE are turbulence, pressure drop, heat transfer coefficient, fouling, ratio of flow rates on the tube side to shell side, length of heat exchanger and type of baffle (Salahuddin et al., 2015). Heat transfer coefficient and pressure drop are two major characteristics for the STHE system (Danielsen, 2009). Thus, promoting the heat transfer coefficient to decrease the heat transfer area and decreasing the pressure drop to save the cost of pump are two major ways to save energy and improve the efficiency of heat exchangers.

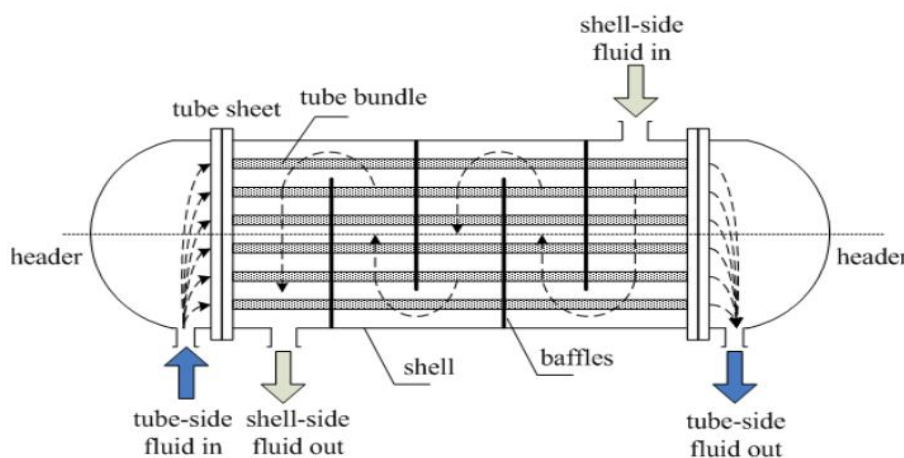


**Figure 2.6 Schematic Diagram of the STHE (Zhang et al., 2012)**

Baffle is one of critical component to significantly influence the overall performance of the STHE system. Besides supporting the tube bundles, baffles forms flow passage for the shell-side working fluid in conjunction with the shell and tube structures (Zhang et al., 2009). Baffle is also responsible to maintain desirable velocity for shell side fluid flow and create turbulence in shell side. It also resists vibrations to enhance the fluid velocity as well as the heat transfer coefficient (Salahuddin et al., 2015). The shape and arrangement of baffles are of essential importance for the performance of the heat

exchanger. Based on the shape, various type of baffles, such as segmental, double segmental, helical, flower, ring, trefoil hole, disc and doughnut type were developed and used in the wide applications of the STHE system (Bichkar et al., 2018). Figure 2.7 show the some types of baffles. Helical baffles require high capital investment due to the complexity of shapes and manufacturing process. Thus, the segmental baffle-based STHE has been widely adopted and probably is still the most commonly used type of STHE. Segmental baffle forces the shell-side fluid going through in a zigzag manner, hence the improvement of heat transfer with acceptable pressure drop. In order to collect more residual heat from flue gas, this study focused to increase heat transfer coefficient by implementation of segmental baffle for the lab-scale STHE prototype.

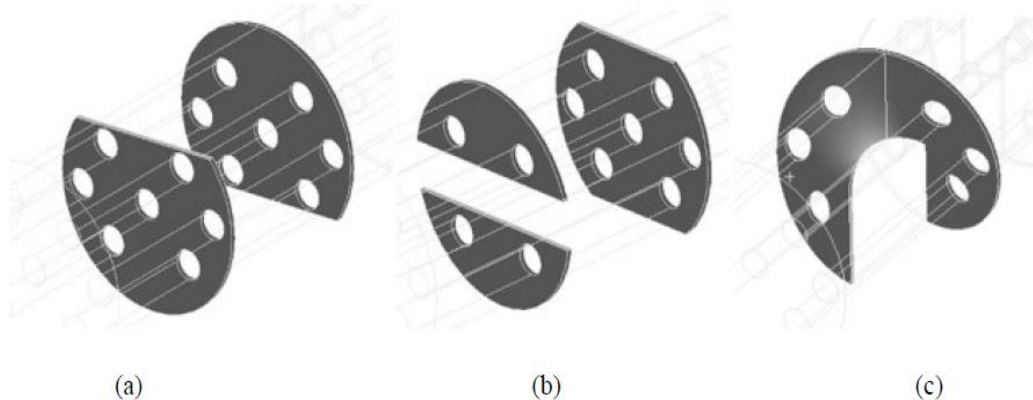


**Figure 2.7: Types of Baffles (a) Segmental, (b) Double Segmental, (c) Helical**

The type of tubes play an important role in heat transfer enhancement technique and effect the heat transfer process. There are several types of tubes, such as plain, twisted and longitudinally finned available in the current market (Dubey et al., 2014). Among the other types of tube, twisted tube is a typical passive heat transfer enhancement technique. Twisted tubes can be manufactured from a full range of materials including carbon steels, stainless steels, titanium, copper and nickel alloys (Danielsen, 2009). Sketch of twisted tube is illustrated in Figure 2.8. Geometrical parameters of the twisted tube are twist pitch

length ( $P$ ), inner major axis ( $a$ ), inner minor axis ( $b$ ), outer major axis ( $A$ ) of the oval section and outer minor axis ( $B$ ) of the oval section. The twist pitch length indicates the tube length between each  $360^\circ$  twist.

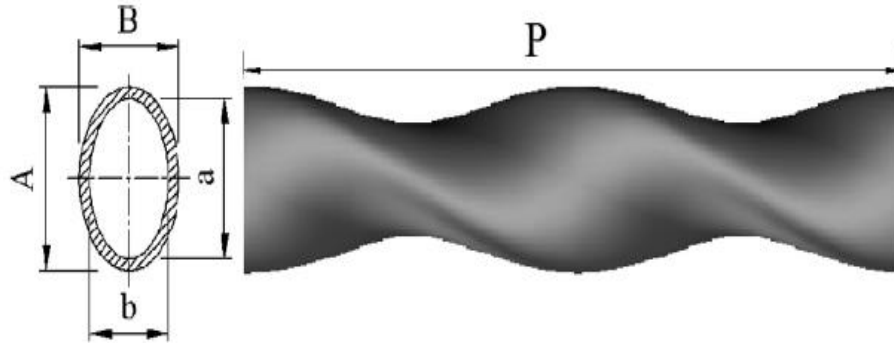


**Figure 2.8: Sketch of the Twisted Oval Tube**

Deformations of tubes also determine the cross-section of tube side in relation to shell side (Danielsen, 2009). As shown in Figure 2.9, the helical channel formed in the inter tubular space can be looked upon as a series of consecutive short sections. In the tube side, the buildup of a steady velocity profile is interrupted by the constant direction change of the flow. These numerous interruptions achieve good transverse mixing and keep the turbulent flow even at relatively low Reynolds numbers. Compared to the laminar flow, the turbulent flow offers substantially high convective heat transfer coefficients. Thus, a high heat transfer performance was secured by keeping the turbulent flow in tube section. These mechanisms contribute to higher heat transfer coefficients on the shell side flow.

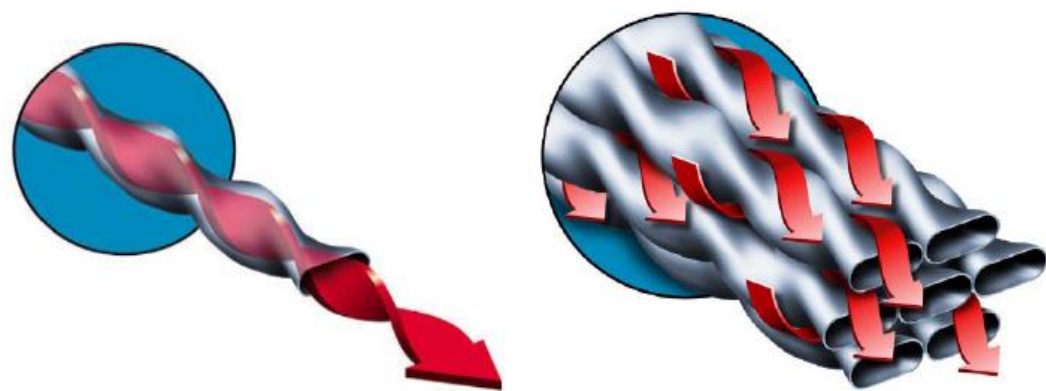


**Figure 2.9: Flow Pattern of the Tube Side and Shell Side**

For the tube side flow, swirl flow of twisted tube produces inertial mass forces, which generate a secondary flow and enhance the tube side mixing. By running cooling fluid inside the tubes as shown in Figure 2.10, the cold fluid was heated near the wall with a lower density compared to the colder flow in tube center because of the induced swirl flow (or secondary flow) create centrifugal forces tent to move cold high density towards the wall securing as high as possible temperature difference across tube.

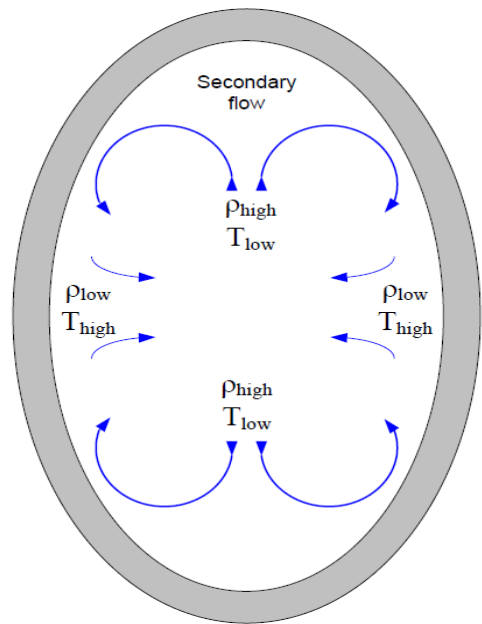


**Figure 2.10: Secondary Flow on the Tube Side**

Few studies have been conducted for the purpose of obtaining the heat transfer and pressure drop performance of the twisted tube. In the early stage, Asmantas et al. (1985) tested the performance of twisted tube to get the heat transfer and pressure drop correlations. In addition, effect of geometrical parameters on the performance of the twisted tube have also been accomplished in the turbulent state (Gao et al., 2008; Yang et al., 2011). Tan et al. (2012) further studied heat transfer and pressure drop performances of twisted oval tube by combination of experiment and numerical simulations. In the experimental study, results showed that heat transfer process of twisted tube can be enhanced with an increasing of pressure drop when compared with the smooth round tube. Tan et al. (2013) experimentally compared the heat transfer and pressure drop performances of a twisted oval tube heat exchanger with other type of heat exchangers. The comparative study showed that the heat transfer coefficient of the twisted oval tube heat exchanger is higher, and the pressure drop is lower than the rod baffle heat exchanger. Li et al. (2018) conducted an experimental research on air side heat transfer and pressure drop of twisted oval tube bundle with staggered layout with cross flow. The twisted oval tube bundle is comprised of 216 twisted oval carbon steel tubes with a diameter of 0.027 m, which are arranged in a triangular pattern with 6 rows of 36 twisted oval tubes. Result indicated that twisted oval tube bundle has an advantage in air side convection heat transfer than round tube bundle with same arrangement in cross flow.

As shown in Table 2.6, investigations on the twisted tubes with various working fluid and tube configurations were performed (Yang et al., 2011). There are various working fluids, such as diesel, air and water were used to test the performance of twisted tubes. However, there is limited study to investigate the heat transfer performance of a

twisted tube in the STHE by using flue gas from biomass combustion process and water as working fluids.

**Table 2.6: Investigations of Twisted Tubes Under Various Conditions**

Sources	Tube Parameters				Working Fluid	
	Thickness	P (mm)	A (mm)	B (mm)	Tube	Shell
Si et al. (1995)	3mm	144, 192, 205	21		Diesel	Steam
Tan et al. (2012)	2.5mm	200	29	19.5	Cold water	Hot Water
Tan et al. (2013)	2.5mm	230	29	19.5	Cold water	Hot Water
Thantharate & Zodpe (2013)		90	18.42	12	Water	Air
Li et al. (2018)	2mm	300	33	16	Water	Air

## **Chapter 3. Fuel Property Characteristics and HHV Prediction**

The objectives of Chapter 3 are to (1) analyze and understand the proximate and ultimate analysis components of poultry litter samples, and (2) develop proximate-based regression models for HHV predictions. In Chapter 3, the methodology and approach to characterize the fuel property and predict the HHV were introduced. The detailed steps and results on sample collection, regression models development and model validation of HHV were also introduced. In the results and discussion part, proximate and ultimate analysis compositions of poultry litter, correlation of proximate analysis components and HHV as well as ultimate analysis components and HHV were summarized. In addition, proximate-based regression models were developed, and validated with additional samples, and also compared with existing proximate-based models to prove the new regression models are more accurate for the HHV prediction of poultry waste samples.

### **3.1 Materials and Methods**

#### **3.1.1 Data Collection, Selection and Normalization**

Various geological locations, farming practices, fuel preparation and processing, handling and storage influence the fuel properties of samples. In this study, a total of forty-eight (48) poultry waste (PW) (also known as poultry litter) samples were collected from the published open literature reviews to include all different scenarios of fuel samples and form a database for derivation, evaluation, and validation of proximate-based HHV models. Complete datasets for the proximate analysis, ultimate analysis, HHV and raw material type are listed in Table S1 (Qian et al., 2018).

During sample selection for the proximate-based HHV models, three samples (#43, 44, and 45) were deleted because only moisture (M) and ash information was provided.

Additionally, two samples (#46 and 47) with HHV of 14.587 J/g and 11.552 J/g were excluded due to extremely low HHV values in contrast to the rest of the samples. In addition, sample (#48) was removed due to uncertainty over whether proximate analysis was conducted under dry-basis or wet-basis conditions. Then, the VM, FC, and ash contents are normalized in dry-basis (moisture free) because dry-basis have been used in most previous HHV prediction studies. The missing data of FC contents are calculated by subtracting VM and ash contents from 100%. Table 3.1 summarizes the FC, VM, ash content and the HHV results of collected PW samples. The collected HHV (e.g., Btu/lb, kJ/kg, GJ/t, and kcal/kg) results are converted into MJ/kg. Composition of proximate analysis components are presented in wt % on dry-basis. In addition, one more poultry litter sample (#49) from a local poultry farm (Bethel Farms, Salisbury, MD, USA) is experimentally analyzed by Mineral Labs Inc. (Salyersville, KY, USA) and results were summarized in the Table 3.1.

For dry-basis ultimate analysis, sum of six major components, carbon (C), hydrogen (H), oxygen (O), nitrogen (N), sulfur (S), and chlorine (Cl) elements and ash content are equal to 100% while wet-basis ultimate analysis include additional M content. For the ultimate analysis, three samples (#19, 33 and 34) were deleted due to the missing three or more elements contents. Then, additional twelve samples where the ultimate analysis in dry basis or wet-basis is not equal to 100% were excluded. But, three samples (#43, 44 and 45) were included because of the available data on the ultimate analysis. After sample selection and normalization process, descriptive statics were applied to study fuel properties of PW samples. For the moisture and Cl contents, only 34 and 11 sample datasets existed to analyze the fuel properties. Before the development of new regression models in

this study, the experimental HHV results from poultry litter samples were plotted with different components of the proximate and ultimate analysis to get a visual insight of their relationship with HHV values.

**Table 3.1 Summary of FC, VM, A and HHV in Dry-basis (Qian et al., 2018)**

No.	FC <sup>1</sup>	VM <sup>2</sup>	ASH <sup>3</sup>	HHV <sup>4</sup>	No.	FC	VM	ASH	HHV
1	2.98	68.25	28.77	10.62	25	27.00	42.30	30.70	19.03
2	6.88	65.16	27.96	11.80	26	35.50	18.30	46.20	14.75
3	9.07	61.20	29.73	12.02	27	16.56	68.83	14.61	16.80
4	11.02	60.77	28.21	12.33	28	5.50	67.90	26.60	13.30
5	5.31	55.61	39.09	9.96	29	9.60	65.70	24.70	14.70
6	2.08	38.46	59.46	6.78	30	12.80	65.56	21.65	13.15
7	13.36	71.26	15.49	18.02	31	14.45	47.42	37.83	14.24
8	14.40	47.93	37.79	13.52	32	14.17	60.99	26.42	10.79
9	14.40	47.82	37.79	14.90	33	13.88	62.55	23.39	12.80
10	11.05	68.63	20.33	12.52	34	25.90	14.30	59.80	11.71
11	12.40	53.60	33.90	12.38	35	3.37	71.54	26.09	10.62
12	15.40	62.70	21.90	14.84	36	55.60	26.70	17.70	27.90
13	15.00	66.30	18.70	14.05	37	4.70	75.10	20.20	12.80
14	17.20	71.90	10.90	17.48	38	14.30	58.64	27.06	12.77
15	14.00	62.20	23.90	14.07	39	11.70	63.10	25.20	11.00
16	13.49	65.10	21.61	14.87	40	9.08	43.57	47.35	10.00
17	2.91	68.28	28.81	10.62	41	8.80	74.30	16.90	15.11
18	12.74	71.11	16.16	17.11	42	4.53	57.93	37.54	10.33
19	13.36	61.49	25.15	14.69	43	-	-	17.20	14.59
20	22.77	66.39	11.54	18.30	44	-	-	25.10	13.67
21	24.40	60.20	15.40	16.00	45	-	-	22.90	15.28
22	23.20	75.30	1.60	20.90	46	-	26.56	10.60	14.587
23	19.42	63.97	16.61	16.80	47	-	64.43	15.41	11.552
24	9.63	69.13	21.25	14.87	48	3.30	54.30	-	10.10
					49	11.98	63.96	24.06	14.34

<sup>1</sup>FC = Fixed Carbon; <sup>2</sup>VM = Volatile Matter; <sup>3</sup>A = Ash; <sup>4</sup>HHV = Higher Heating Value

### 3.1.2 Regression Methods and Proposed HHV Models

Regression analysis is one of the most important industrial engineering analysis methods to determine the relationship between the dependent variable and the independent variables (Moka, 2012). It has been successfully used in quality inspection, reliability engineering, and many other applications. It has been used to model and explore the relationships between variables that are related in a nondeterministic manner. Regression

analysis dealing with the equations either linear or nonlinear with variables more than two is called as multiple regression analysis. It allows us to control the several other factors that simultaneously affect the dependent variable. Regression method can be used to create empirical equations and predict the response based on experimental data (Montgomery, 2017). In general, the dependent variable or response,  $Y$  may be related to  $k$  independent variables. This following model is called multiple linear regression model,

$$Y = \beta_0 + \beta_1 x_1 + \beta_2 x_2 + \cdots + \beta_k x_k + \epsilon$$

Where this model has  $k$  independent variables,  $x_1, x_2, \dots, x_k$ , the parameter,  $\beta_0, \beta_1, \dots, \beta_k$  are called regression coefficients and  $\epsilon$  is a random error term. The model describes a hyperplane in the  $k$ -dimensional space of the independent variables. The parameter represents the expected change in response  $Y$  per unit change in when all the remaining independents are hold constant. The method of least square can be used to estimate the regression coefficients in the multiple regression model (Montgomery and Runger, 2010; Montgomery, 2017). Suppose  $n > k$  observations are available, and let  $x_{ij}$  denote the  $i$  th observation or level of variable  $x_j$ . The observations are

$$(x_{i1}, x_{i2}, \dots, x_{ik}, y_i), i = 1, 2, \dots, n \text{ and } n > k$$

It is customary to present the data for multiple regression in a table such as Table 3.2,

**Table 3.2: Data for Multiple Linear Regression**

$y$	$x_1$	$x_2$	$\cdots$	$x_k$
$y_1$	$x_{11}$	$x_{12}$	$\cdots$	$x_{1k}$
$y_2$	$x_{21}$	$x_{22}$	$\cdots$	$x_{2k}$
$\vdots$	$\vdots$	$\vdots$	$\cdots$	$\vdots$
$y_n$	$x_{n1}$	$x_{n2}$	$\cdots$	$x_{nk}$

Each observation  $(x_{i1}, x_{i2}, \dots, x_{ik}, y_i)$ , satisfies the model in equation,



fifteen new regression models were proposed to establish the relationship between the HHV and proximate analysis components from selected thirty-seven poultry waste samples (#1–37), and ultimately predict the HHV of samples from proximate analysis results.

**Table 3.3: List of Proposed Regression Models**

No.	Proposed New Models *	Note
1	$HHV = a + bFC + cVM + dA$	Linear (FC, VM, A)
2	$HHV = a + bFC + cVM$	Linear (FC, VM)
3	$HHV = a + bFC + cASH$	Linear (FC, A)
4	$HHV = a + bVM + cASH$	Linear (VM, A)
5	$HHV = a + bFC^2 + cVM + dA$	Quadratic (FC), Linear (VM, A)
6	$HHV = a + bFC + cVM^2 + dA$	Quadratic (VM), Linear (FC, A)
7	$HHV = a + bFC + cVM + dA^2$	Quadratic (A), Linear (FC, VM)
8	$HHV = a + bFC^2 + cVM^2 + dA$	Quadratic (FC, VM), Linear (A)
9	$HHV = a + bFC^2 + cVM + dA^2$	Quadratic (FC, A), Linear (VM)
10	$HHV = a + bFC^2 + cVM^2 + dA^2$	Quadratic (FC, VM, A)
11	$HHV = a + bFC + cVM + dA + eVM^2 + fVM^3$	Linear (FC, VM, A), Quadratic & Cubic (VM)
12	$HHV = a + bFC + cVM + dA + eFC \times VM$	Linear (FC, VM, A), Interaction (FC&VM)
13	$HHV = a + bFC + cVM + dA + eFC \times A$	Linear (FC, VM, A), Interaction (FC&A)
14	$HHV = a + bFC + cVM + dA + eVM \times A$	Linear (FC, VM, A), Interaction (VM&A)
15	$HHV = a + bFC + cVM + dA + eVM^2 + fVM^3 + gFC \times A$	Linear (FC, VM, A), Quadratic & Cubic (VM), Interaction (FC&A)

\*Note: a, b, c, d, e, f and g are the constant terms for the proposed regression models.

Equation (1) considers that all components of the proximate analysis have linear relationships with the HHV. Equations (2) – (4) only consider that two components of proximate analysis have linear relationships with HHV. Equations (5) – (7) consider two components as linear and one component as a polynomial (quadratic) relationship with HHV while Equations (8) and (9) consider one component as linear and two components as quadratic for its relationship with the HHV. Equation (10) considers all components as quadratic relationship with the HHV. Among Equations (1) through (10), the most suitable and simple multiple linear regression model (Equation (1)) is used to further improve the

accuracy of HHV prediction. Equation (11) combines Equation (1) and polynomial terms (both quadratic and cubic) of VM contents. Equations (12) – (14) are used to compare the different interaction effects between two components on the accuracy of HHV prediction. Equation (15) combines Equation 1 plus polynomial terms of VM and best interaction effect to get a best-fit proximate-based HHV model. The constant terms of proposed regression models are calculated and determined according to the Least Squares Method. Data for selected PW samples are inserted into one of statistical software, Minitab to perform curve fitting, calculate constant terms, and derive the proposed regression models.

### 3.1.3 Evaluation and Validation of New Regression Models

Three statistical parameters, average absolute error (AAE), average biased error (ABE), and coefficient of determination ( $R^2$ ), are employed to evaluate the accuracy and suitability of the new regression models. Estimation errors such as ABE calculate the degree of overestimation and underestimation of models while AAE measures the degree of closeness between the predicted and measured results.  $R^2$  value is used widely in statistical and regression analyses to determine the degree of goodness and accuracy of models. The "coefficient of determination" or "*r*-squared" denoted  $r^2$ , is equal to the square of the correlation coefficient. The  $r^2$  is equal to the regression sum of squares ( $SS_{\text{regression}}$ ) (explained sum of squares) in *y* divided by the total sum of squares ( $SS_{\text{total}}$ ). Alternatively, since the  $SS_{\text{total}} = SS_{\text{regression}} + SS_{\text{error}}$  (sum of squares errors, residual sum of squares, unexplained sum of squares), the quantity  $r^2$  also equals one minus the ratio of the  $SS_{\text{error}}$  to the  $SS_{\text{total}}$ :

$$r^2 = \frac{SS_{\text{regression}}}{SS_{\text{total}}} = 1 - \frac{SS_{\text{error}}}{SS_{\text{total}}} = 1 - \frac{\sum_{i=1}^n (\text{Actual} - \text{Prediction})^2}{\sum_{i=1}^n (\text{Actual} - \text{Mean of Actual})^2}$$

where  $SS_{total}$  = total variation of y from mean,  $y=(y_1 - \bar{y})^2+(y_2 - \bar{y})^2 \dots+(y_n - \bar{y})^2$ .  
 $SS_{error}$  = variation y from predicted regression line  $= (y_1 - predicted\ y_1)^2 + (y_2 - predicted\ y_2)^2 + (y_n - predicted\ y_n)^2$ . In the above equation,  $SS_{error}/SS_{total}$  is percentage of variation is not described by the variation of y. R-squared (or  $r^2$ ) means the percentage of variation which is described by the regress line. R-squared is Pearson's regression coefficient which ranges from 0 to 1. R-squared value above 0.5 is valid and above 0.7 is the best R-squared value for a given correlation (Moka, 2012). Validation of Correlations will be conducted to confirm the validity of regression equations. A variety of various emissions under different operation conditions and fuel properties will be selected and examined to validate the correlations. Thus, all the estimation errors and  $R^2$  are derived from equations listed below:

$$AAE = \frac{(\sum_{i=1}^n \frac{|P_i - M_i|}{M_i})}{n} \times 100\%,$$

$$ABE = \frac{(\sum_{i=1}^n \frac{(P_i - M_i)}{M_i})}{n} \times 100\%,$$

$$R^2 = 1 - \frac{\sum_{i=1}^n (P_i - M_i)^2}{\sum_{i=1}^n (M_i - \bar{M})^2},$$

where P, M,  $\bar{M}$ , i and n represent predicted results, measured results, average of measured results, specific sample number, and total number of samples, respectively.

$R^2$  values in this study are calculated along with the derivation of regression models while the AAE and ABE of regression models are calculated separately with Microsoft Excel. The developed model is determined to be best fit model when estimation errors, AAE and ABE, tended to be zero and the  $R^2$  value was close to 1 (Sheng et al., 2005; Nhuchhen & Salam, 2012). Experimental results and predicted results from the new regression models were also compared. To further confirm the validity, additional five

poultry waste samples (#38–42) and one experimentally tested sample (#49) in Table 3.1 were used to calculate estimation errors. In addition, the estimation errors of the simple multiple linear regression model (N1) and best-fit regression model (N15) were compared with other published seventeen proximate-based models (for biomass and solid fuels as shown in Table 2.5) by using the same samples data points (#1–37) in Table 3.1 to further determine the accuracy and necessity of new proximate-based HHV models.

## 3.2 Results and Discussion

### 3.2.1 Fuel Properties of PW samples

In order to improve the accuracy of fuel properties, different sample sizes were selected for different elements. Descriptive statistics of the datasets collected from published open literatures are presented in Table 3.4, where mean, sample standard deviation (SD), minimum, 25% percentile, median, 75% percentiles and maximum were included to analyze and understand the composition and HHV of PW samples from proximate and ultimate analysis.

**Table 3.4: Descriptive Statics of Fuel Properties for Poultry Litter Samples**

VARIABLES	DESCRIPTIVE STATISTICS							
	No.	Mean	SD	Min.	Q1	Median	Q3	Max.
<b>C (%)</b>	30	49.20	6.79	38.90	45.19	47.79	52.36	67.93
<b>H (%)</b>	30	6.37	0.86	5.11	5.95	6.37	6.71	9.96
<b>O (%)</b>	30	37.26	8.62	7.53	34.62	38.79	41.77	48.84
<b>N (%)</b>	30	6.25	2.24	1.57	5.00	5.95	6.71	12.88
<b>S (%)</b>	30	0.87	0.39	0.12	0.56	0.98	1.18	1.83
<b>CL (%)</b>	11	0.82	0.37	0.34	0.63	0.80	0.89	1.66
<b>M (%)</b>	34	17.99	11.05	5.00	9.30	14.85	24.67	43.01
<b>FC (%)</b>	42	14.14	9.68	2.08	9.00	13.36	15.69	55.60
<b>VM (%)</b>	42	59.63	14.27	14.30	55.10	62.90	68.36	75.30
<b>ASH (%)</b>	42	26.71	11.98	1.60	18.45	25.17	31.50	59.80
<b>HHV (MJ/KG)</b>	42	14.08	3.59	6.78	11.78	13.78	15.3	27.90

Results show the HHV of PW samples varies from 6.78 to 27.90 MJ/kg and has an average of 14.08 MJ/kg. Chastain et al. (2012) also reported the average HHV for broiler litter is around 14.3 MJ/kg. This inferred that average and range of HHV values from this study were accurate and very close to previous studies. The M content is in the wide range because PW samples were collected from various farm locations along with different type of bed materials. Topal & Amirabedin (2012) also reported the M content with bedding material of sawdust is 18.16% while bedding material of rice husk is 32.57% (as-received, wt%) for poultry litter samples. It concluded that appropriate bedding materials are required in the poultry farm to potentially reduce the M content that ultimately maintain the steady fuel feeding and improve combustion performance during the PW conversion process (Topal & Amirabedin, 2012). Ash content is also critical in the biomass combustion system development because of the relatively high content of Ca, K, P and Na, and low Si in ash may allow lower fusion temperature and higher sulfur-retention ability (Li et al., 2008). In this study, the mass fraction of ash has a mean value of 26.71% and it fall into the range of previous study, 15.7 and 28.8 % (dry-basis, wt%; Font-Palma, 2012). In addition, High VM content in PW samples indicated that it is extremely reactive biomass fuel and easier to ignite even at relative low temperatures. The quick release of VM makes it necessary to have longer high temperature zones and sufficient mixing time to achieve complete combustion along with relative low CO emissions (Khan et al., 2009). PW samples contain on average 14.14% FC and it was suggested to keep a shallow bed that provide necessary heat for the rapid de-volatilization of the fuels as soon as it entered the combustor (Abelha et al., 2003). In summary, high moisture and ash contents as well as lower HHV of PW may result in corrosion and agglomeration issues. Therefore, co-

combustion of PW with other fossil fuels (e.g. coal, natural gas) can be suggested as a better alternative remedy to process PW in clean and efficient manner.

In this study, the C content of PW samples was found to be in the range of 38.90%-67.93% (db) and it has wide range than the previous results of 42.02%-48.61% in dry-basis (Lynch et al., 2013a). Different bedding materials, husbandry practices and possible storage conditions may explain the carbon difference. As many previous studies found that the S and N can generate acidic oxides (e.g., SO<sub>2</sub> and NO<sub>x</sub> emissions), while Cl could give rise to the formation of chlorinated compounds (e.g., hydrochloric acid and dioxins; Florin et al., 2009). The content of N, S and Cl in biomass fuels are critical on the conversion process. Quiroga et al. (2010) proposed the Cl and S content in poultry manure vary around mean values of 0.64% and 0.11% while N content in biomass fuels were found usually less than 1% (Khan et al., 2009). Results indicated that PW samples in this study has average values of N, S and Cl in 6.25%, 0.82% and 0.88%, respectively. The mean value of N, Cl and S in this study were higher than previous results. These results indicated that PW might have a potential to create adverse environmental problems (e.g., acid rain, climate change, ash deposition, corrosion and fouling) and must to be considered in the development and design process of PW disposal systems.

### **3.2.2 Effects of Proximate and Ultimate Analysis Composition on HHV**

As shown in Figure 3.1, the HHV of PW samples are plotted as a function of FC, VM, and ash components (in wt %, dry-basis) by using scatter plots to show how HHV results vary with different composition of proximate analysis data. It was clear that HHV results were increased with the increasing FC contents. In contrast, there is a clear trend in HHV results decreasing with the increase of ash contents. Previous studies have drawn

similar conclusions in that FC content has a positive effect whereas ash content has a negative effect on the HHV of both raw biomass and torrefied biomass materials (Nhuchhen et al., 2017). For the case of coal, Majumder et al. (2008) also found the same trend. This may be possible due to ash having an inert effect on the heating value. Some detrimental effect on the apparent heat obtained during the biomass combustion process because thermal breakdown and phase transition energy of ash forming is taken from biomass combustion process (Özyuğuran & Yaman, 2017). These results further confirm that ash content is one of the most important fuel properties directly affecting the HHV, with high amounts may making PW less desirable as energy resource during the conversion processes. But, the effect of VM composition on the HHV of PW is less obvious. Previous studies also found that the effect of VM content on HHV is much more complicated and inconclusive. High VM does not guarantee a high calorific value since some of the ingredients in VM are formed from non-combustible gases, such as CO<sub>2</sub> and H<sub>2</sub>O (García et al., 2014; Özyuğuran & Yaman, 2017). Therefore, the results infer that linear regression models for VM may not represent the most appropriate solution to accurately estimate the HHV of PW samples. As such, the polynomial terms, such as quadratic, cubic, and interaction effect in the proposed models ensure to predict the precise HHV of PW samples. Correlation is evaluated to measure the strength of the association between the factors (e.g., FC, VM, ash) and response variables (i.e., HHV).

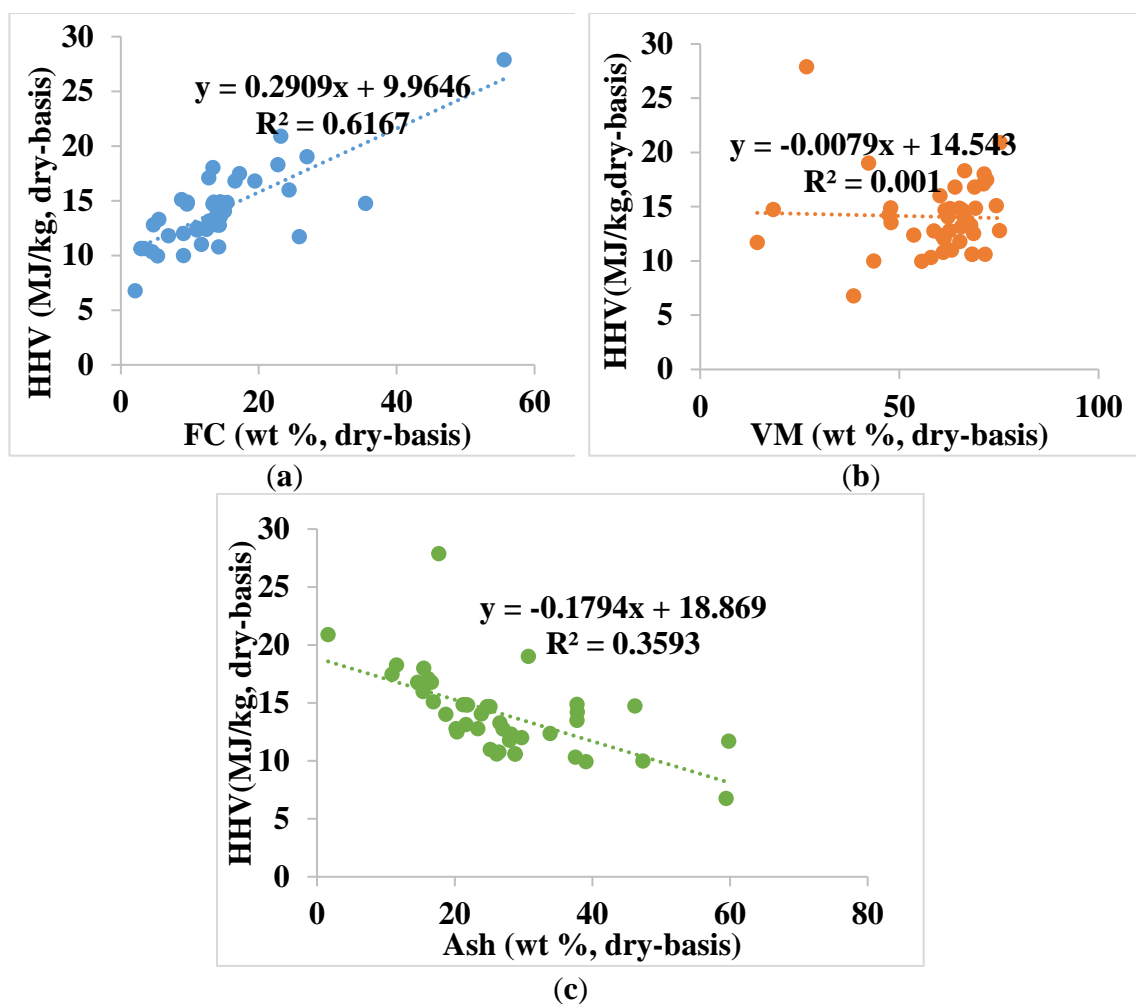


**Figure 3.1: Relationships between HHV and (a) FC; (b) VM; (c) Ash**

As shown in Figure 3.1, there is a relatively strong linear correlation between the HHV and FC ( $R^2 = 0.6167$ ) while only a moderate correlation exists between the HHV and ash ( $R^2 = 0.3593$ ) with the current PW database. However, Sheng and Azevedo (2005) found a different phenomenon for biomass, in that there exists a significant correlation between HHV and ash ( $R^2 = 0.625$ ) while only a trend exists between the HHV and VM ( $R^2 = 0.307$ ). In addition, Akkaya et al. (2009) observed a linear relationship between the HHV and two components (VM and FC), as well as a stronger non-linear dependence for percentages of other two components (M and ash) with coal samples. Compared with biomass and coal samples, the correlation between proximate analysis components and

HHV for PW samples is significantly different. This suggests that the existing correlation of proximate-based models for biomass and coal may not appropriate for estimating the HHV of PW samples. Thus, fifteen new regression models are proposed to correlate the HHV and proximate analysis components of PW samples.

As shown in Figure 3.2, individual concentration of C, H and O were plotted against the corresponding HHV values to explore the appropriateness of the relationship between major elements (C, H, and O) and HHV values. It can be found that major elements of ultimate analysis have better linear dependence than the proximate analysis data. It can thus be inferred that ultimate-based linear models may provide more accuracy than the proximate-based linear models (Sheng and Azevedo, 2005). However, ultimate analysis suffered a drawback; it needs an elemental analysis as an input data, which needs expensive equipment and highly skilled analysts (Parikh et al., 2005). Thus, this study focused on proximate-based mathematical correlation models.

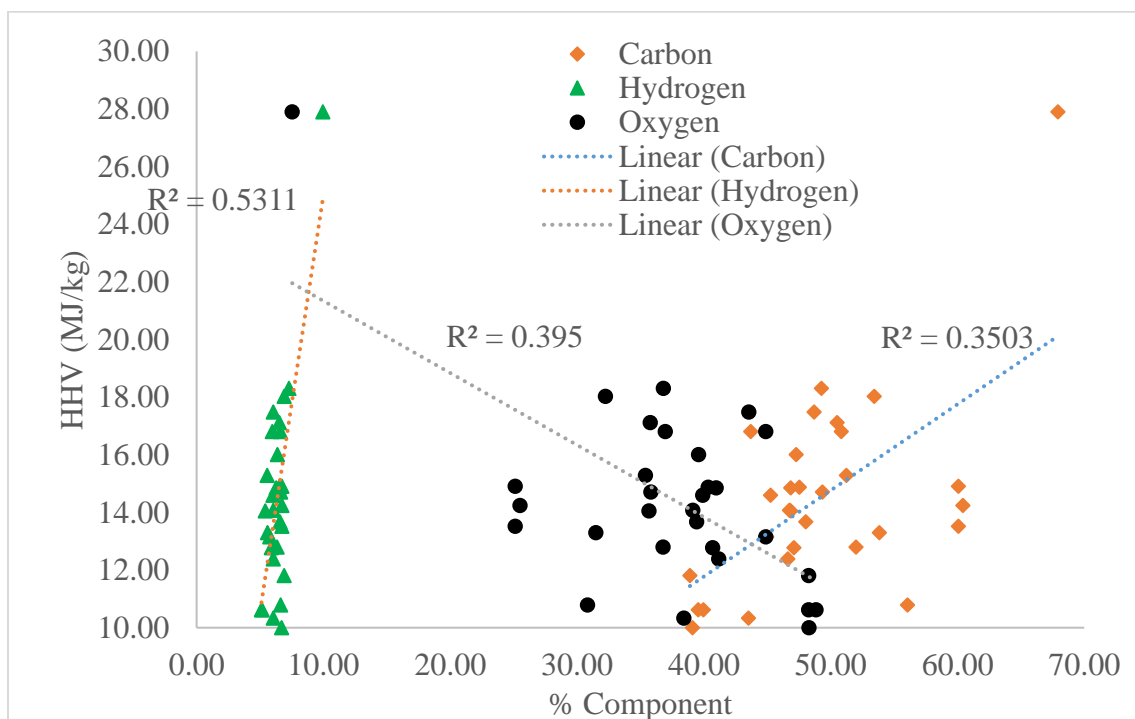


**Figure 3.2: Scatter Plot of HHV and Ultimate Analysis Elements**

### 3.2.3 Derivation of the New Regression Models

As shown in Table 3.5, fifteen new regression models are developed by using proximate analysis data of thirty-seven PW samples.  $R^2$  value, adjusted  $R^2$  value, along with AAE and ABE, are also calculated and summarized.

**Table 3.5: Summary of New Regression Models for PW Samples**

No.	Developed New Regression Model *	Percentage (%)			
		$R^2$	$R^2_{(adj)}$	AAE	ABE
N1	$HHV = 174.3 - 1.335 FC - 1.596 VM - 1.749 A$	88.15	87.08	7.02	0.68
N2	$HHV = -0.33 + 0.4109 FC + 0.1461 VM$	85.72	84.88	7.50	0.70
N3	$HHV = 14.355 + 0.2642 FC - 0.1480 A$	86.11	85.29	7.42	0.69
N4	$HHV = 40.89 - 0.2651 VM - 0.4138 A$	86.73	85.95	7.25	0.61
N5	$HHV = 36.27 + 0.00104 FC^2 - 0.2140 VM - 0.3651 A$	87.03	85.85	7.23	0.75
N6	$HHV = 20.60 + 0.1900 FC - 0.000823 VM^2 - 0.2281 A$	86.43	85.20	7.28	0.66
N7	$HHV = -0.02 + 0.4077 FC + 0.1426 VM - 0.00006 A^2$	85.72	84.42	7.53	0.73
N8	$HHV = 28.46 + 0.002104 FC^2 - 0.001712 VM^2 - 0.3205 A$	86.38	85.14	7.73	0.90
N9	$HHV = 18.16 + 0.00425 FC^2 - 0.0463 VM - 0.00288 A^2$	78.37	76.40	10.36	1.47
N10	$HHV = 15.41 + 0.004800 FC^2 - 0.000145 VM^2 - 0.002430 A^2$	78.14	76.15	10.31	1.53
N11	$HHV = 143.7 - 1.161 FC - 0.364 VM - 1.562 A - 0.02458 VM^2 + 0.000173 VM^3$	91.54	90.18	6.05	0.47
N12	$HHV = 174.3 - 1.331 FC - 1.595 VM - 1.751 A - 0.00012 FC \times VM$	88.16	86.68	7.01	0.46
N13	$HHV = 172.2 - 1.262 FC - 1.587 VM - 1.698 A - 0.00237 FC \times A$	88.91	87.53	6.74	0.57
N14	$HHV = 175.2 - 1.332 FC - 1.615 VM - 1.780 A + 0.000652 VM \times A$	88.32	86.86	7.05	0.20
N15	$HHV = 140.2 - 1.167 FC - 0.210 VM - 1.558 A - 0.02739 VM^2 + 0.000191 VM^3 + 0.00104 FC \times A$	91.62	89.94	5.98	-0.35

\* HHV = Higher Heating Value; FC = Fixed Carbon; VM = Volatile Matter.

Results indicate that new proximate-based regression models can predict the HHV of PW with  $R^2$  values ranging between 78.14% and 91.62%. The estimation errors are found to be in the range of 5.98% to 10.36% for AAE, and -0.35% to 1.53% for ABE,

respectively. In the following section, letter “N” indicates the new regression models derived from this study and “E” indicates the existing models that were developed by other researchers. For instance, N1 indicates the new regression model 1. Excluding N9 and N10, the rest of the new regression models have better  $R^2$  values ( $>0.85$ ) than the previous models. One possible reason for relatively high  $R^2$  value is that only one subclass of fuel (PW samples) is being used. Sheng and Azevedo (2005) had a similar explanation for why their  $R^2$  value was very low ( $<0.85$ ) because a wide range of biomass species were selected and compromised the accuracy of estimation. This infers that considering only PW samples could improve the accuracy of HHV prediction.

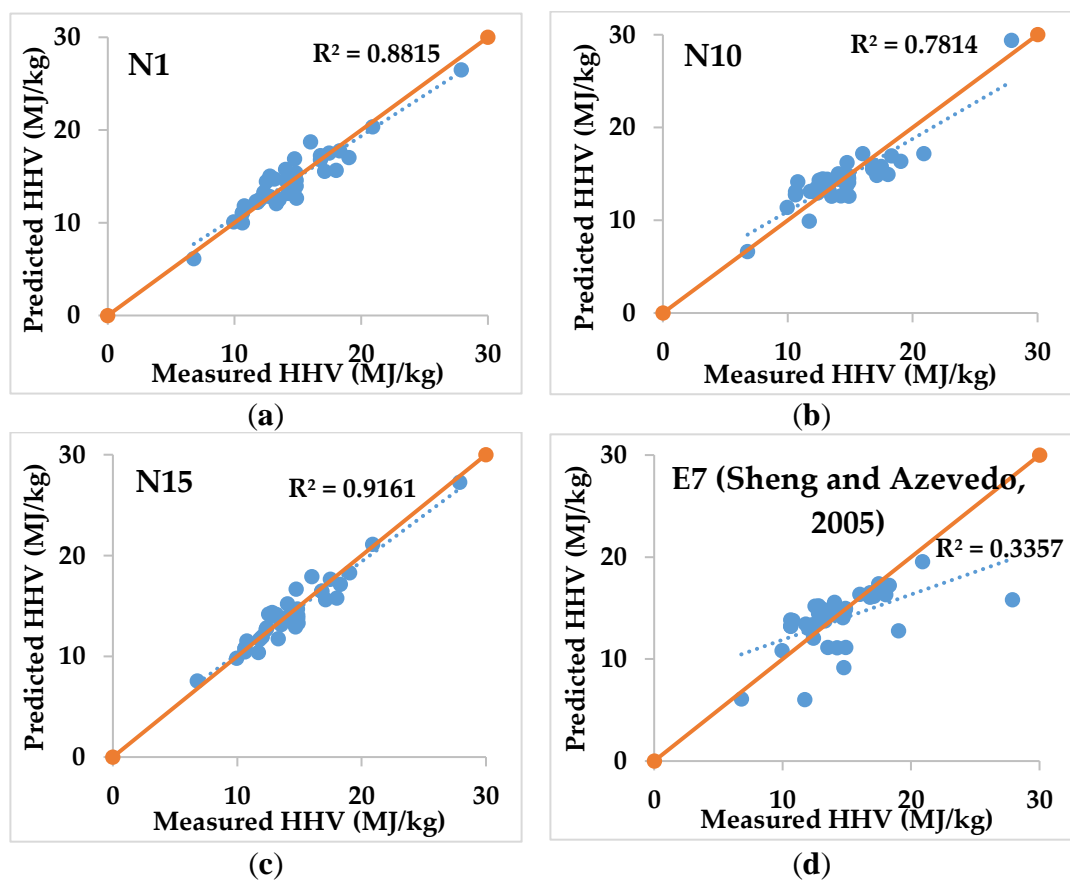
According to previous studies, Cordero et al. (2001) identified a simple equation based on proximate analysis (VM and FC) that could predict the HHV of lignocellulosic materials as well as char coals. Yin (2011) also found that a simple empirical equation based on proximate analysis (VM and FC) is sufficient for estimating the HHV of biomass. However, consideration of only two components (VM and FC) of proximate analysis in N2 has lower  $R^2$  value and higher estimation errors than N1, where all three proximate analysis components are included for PW samples. This indicates that a proximate-based regression model in HHV predictions of PW samples should consider FC, VM and ash content. Parikh et al. (2005) and Nhuchhen (2012) used a similar approach and concluded that developed models with all three components of proximate analysis are required to lower estimation errors. In Table 3.5, AAE in N1 to N8 is also observed to be lower than N9 and N10 (about 3%). Since both FC and ash content are applied as quadratic in both N9 and N10, while at least one linear correlation (either FC or ash) are included in N1 to

N8, it concludes that the multiple linear regression model of all three components of proximate analysis (N1) is the most accurate regression model among N1 to N10.

In further refining the steps (derivation of N11), polynomial relationships (quadratic and cubic) with VM are added to the simple multiple linear regression model (N1) because the observation from Figure 1b identified as the linear model for VM may not represent the most appropriate solution to accurately estimating the HHV of PW samples. This addition shows a further increment of  $R^2$  and a reduction of estimation errors. In addition, N12, N13 and N14 are proposed to compare the interaction effect between two proximate components. Even though the interaction effect provides a small contribution in reducing the estimation errors, a significant interaction effect of FC and ash has been identified. Therefore, N15 is developed by combining the simple multiple linear regression model (N1), the polynomial terms of VM (quadratic, cubic), and the best interaction effect (FC and ash). The best-fit regression model (N15) has the highest  $R^2$  in 91.62%, lowest AAE in 5.98%, and the lowest ABE in  $-0.35\%$ . This suggests that consideration of a polynomial dependence of VM as well as interaction effects of FC and ash can improve the accuracy of predicting the HHV of PW samples.

As shown in Figure 3.3, the comparison between experimental and predicted HHV results from new regression models (N1, N10 and N15) as well as three existing proximate-based models (E7, E14 and E17) are plotted by using the sample data points (Sample #1–37). Figure 3.3, d–f indicate that the predicted HHV from existing proximate-based models are far away from the diagonal line of  $HHV_{\text{predicted}} = HHV_{\text{experimental}}$  (orange lines in Figure 3.3) and therefore not applicable in predicting the HHV of PW samples. On the other hand, the results show most of the estimated HHV results from new regression models (N1, N10

and N15) are close to the line of  $\text{HHV}_{\text{predicted}} = \text{HHV}_{\text{experimental}}$ , indicating good accuracy for HHV predictions of PW samples. The results further confirm that the new regression models have better accuracy than existing proximate-based models in predicting the HHV of PW samples. It is especially apparent that the predicted points from the best-fit regression model (N15) are close to the measured values while slightly over-predicting or under-predicting the HHV at different points in the curve.



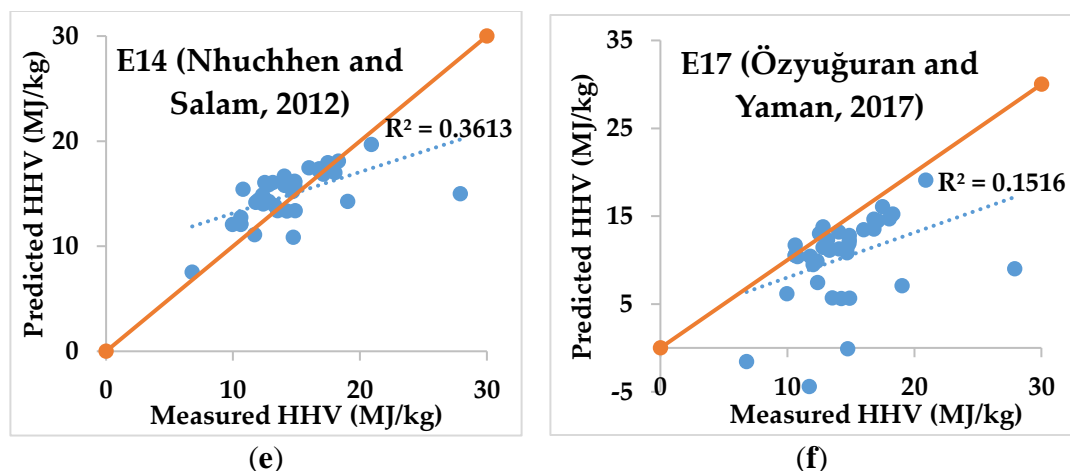


**Figure 3.3: Comparison between Predicted and Experimental HHV Results**

The validations are carried out for the 15 new regression models to ensure the compatibility with other PW samples with different characteristics. As shown in Figure 3.4, the AAE and ABE of 15 new regression models are calculated by using additional six samples (#38–42, #49) and presented by the bar chart. Results indicate new regression models have an AAE of 7.81 to 9.57% and ABE of 3.37 to 7.21%. Both AAE and ABE are lower than 10% which infer that new regression models can be used to estimate the HHV of PW samples from proximate analysis data with high accuracy. There is no relationship between each bar in the graph. Each bar represents the estimation error for each developed regression model (This study develop 15 different models based on different relationship between proximate analysis components and HHV).

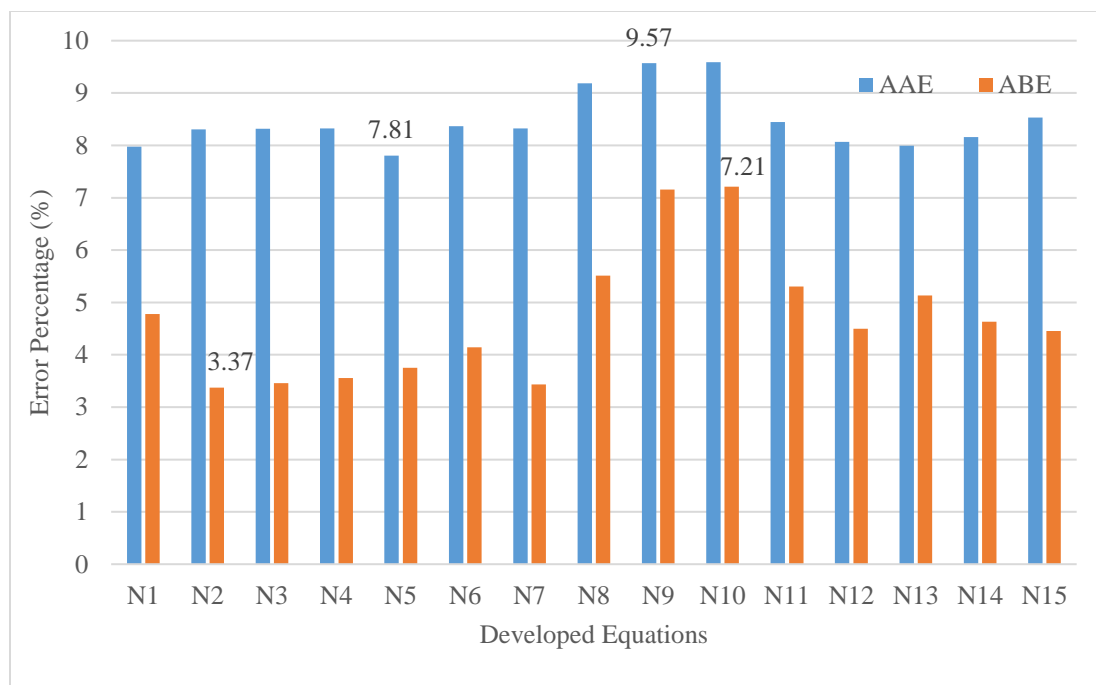


**Figure 3.4: Summary of AAE and ABE of New Developed Models**

Detailed ABE and AAE results of existing proximate-based models (E1 to E17) are further calculated using the same data points (#1–37) to identify if the existing models may be able to predict the HHV of poultry litter. Overall, the results in Figure 3.5 indicate that the new regression models (N1, N15) have lower estimation errors than existing proximate-based models (E1 to E17). It is not surprising that the resulting estimation errors from existing proximate-based are very different because the coefficients of the formula and constituent of proximate analysis are considerably different for each case. Three existing proximate-based models, E5, E11 and E15, are excluded due to extremely large estimation errors compared to the other models. AAE of existing models, E2 (coal), E3 (biomass) and E17 (biomass) is overestimated compared to the measured HHV (AAE > 20%) because they were developed for coal and biomass samples. Raw materials of biomass and coal were selected from a wide range of species and are expected to cause large variations. In addition, the existing proximate-based model for subclass of fuels, E6 (municipal solid

waste) and E9 (sewage sludge), also have larger AAE values (>25%) due to existing proximate-based models for one specific subclass fuel (e.g., municipal solid waste, sewage sludge) that are not appropriate for the other subclass of fuel (i.e., PW). It was found that the ABE of E1 (-13.48%) and E17 (-15.09%) is negative value. These negative results mean that the estimated HHV for these two models are lower than the measured HHV from experiment. However, relatively low AAE and ABE prove that the new regression models can generally have higher accuracy than the existing proximate-based models in HHV predictions of PW samples. Among the 15 new regression models, the simple multiple linear regression model (N1) has a  $R^2$  value of 88.15% for predicting HHV of PW samples. The best-fit regression model (N15) has the highest  $R^2$  value of 91.62%, lowest AAE at 5.98% and provides a marginal lower estimation at just 0.35%, further validating the model's capability in predicting the HHV of PW samples.

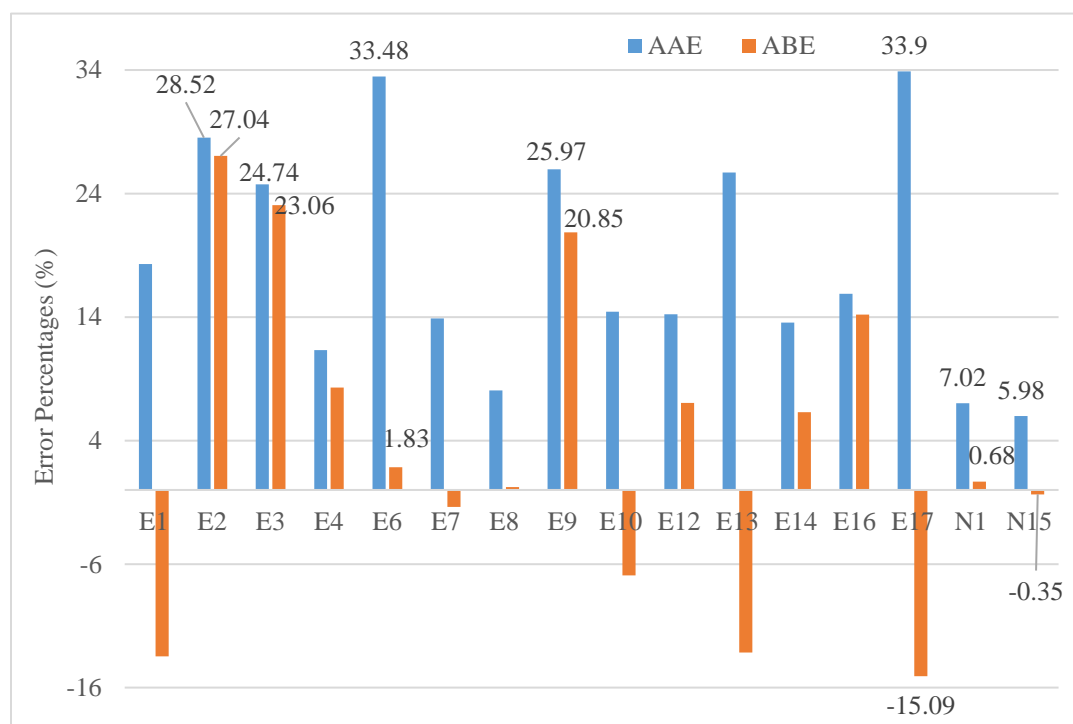


**Figure 3.5: Comparison of Estimation Errors between Existing Proximate-based Models (E1–E17) and New Regression Models (N1, N15)**

In this study, 48 poultry waste sample data were collected from different sources to analyze and characterize fuel properties. The correlation between ultimate and proximate components and HHV were plotted to investigate the relationship between fuel properties and HHV. Results show that ultimate analysis data has a better relationship with HHV than proximate analysis data. However, proximate-based regression model is developed to predict HHV of PW samples because it is relatively simple and cheap to perform in any laboratory with limited resources. Results show that the simple multiple linear regression model (N1) compromise all proximate analysis components. Results also show that the polynomial terms for VM, as well as interaction effects of FC and ash, are necessary for the best-fit regression model (N15) to further lower estimation errors. In addition, these new regression models for poultry waste samples provide better prediction power than the existing proximate-based models (E1 to E17) for other materials. Therefore, this new regression models can be an excellent tool for predicting the HHV of PW and does not require any expensive equipment that measures HHV directly or predicted from elemental compositions. In future study, more various farm samples and powerful tools (e.g., data mining, neural networks, machine learning) will be adopted to reduce errors and provide much more robust HHV prediction results for both poultry litter and other biomass fuels.

## **Chapter 4. Evaluation of Electricity in the Stirling Engine-based Biomass Conversion System**

In response to the fossil fuel depletion issue, high water consumption and adverse environmental issues found in current power plants, the Stirling engine-based biomass conversion (SEBC) system was designed, fabricated, and developed with integration of the 1 kW Stirling engine (SE) and an existing advanced lab-scale swirling fluidized bed combustion (SFBC) prototype. In Chapter 4, the effects of operating factors on performance (e.g., electricity output, temperature profiles and emissions) of the SEBC system during the poultry litter and natural co-combustion process was analyzed and evaluated with statistical methods.

### **4.1 Materials and Methods**

#### **4.1.1 Apparatus and Experiment Setup**

As shown in Figure 4.1, the SEBC system was designed, fabricated, and developed by the Center for Advanced Energy Systems and Environmental Control Technologies (CAESECT) research group at Morgan State University. This lab-scale SEBC system includes Stirling engine (SE), advanced SFBC, fuel feeding system, air supply system, cyclone system, among other instrumentations. The cylinder combustion chamber of 1500mm height with an inner diameter of 200 mm was constructed by stainless steel. The screw-type feeder (Acison, USA) was used to feed materials into the chamber at a height of 228.6 mm. A speed motor controller was used to change the fuel feeding rate by changing the rotational speed (rpm) of the screw feeder's motor. The combustion air was supplied by two streams, PA and SA. Primary air (PA) was injected from a 1/8 hp blower through the wind box and PA distributor, which allowed PA to act as both fluidization and combustion air. Secondary air (SA) was injected symmetrically through four nozzles above

the PA distributor at three different heights (650 mm, 850 mm and 1100 mm) and from a 1/125 hp blower. Control value along with voltage regulators was used to modulate fan speed and ultimately control the PA and SA flow rates. The 1kW free piston SE (E1.4B-00001) from the Microgen Company was integrated into the existing lab-scale SFBC system at a height of 406.4 mm to produce electricity during poultry litter and natural gas co-combustion process. The cooling system for the SE consisted of a radiator, cooling fan, and hot water pump for heat rejection.

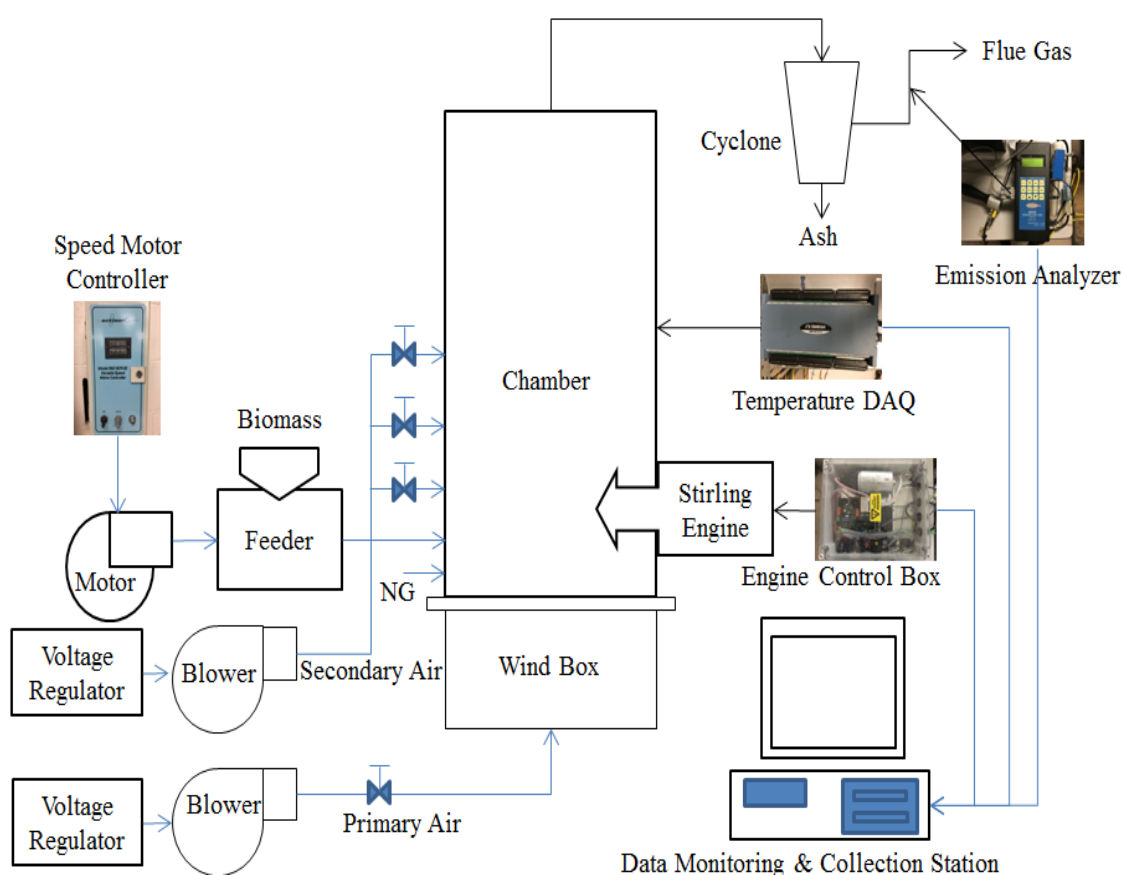


**Figure 4.1: Schematics of the SEBC System and Instrumentations**

At the beginning of the experiment, small amount of PA and natural gas was provided at a height of 120mm above the PA distributor to preheat the chamber. After the chamber environment stabilized between 595 °C and 610 °C at a height of 431.8 mm, the waste biomass materials were fed into the chamber from the volumetric screw feeder at

different speeds with the speed motor controller. Air flow rates were supplied according to the experimental levels. Co-combustion of poultry litter and natural gas was conducted in the SEBC system. SE was used to produce the electricity through the engine control box to the grid (220-230 volts).

For the performance measurement, six (6) rugged heavy-duty transition joint K-type thermocouples (Omega TJ36-CASS-18U-6), along with a data logger (Omega OMB-DAQ-2416), were installed to measure, monitor, and collect real-time axial temperature changes along the combustion chamber at a height of 177.8 mm, 431.8 mm, 635 mm, 889 mm, 1143 mm, 1574.8 mm above the PA distributor, respectively. At the end of each run, gas samples were collected after the cyclone system. The emission analyzer (Enerac 500), along with ENERCOM software, were used to record and analyze the combustion efficiency and the concentration levels of major gaseous emissions (e.g., CO, NO<sub>x</sub> and SO<sub>2</sub>) found in the flue gas sample. The head control temperature and the flow rate were measured by the mounted K-type thermocouple and water flow sensor, respectively. In addition, the electricity output was measured, calculated, and monitored by using an engine control box, along with the Microgen Test Rig Data Viewer. All collected data on electricity, temperature, and emissions were then monitored and stored into the data monitoring and collection station for statistical analysis and system evaluation. For the particulate matter (PM) collection and measurement, the collection filter (Quartz Microfiber Filters (Whatman<sup>TM</sup>, 203mm\*254mm) and weight measurement (Micro-scale, High Resolution Balance, 600g, 0.01 g) were used. PM samples were collected after the cyclone and before exit the chimney. In this study, PM filter was inserted to collect PM particles during the combustion test at duration of 2 hrs.

### 4.1.2 Materials

The biomass fuel used in this study was poultry litter (where the bedding material was sawdust). The poultry litter samples were collected from a local poultry farm (Bethel Farms, Salisbury, Maryland, USA). The waste biomass fuels were characterized by proximate analysis (as-received) and used as dry basis for the ultimate analysis. The proximate and ultimate analysis results of these fuels are presented in Table 4.1. From the analysis results, it was clear that the poultry litter sample reflected high levels of both moisture (around 21%) and ash content (about 19%), which may result in lower heating value than the coal sample.

**Table 4.1: Proximate and Ultimate Analysis of Poultry Litter**

Fuel	Poultry Litter
<b>Proximate Analysis (as received, wt%)</b>	
Moisture	21.20
Volatile Matter	50.40
Fixed Carbon	9.44
Ash	18.96
<b>Ultimate Analysis (dry, wt%)</b>	
Carbon (C)	26.88
Hydrogen (H)	4.44
Oxygen (O)	24.80
Nitrogen (N)	3.28
Sulfur (S)	1.04
Ash	18.96
Heating Value (kJ/kg)	11,295

### 4.1.3 Statistical Methods

In order to identify the effect of operating factors on system performance, the design of experimental method and statistical tool were used. As shown in Table 4.2, the control factors for this study were PA flow rate, SA flow rate, and fuel feeding rate. Each control factor was associated with their individual levels. The fuel feeding rates were characterized in kilograms per hour (kg/hr) across different various rotational speeds (rpm).

Measurements of the voltage regulator in percentage were characterized in cubic feet per minute (cfm) by using the Fluke Air Meter and subsequently converted into cubic meter per hour (m<sup>3</sup>/hr). Air supply was varied and the average air flow rate at the individual level was calculated and summarized in Table 4.2.

**Table 4.2: Factors and Individual Levels for Mixed Level Factorial (2<sup>1</sup>×3<sup>3</sup>) Design**

Levels	PA, % (m <sup>3</sup> /hr)	SA, % (m <sup>3</sup> /hr)	Fuel Feeding Rate, rpm (kg/hr)
Low	32 (20.38)	15 (10.19)	55 (7)
Medium		17(16.98)	65 (10)
High	34 (35.66)	25 (33.96)	75 (13)

Depending on the number of factors and its level, a 2<sup>1</sup>×3<sup>2</sup> mixed level factorial design approach was used to evaluate the system's performance. The most interesting response variables turned out to be the temperature captured near the SE head (T1 at height of 431.8 mm), flue gas temperature right above the chamber (T6, at height of 1574.8 mm), and the gases being emitted (CO, NO<sub>x</sub> and SO<sub>x</sub>). The effects of these operational factors were also evaluated on the electricity output. Analysis of variance (ANOVA) test, contour plot, and statistical software (Minitab Version 17) were used to analyze the significance of these factors and their interactive effect on the response variables. Statistical significance level was set at 5% and compared with P-value to consider statistically significant for this study.

## 4.2 Results and Discussion

### 4.2.1 Electricity Outputs

The electricity output was one of the most important performance factors in developing SEBC system. Experimental results indicated that the electricity output level was determined by the engine head temperature as well as the water inlet flow rate. The

temperature difference between the water inlet and outlet was kept at 3-5°C. The electricity output at various head temperature and water flow rate is provided in Figure 4.2. The results of these tests indicated that higher head control temperature and higher electricity output were achievable. The maximum power output is 905 Watts at a head temperature of 584 °C and the water flow rate at 13.1 L/min. Compared with other water flow rates, the highest electricity output was measured at a water flow rate of 13.1 L/min. When the engine head temperature was lower than 350°C, the minimum threshold of electricity output was found at a maximum water flow of 19.5L/min. However, when the temperature eclipsed 400°C, the minimum threshold of electricity output was found at a water flow of 9 L/min. These results indicated that high (19.5L/min) or low (9L/min) water flow rate was not sufficient for the electricity output. The SEBC system required a certain water flow rate (13.1 L/min) to reject a enough heat and thereby improve the overall system performance.

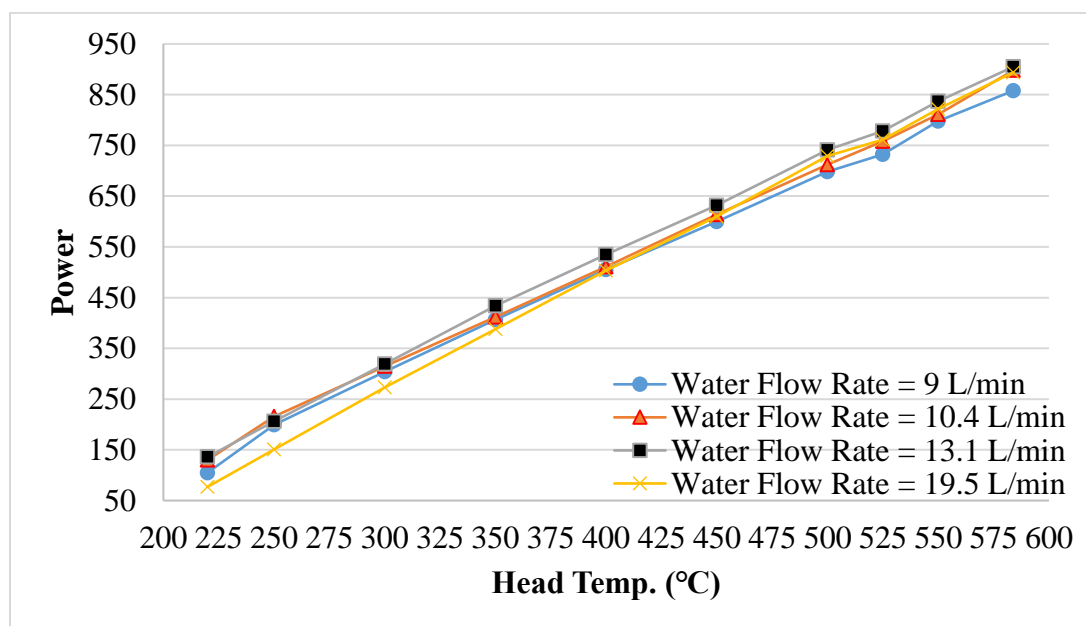


**Figure 4.2: Power out Vs. Head Temperature at Various Water Flow Rates**

#### 4.2.2 Temperature Profiles

Table 4.3 shows the mixed level design worksheet, which shows the axial temperature results at different heights, along with various PA flow rates (A), SA flow rates (B) and fuel feeding rates (C). All the experimental scenarios were conducted randomly based on the mixed level design sheet. In this study, the temperatures found at a height of 431.8 mm and 1574.8 mm had the most interesting response factors because their portion of heat output was used to produce electricity and ultimately hot water (in Chapter 5). This allowed for space heating to be generated by different heat exchanger applications. The temperature profile indicated that the chamber internal temperature was in the wide range of 712°C-962 °C when measured at a height of 431.8 mm. The hot flue temperature ranged from 304°C to 517 °C when measured at a height of 1574.8mm.

**Table 4.3: Summary of Temperature Distribution in Combustion Chamber**

<b>A (PA, %)</b>	<b>B (SA, %)</b>	<b>C (Feeding Rate, rpm)</b>	<b>T0 (°C)</b>	<b>T1 (°C)</b>	<b>T2 (°C)</b>	<b>T3 (°C)</b>	<b>T4 (°C)</b>	<b>T5 (°C)</b>
34	25	55	812	890	797	682	590	497
32	17	55	780	851	783	658	548	408
34	15	55	852	948	904	773	605	451
34	17	75	885	929	920	797	668	486
34	15	65	802	866	740	662	515	438
32	25	75	863	903	875	742	637	459
32	15	65	705	755	656	558	438	305
32	17	75	785	838	839	748	633	465
34	17	65	820	895	756	658	521	408
34	25	75	914	962	891	743	644	517
32	25	55	765	841	819	707	531	429
32	25	65	785	860	827	685	582	424
34	17	55	832	938	839	757	612	470
32	15	55	652	712	646	523	437	304
34	15	75	856	907	903	798	672	517
32	15	75	811	868	852	742	621	445
32	17	65	831	870	829	696	584	421
34	25	65	792	857	767	646	556	467

The ANOVA results are shown in Table 4.4 and indicate that the PA was a significant ( $P\text{-value}=0.018<0.05$ ) factor in controlling the temperature (T1) near SE as well as producing efficient electricity from SE.

**Table 4.4 Summary of ANOVA Table for T1 (H =431.8 mm)**

Source	DF	Adj SS	Adj MS	F-value	P-value
<b>A</b>	1	26760	26760	14.85	0.018
<b>B</b>	2	7575	3787	2.10	0.238
<b>C</b>	2	8328	4164	2.31	0.215
<b>A*B</b>	2	6781	3390	1.88	0.265
<b>A*C</b>	2	5208	2604	1.45	0.337
<b>B*C</b>	4	4936	1234	0.68	0.639
<b>Error</b>	4	7206	1802		
<b>Total</b>	17	66793			

*Abbreviations: DF, Degree of freedom; Adj SS, Adjust sum of square; Adj MS, Adjust mean square*

At feeding rate of 10 kg/hr for various PA and SA flow rates, the detailed axial temperature distribution along with combustor height are shown in Figure 4.3. The highest temperature was found to be between the fuel injection and first layer of the SA injection (431.8 mm). Experimental results show that the temperature varied typically in the range of 755°C-895°C. With the injection of PA=20.38m<sup>3</sup>/hr, increasing SA injection was found to increase its temperature at a height of 889 mm (from 558°C to 705°C), 1143mm (from 438°C to 592°C), and 1574.8 mm (from 320°C to 424°C). This observation inferred that the temperature increased most significantly when above the SA injection area because of SA injection has a contribution in burning unburned fine particles and prolonging the particle residence time (Zhu and Lee, 2005). However, in the case of PA=35.66m<sup>3</sup>/hr, increasing SA=17m<sup>3</sup>/hr, to SA=34m<sup>3</sup>/hr was found to decrease temperature at a height of 889 mm, 1143mm, and 1574.8 mm, possibly due to the strong PA flow rate bring a relatively high quantity of unburned sawdust particles to the top of chamber.

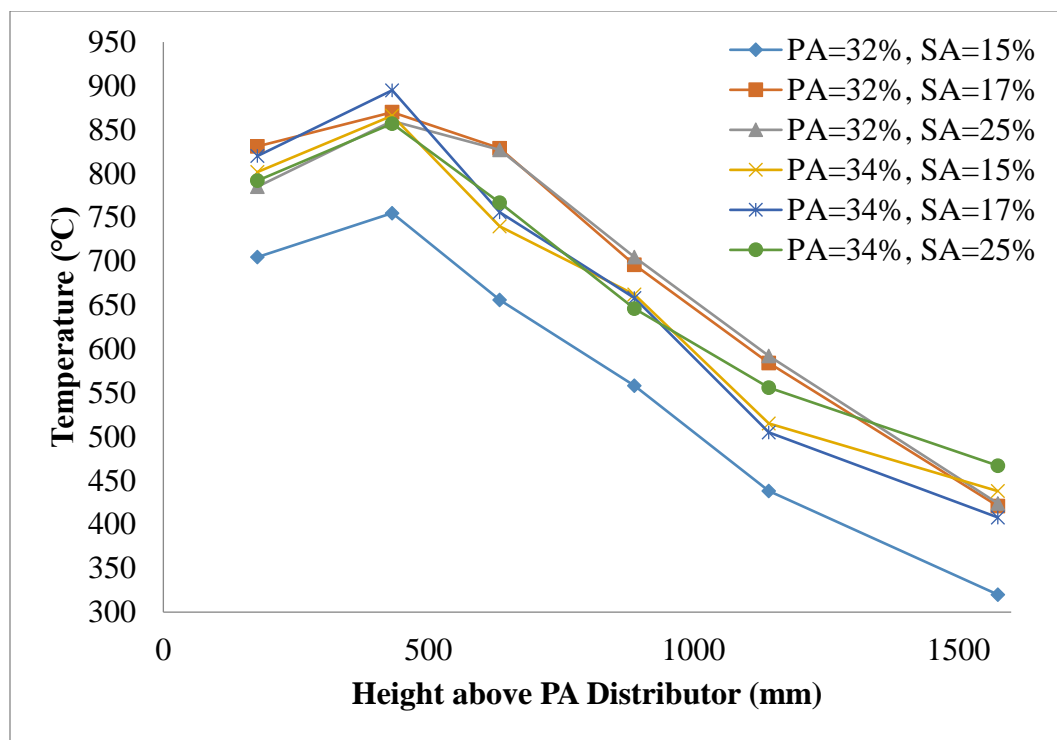


**Figure 4.3: Axial Temperature Profiles at Various Combustor Heights**

#### 4.2.3 Emissions Performance

With respect to the  $\text{NO}_x$  emissions, the ANOVA results suggested that the PA (P-value=0.006) was more significant than both the SA flow rate (P-value= 0.155) and fuel feeding rate (P-value=0.322). In this study, the  $\text{NO}_x$  emissions were measured to be between 31 ppm and 140 ppm across various operating conditions. The system had relatively low  $\text{NO}_x$  emissions when operating temperature was lower (700-900°C) in the combustion chamber, which significantly limited the emission of thermal  $\text{NO}_x$  and prompt  $\text{NO}_x$  (Duan et al., 2013). It was found that the  $\text{NO}_x$  emissions were more likely to be reduced when bed temperature and  $\text{O}_2$  concentration in the bed are both reduced by the adjustment of PA injection (Kuprianov et al., 2011; Suksankraisorn et al., 2004).

For CO emissions, the ANOVA results indicate that the SA (P-value=0.008) was a more significant factor than the PA flow rate (P-value= 0.021) and fuel feeding rate (P-

value=0.447) at different operating conditions. Figure 4.4 shows the concentration of CO emissions in the flue gas in relative to other total flow rates. The concentration of CO varied from 15 ppm to 2090 ppm. In order to reduce the maximum CO concentration value (1048 ppm) by half, the total air flow rate needed to exceed  $45.85\text{m}^3/\text{hr}$ . These results concluded that with an increase of total air flow rate to a threshold, it is able to create EA and provide enough oxygen during combustion process to mitigate CO formation and thereby decrease the CO concentration (Permchart & Kouprianov, 2004; Varol et al., 2014b). It confirms the importance of EA in the poultry litter and natural gas combustion process.

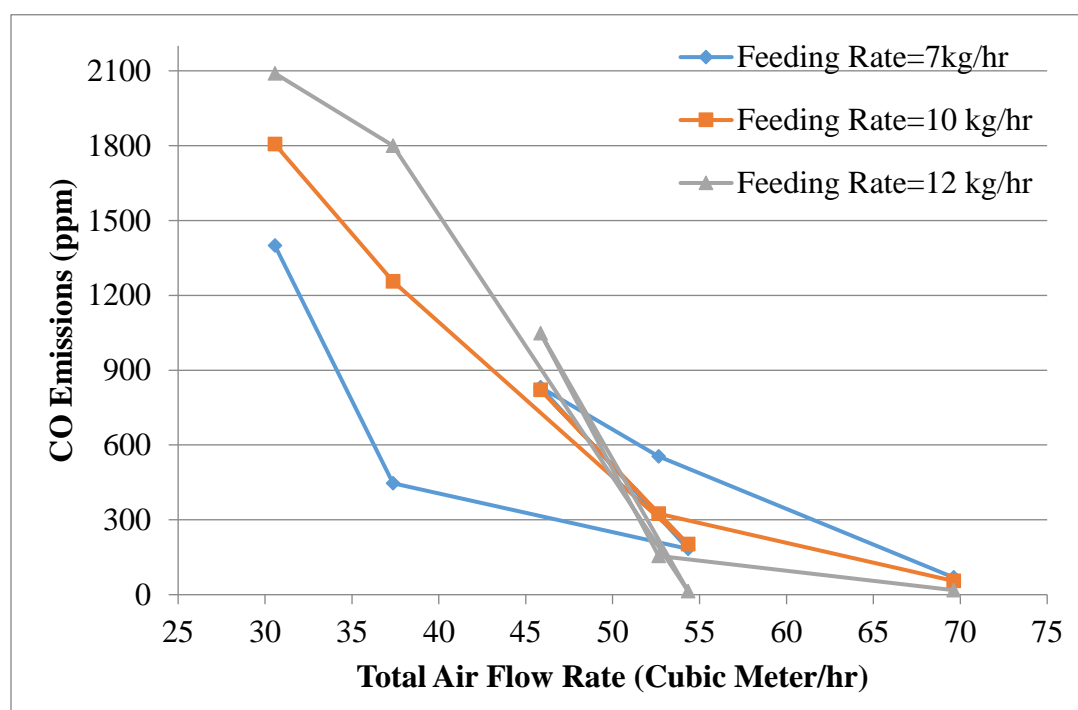


**Figure 4.4: Total Air Flow Rate Vs. CO Emissions**

Then, the effect of EA ratio on emissions were further investigated. Figure 4.5 shows the effect of EA ratios on CO, NO<sub>x</sub>, and SO<sub>2</sub> emissions in the range of EA, between 0.44 and 2.28 at a feeding rate of WBM=7kg/h.

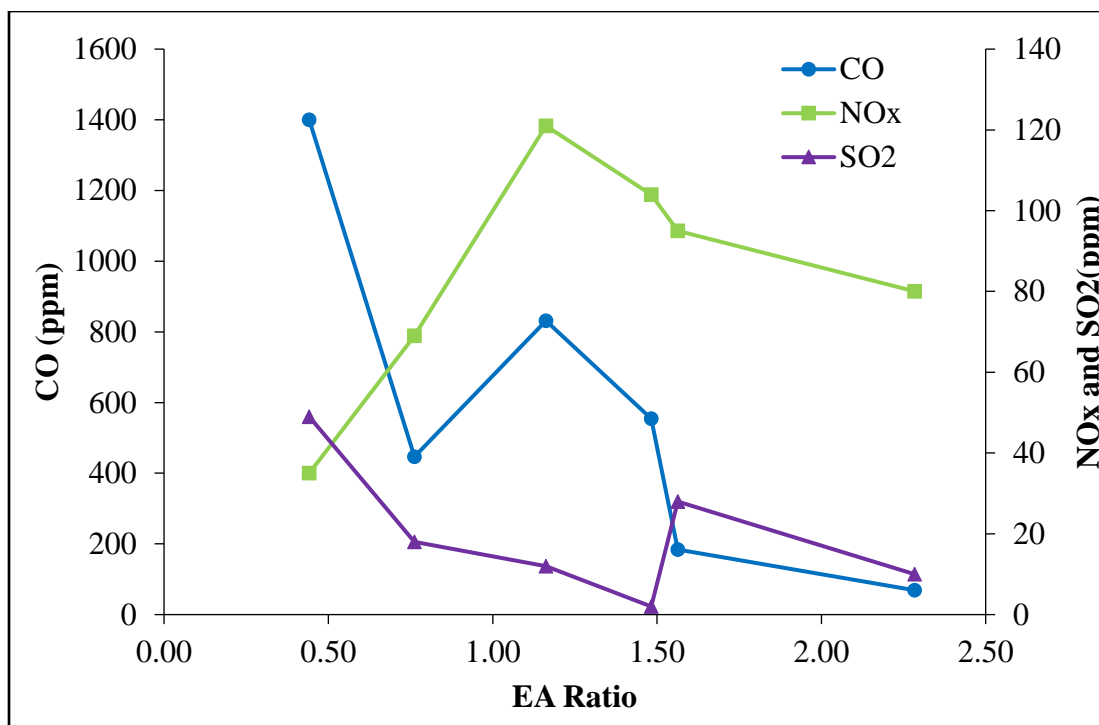


**Figure 4.5: Effect of EA on CO, NO<sub>x</sub> and SO<sub>2</sub> Emissions**

Results indicate that the EA ratio had minor effect on SO<sub>2</sub> emissions. However, the EA ratio is shown to have a bigger role in reducing CO emissions, with exception of a slight increment when the EA ratio=1.16. EA exhibited roughly 570-1330 ppm of CO reduction by enhancing the rate of CO oxidation into CO<sub>2</sub> (Kuprianov et al., 2011; Duan et al., 2013). Fang et al. (2004) and Kuprianov et al. (2011) also concluded that EA is an important factor in reducing CO emissions during biomass co-combustion process. NO<sub>x</sub> was found to have increased with increasing EA between 0.44 and 1.16. This result is concordant with similar studies that show increased levels of NO emission when there is an increase in the EA ratio (Duan et al, 2013). This phenomenon can perhaps be explained by the fact that an increased oxygen concentration in EA may have increased the chance of converting fuel-N into NO<sub>x</sub> emissions (Madhiyannon et al., 2010). On the other hand, NO<sub>x</sub> was found to have decreased whenever the EA ratio was between 1.16-1.48. When the EA ratio was greater than 1.56, the higher EA ratio exhibited more NO<sub>x</sub> reduction, as

well as CO and SO<sub>2</sub> emissions. However, the elevated EA can be attributed to an initial increase and subsequent deterioration of combustion behavior caused by an increase in heat loss with waste gas (affected by a significant volume of EA; Zhu et al., 2005; Topal et al., 2012). Therefore, the optimal EA ratio is suggested to be within the range of 1.16-1.48 for minimizing all three emissions during PL and NG co-combustion processes.

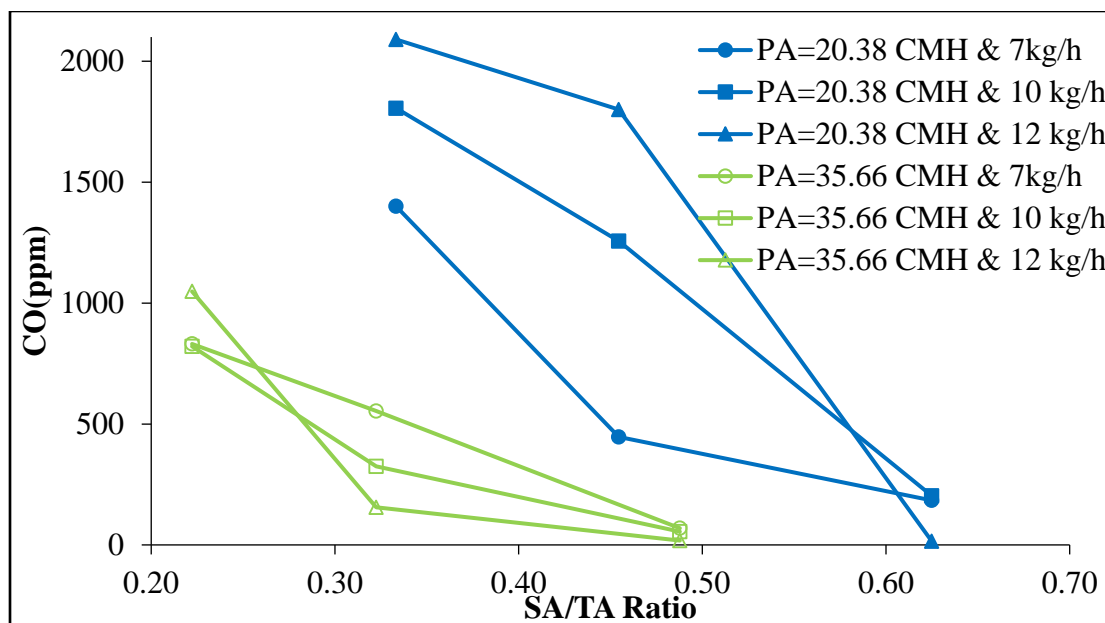


**Figure 4.6: Effect of SA/TA on CO emissions**

Figure 4.6 shows the effect of SA/TA ratios on CO emissions at various PA flow rates and feeding rates. For PA of 20.38m<sup>3</sup>/h (cubic meter per hour, CMH), CO emission levels reduced with the increase in SA/TA ratio from 0.22 to 0.49. Similar reduction tendencies were discovered at PA at 35.66m<sup>3</sup>/h when SA/TA ratio increased from 0.33 to 0.62. These results strongly suggested that SA was significantly responsible for the reduction of CO emissions. However, some studies report that SA/TA (or air staging) has a relatively weak role in determining CO emission levels during biomass combustion (Fang et al., 2004; Chyang et al., 2007; Kuprinov et al., 2011). Basically, conflicting conclusions may be explained by different SA injection locations, and the varying number of SA layers.

In previous studies, SA was injected into a splash zone (Kuprinov et al., 2011), or freeboard by using one layer of SA (Fang et al., 2004) or two layers of SA (Chyang et al., 2007). Such studies concluded that three layers of SA injection into freeboard of the lab-scale SFBC at a height of 650 mm, 850 mm, and 1100 mm can reduce CO emission levels from promotion of oxygen distribution, swirling effects, and increased residence time.

In addition, the effect of mixing ratio on emissions were further studied. Figure 4.7 shows relationship between mixing ratio and average concentration levels of CO, NO<sub>x</sub>, and SO<sub>2</sub> emissions across six different scenarios. A clear increase in mixing ratio (by heat content) of PL from 1.45 to 2.49 can be seen, as well as notable increases in CO emissions, from 580.3ppm to 854.3 ppm. This may be caused by the following reasons: (1) Higher biomass share in a dense zone creates a reducing atmosphere that promotes CO emissions, (2) Higher levels of volatile matter released from biomass increases the hydrocarbon concentration and therefore prevents further CO oxidation, (3) Unburned volatile matter from low density sawdust contributes as an additional source of CO emissions (Sun et al., 2013). The increase in mixing ratio reduces NO<sub>x</sub> emissions because the presence of CO promotes the reduction rate of NO emissions by char catalysis (Sun et al., 2013), and an increase in organic N fraction (e.g., NH<sub>3</sub>, urea) in PL can act as NO and ultimately reduce the formation of NO<sub>x</sub> (Li et al., 2008).

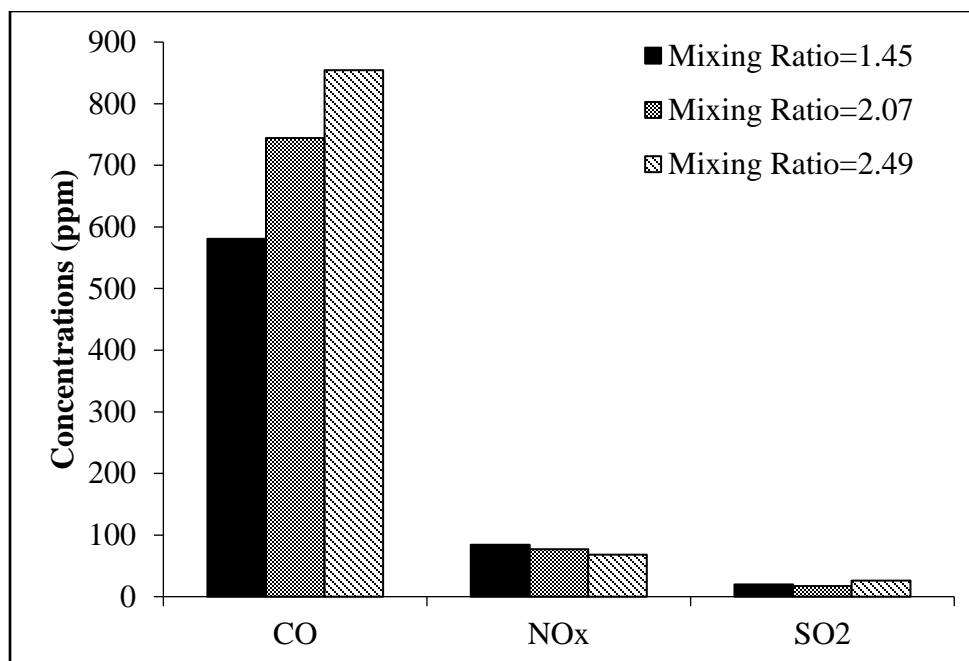


**Figure 4.7: Effect of Mixing Ratio on CO, NO<sub>x</sub> and SO<sub>2</sub> Emissions**

In this study, biomass co-combustion was observed to release relatively low emissions of SO<sub>2</sub> (1 ppm to 49 ppm) because both poultry litter have relatively small fuel-S content. The ANOVA results also indicated that PA (P-value = 0.041) was a more significant factor than the SA flow rate (P-value = 0.222) and fuel feeding rate (P-value = 0.323). Figure 4.8 shows the contour plot that graphs the relationship between PA and fuel feeding rate, as it relates to SO<sub>2</sub> emissions. An increase in fuel feeding rate was found to have higher emissions of SO<sub>2</sub>. This is due to an increased level of fuel-S in the fuel mixture as well as calcium present in ash act to reduce SO<sub>2</sub> in the flue gas through formation of CaSO<sub>4</sub> (Li et al., 2008; Abelha et al., 2003; Henihan et al., 2003). However, the PA flow rate was shown to have a significant effect on SO<sub>2</sub> emissions and relatively higher amounts of PA may be responsible for reducing SO<sub>2</sub> emissions down to 10 ppm at a fuel feeding rate of between 7-10 kg/hr.

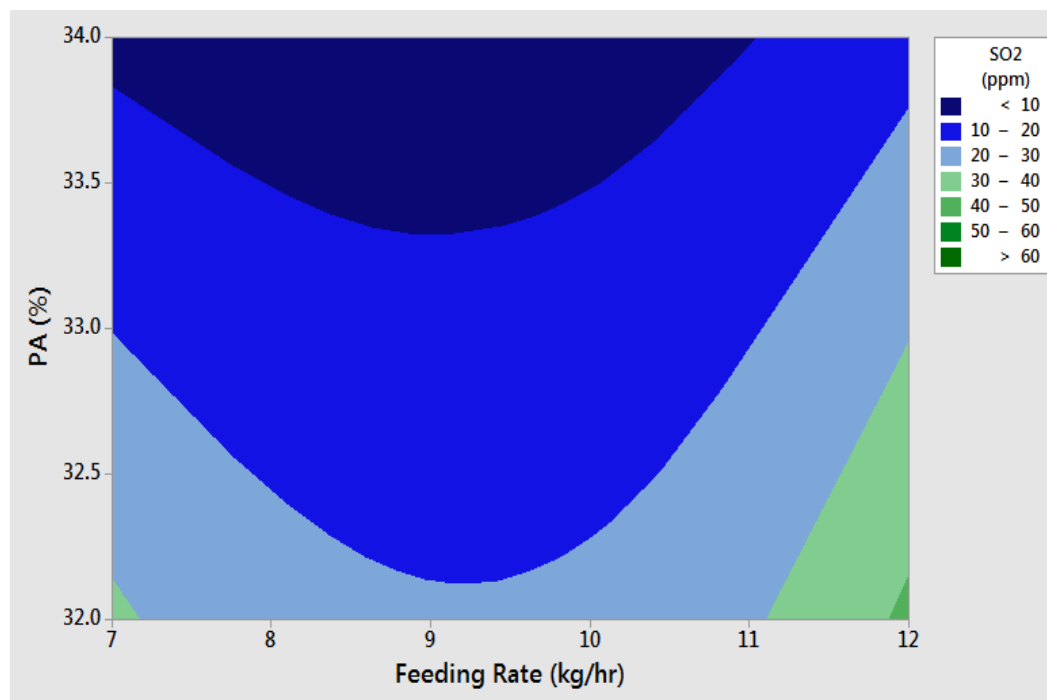


**Figure 4.8: SO<sub>2</sub> Emissions Vs. PA & Feeding Rates**

During the 2 hours test, the heating value of samples was 4856 Btu/lb and total heating value of sample was 168, 104 Btu at feeding rate of 17 lb/hr. Weight of collected PM samples are 0.00033 lb and calculated emission factor of PM particle is 0.002 lb/MMBtu. PM emissions results showed less than MD permitting thresholds of 0.35 lb/MMBtu.

In this chapter, the Stirling engine-based biomass conversion (SEBC) system was developed to study the electricity generation and emissions during poultry litter and natural gas co-combustion process. The effects of operating factors on electricity output, temperature changes, and emission performance were analyzed and evaluated with statistical methods, include mixed level factorial design and analysis of variance (ANOVA) method. Results indicated that maximum power output reached about 905 Watts at head temperature of 584 °C and water flow rate of 13.1 L/min. The PA flow rate was found to have a significant effect on the temperature (P-value = 0.018), NO<sub>x</sub> (P-value = 0.006) and

SO<sub>2</sub> (P-value = 0.041). Furthermore, the CO emissions (P-value = 0.008) was significantly affected by the SA flow rate. This study also showed that the SEBC system is possible to create electricity (close to 1kW) during poultry litter and natural gas co-combustion process with relatively low emissions (NO<sub>x</sub> ranges from 31-140 ppm, SO<sub>2</sub> ranges from 1 to 50 ppm and, CO emissions varies from 15-1048 ppm). PM emissions results showed less than MD permitting thresholds of 0.35 lb/MMBtu.

## **Chapter 5. Evaluation of Heat Generation by Using the Lab-scale Shell and Tube Heat Exchanger**

In the Chapter 4, electricity generation during the poultry litter and natural gas co-combustion process were evaluated. There is still large amount of residual heat in the hot flue gas during co-combustion can be used. In order to collect more residual heat from flue gas, this study focused to increase heat transfer coefficient by implementation of segmental baffle and twisted tubes in the lab-scale shell and tube heat exchanger (STHE) prototype. In the Chapter 5, the detailed steps in the design phase, fabrication phase, testing and evaluation of the lab-scale STHE prototype were included. Evaluation results indicated that the lab-scale STHE system can effectively collect residual heat during poultry litter and natural gas co-combustion process to generate hot water and provide space heating of the mobile trailer.

### **5.1 Methodologies**

#### **5.1.1 Design Phase**

During the design phase, the 2D and 3D lab-scale STHE porotype were completed. AutoCAD software was used to design each component of the 2D lab-scale STHE system based on the design requirements and constrains. The 2D design along with detailed dimensions (e.g. length, outer diameter, inner diameter, thickness) of shell, tube and segmental baffle are illustrated Figure 5.1 and Figure 5.2. Shell with a length of 28.5 inch is a large pressure vessel to carry one fluid. The inner dimeter of each tube is 0.625 inch to carry another fluid. In the baffle design, there are six holes with a diameter of 0.625 inch to provide support for the tubes.

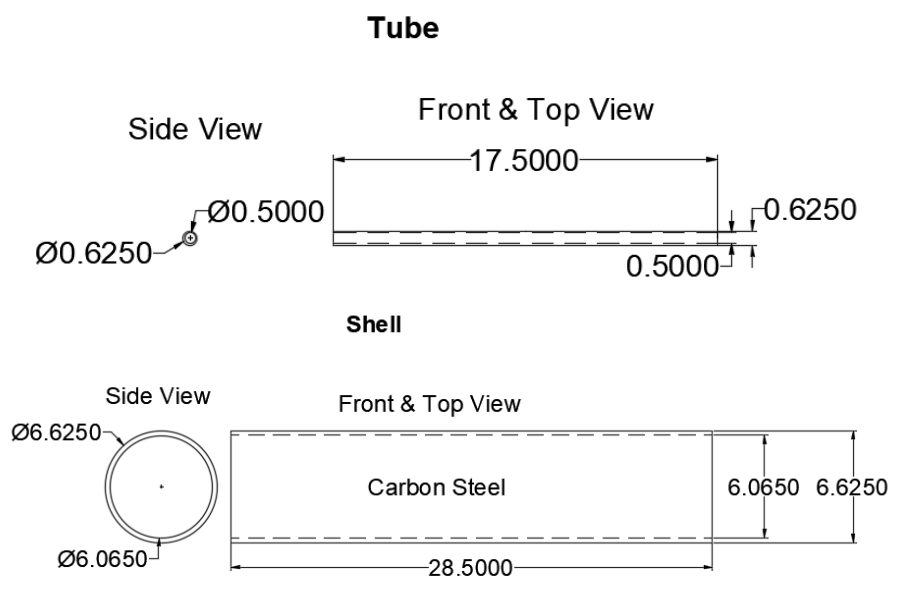


**Figure 5.1: 2D Design of Shell and Tube**

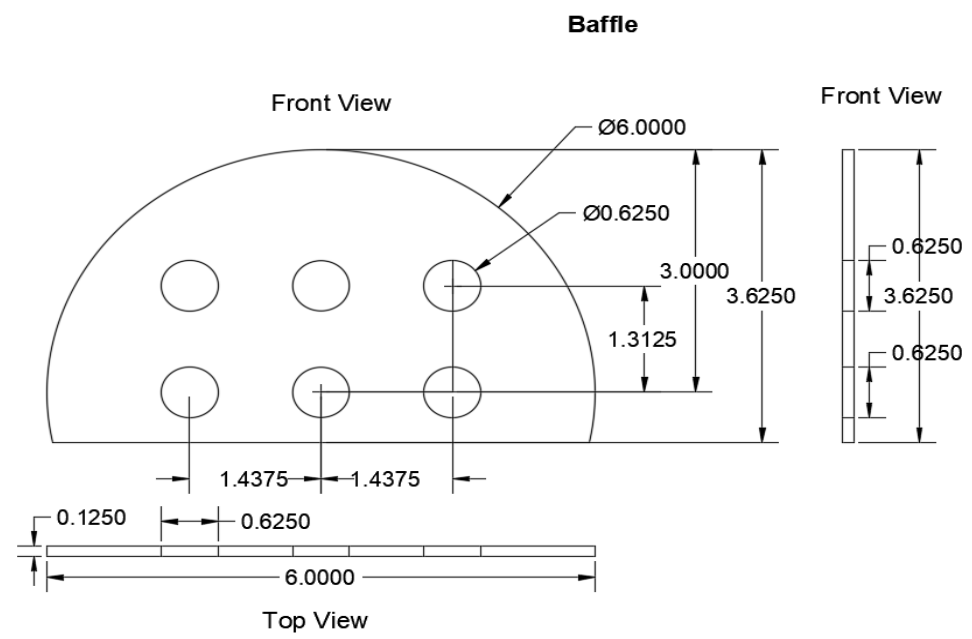


**Figure 5.2: 2D Design of Baffle**

As shown in Figure 5.3, there are two flanges were designed to make the proper connections. Circular flange was used to connect between the lab-scale STHE and cyclone while the rectangular flange was used to connect between the lab-scale STHE and



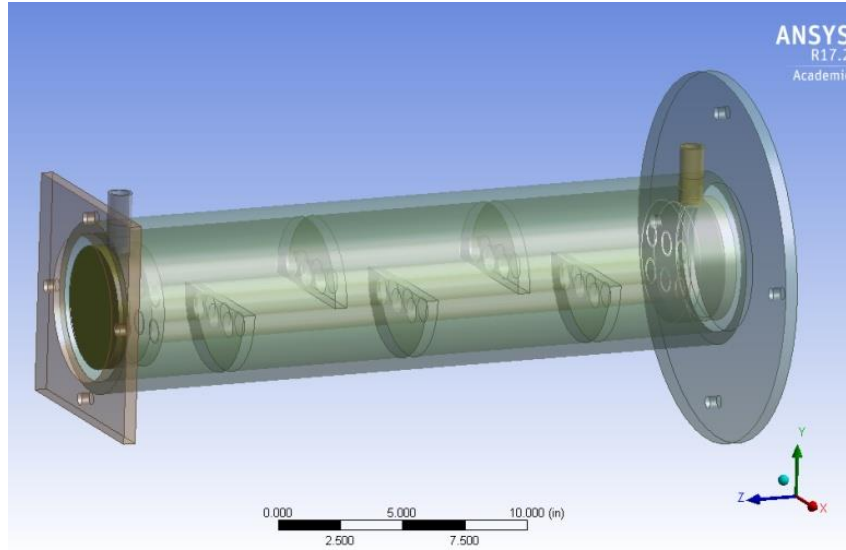


**Figure 5.4: Preliminary 3D Modeling of the STHE System**

Typically, the ends of each tube in the traditional STHE are connected to plenums (also known as water boxes) through holes in tube sheets. However, there is lack of larger copper water box and high cost to fabricate a customized copper water box. As shown in Figure 5.5, special water connection was designed in this study, connections between tubes were linked by using combination of various market available fittings. New design has a large heat exchanger area than the single water box to improve the heat transfer coefficient and solve the existing challenges of availability and cost. In addition, this study used one pass tube side due to the disadvantages of high investment and easily break for two pass heat exchangers.

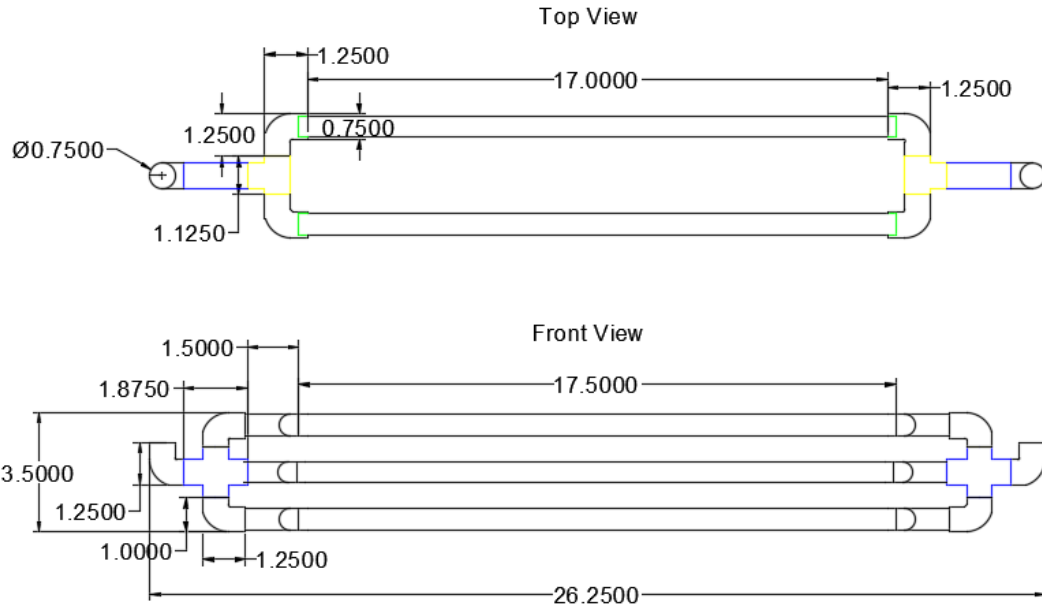


**Figure 5.5: 2D Design of Lab-scale STHE**

### 5.1.2 Fabrication Phase

During the fabrication process, materials for each component were carefully reviewed and selected based on requirements of heat transfer, individual characteristics (e.g. physical and chemical properties) as well as cost consideration. Hot flue gas from the co-combustion of poultry litter and natural gas was used as one fluid in the lab-scale STHE. Thus, the possible chemical reaction between flue gas compositions (e.g.  $\text{SO}_2$ ,  $\text{NO}_x$ ) and material surface should be considered during material selection.

As shown in Figure 5.6, tubes (copper, 0.625" outer diameter with 0.50" inner diameter), fittings (1/2 in.  $\times$  1/2 in. copper, 90° elbow (Everbilt), 1/2 in. Copper Tees, copper pipe cross (0.5", NIBCO, Cast Copper), aluminum plates (0.125" thickness, 12" length\*12" width), carbon steel pipe (6" schedule 40, 6.625" outer diameter, 6.065" inner diameter, 28.5" length), were selected as raw materials for tube, connections, baffle, and shell, respectively. Tools, such as pipe cutting tool, drill bits, hydraulic driller and plates cutter were used to precisely fabricated each component of the lab-scale STHE system.



**Figure 5.6: Raw Materials for SHTE Components**

As shown in Figure 5.7, manufacturing of flanges was performed by company (DS Pipe & Steel Supply, MD, USA). Standard size carbon steel pipe was acquired. The length, inner and outer diameter of shell are 28.5 inches, 6 inches and 7 inches, respectively. Welding between shell and flanges were performed by physical plant staff at Morgan State University.



**Figure 5.7: Flanges and Shell of the STHE System**

As shown in Figure 5.8, segmental baffles have four (4) circular holes for the tubes and a cut off opening for the shell side to change fluid flow path. Baffles are used to direct flow perpendicular to tubes in order to enhance transfer rate. In addition, baffle also used to support the tubes in order to prevent vibration. The length, inner and out diameter of straight copper tube are 23 inches, 0.625 inches and 0.5 inches, respectively. As shown in Figure 5.8, twisted tubes were fabricated by the Dr. Lee's team at Morgan State University due to the lack of manufacturing capability within the U.S. As shown in Figure 5.9, more than 20 tubes were fabricated and most uniform and accurate tubes (6 tubes) were selected

for the lab-scale STHE prototype. Connections were modified from different fittings and adjusted to connect pipes and provide inlet and outlet of the cold and hot waters.



**Figure 5.8: Components of the Lab-scale STHE System**



**Figure 5.9: Parts and Twisted Tubes of the Lab-scale STHE System**

As shown in Figure 5.10, soft soldering and hard soldering were both tried to make a strong connection that no water leakage and disturbance between two working fluids. Pencil flame brass torch kit (Bernzomatic, UL 2317, Propane gas) along with paste flux, sand abrasive and propane gas were used to perform tin-based lead-free (95/5 Tin Antimony) soft soldering of connections at relatively lower temperature (about 180-200 °C, smaller than 400 °C). Pre-test results indicated that soft soldering may not appropriate for resisting the high temperature of residual fuel gas. Due to the high temperature of residual flue gas (about 500 °C), there is some leakage of water were observed during the preliminary test. Premium troch kit (Bernzomatic, TS4000, MAP/PRO gas) and 5% silver solder brazing alloy (Harris Stay-Silv Solder) were used to perform hard soldering at

relatively high temperature (above 500°C) that make more strong connections to avoid water leakage.

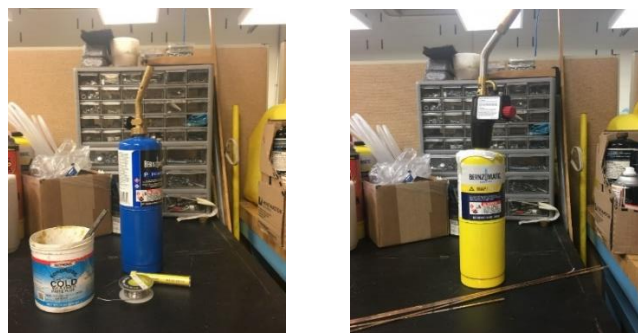


**Figure 5.10: Tools of Soft Soldering (Left) and Hard Soldering (Right)**

As shown in Figure 5.11, twisted tube-based lab-scale STHE system without shell section were completed. It consists of 6 tubes, 5 segmental baffles and connection parts. Then, it was inserted into shell as shown in the right-hand side. Water inlet and outlet were passed through the shell and connected to the connection part. Side-view of the lab-scale STHE along with shell and connection parts were illustrated.

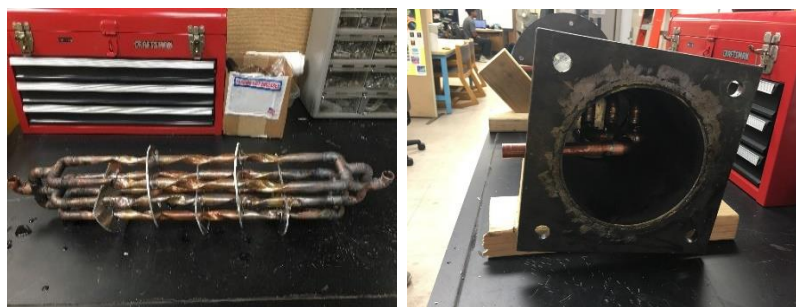


**Figure 5.11: Twisted Tube-based Lab-scale STHE without Shell and Side View**

### 5.1.3 Testing and Evaluation of the Lab-scale STHE System

The detailed layout of systems and instrumentations were illustrated in Figure 5.12. Testing and evaluation of the lab-scale STHE system involved the combustion chamber, fuel feeding system, air supply system, cyclone system, among other instrumentations. The lab-scale STHE system were inserted between combustion chamber and cyclone to observe

the residual heat from the hot flue gas. Poultry litter (PL) was supplied via fuel feeder and natural gas (NG) was supplied via gas line. Then, these fuel resources and air from fans were burned in the combustion chamber and generate hot flue gas to the lab-scale STHE system. Hot flue gas was used to produce hot water and supplied to the radiators. There were 5 radiators (24”H\*64”W, Ecostyle 12,138 Btu, eComfort Company) installed in the mobile trailer. The processed hot water from the lab-scale STHE system were supplied via high temperature resisted hose into the mobile mini trailer to simulate the space heating of poultry house.

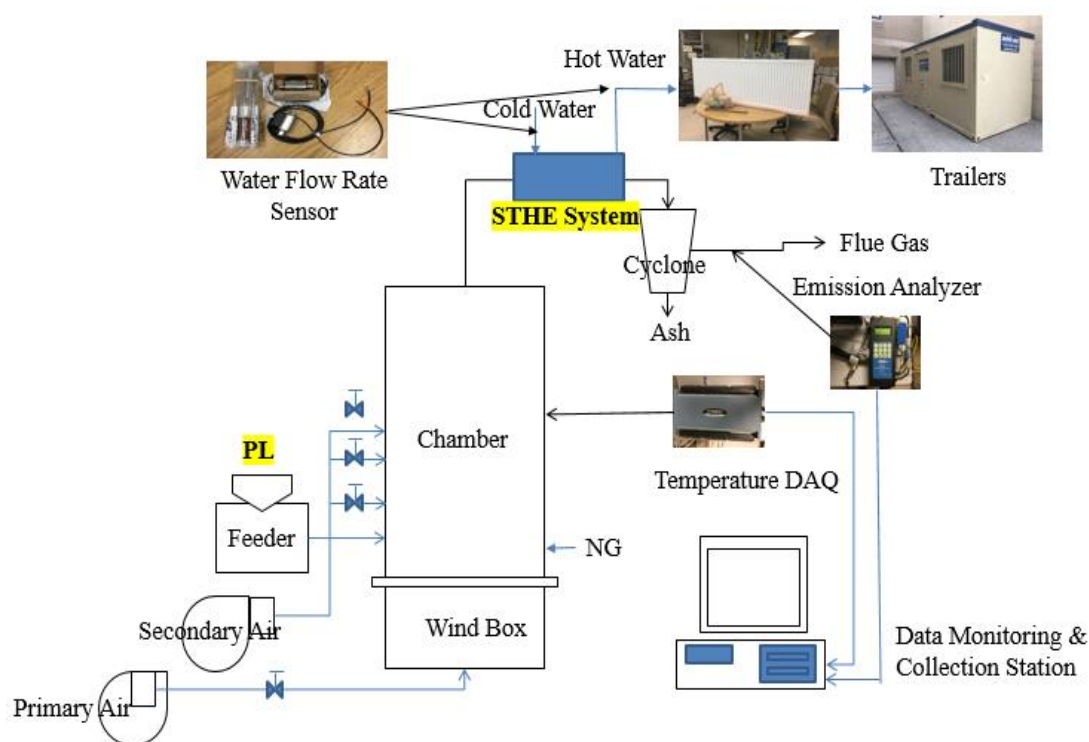


**Figure 5.12: Experimental Setup of the Lab-scale STHE System Evaluation**

During the testing and evaluation of the lab-scale STHE system, flow rates of NG were controlled by valve and feeding rate of PL was controlled by variable speed motor controller (Model 060 SCR-DC, Acrision, USA). Primary air and secondary air were controlled by variable-speed controller. Cold water inlet and hot water outlet temperatures

and flow rates were measured by using flow meter (ifm, SV 4610). Hot flue gas inlet/outlet temperature were measured by using the K-type thermal-couple (Omega, TJ120-CAXL-18U-6) along with data acquisition system (Omega, OMB-DAQ-2416). Meter (Testo, 510i) and pitot tube were used to measure the pressure before and after the lab-scale STHE to calculate the pressure drop under air and fuel mixing ratios. Combustion analyzer (ENERAC™ Model 500, Enerac Inc., USA) were used to measure the emissions (CO, NO<sub>x</sub>, and SO<sub>2</sub>) during the combustion and residual heat collection process. Outside temperature, room temperature, temperature changes of water in and out were also measured. Heat absorption of the lab-scale STHE system were also calculated.

### **5.3 Results and Discussion**

In order to test and evaluate the performance of the lab-scale STHE system, three different fuel conditions (NG: 32 Standard Cubic Feet Per Hour (SCFH); NG: 36 SCFH; NG:36 SCFH+PL:15 lb/hr) were used to produce the hot flue gas in shell section. First two conditions were used to conduct the feasibility of producing hot water by the lab-scale STHE system while third condition was used to prove the feasibility of generating hot water under PL and NG co-combustion condition. Constant cold water (around 75 °F) was supplied to the tube sections of the lab-scale STHE system. As shown in Figure 5.13, the lab-scale STHE system can produce hot water in the range of 86 °F and 109°F from the cold water (around 75 °F) under various fuel mixture conditions. Results also indicated that the highest hot water temperature was 109 °F at rate of 0.30 gallon per minutes (GPM) under co-combustion process of PL and NG in the lab-scale STHE system. It showed that adding PL to NG can increase flue gas temperature (around 324°C-350°C) and hot water temperature between 5 °F (at 1.00 GPM) to 12 °F (at 0.60 GPM) under different water

flow rate conditions. These results indicated the possibility of producing wide range of hot water at various flow rates under different fuel-mixture conditions by using the lab-scale STHE system.

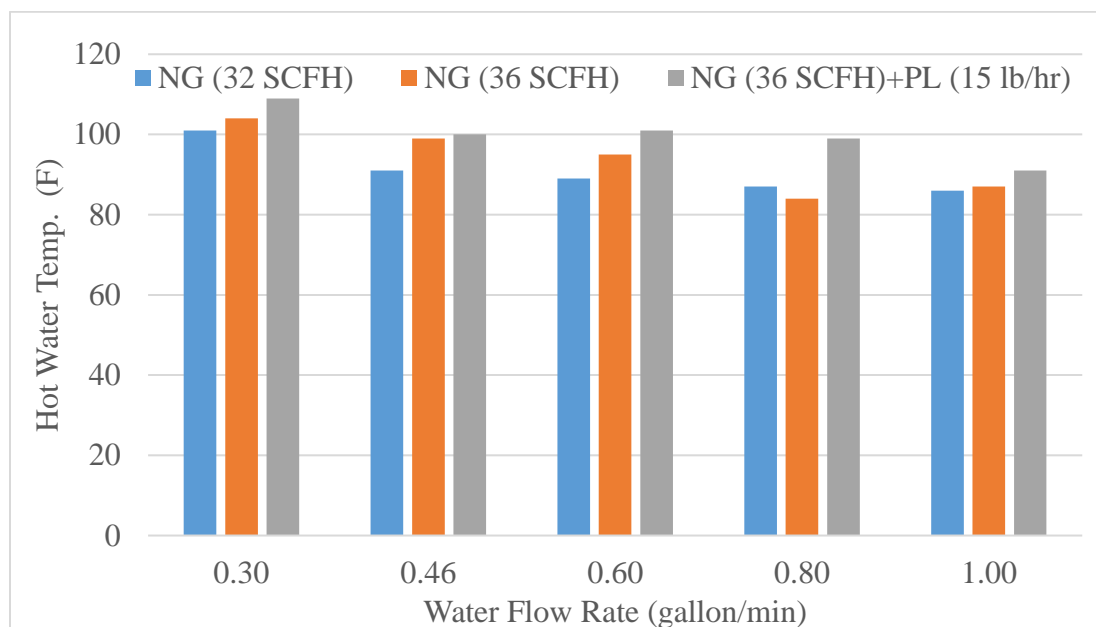


**Figure 5.13: Hot Water Temperature of the Lab-scale STHE System**

Then, specific heat and temperature changes of water and flue gas were used to calculate the energy changes inside the tubes and shells. Multiplication of the specific heat of water and water temperature changes represented the heat content of water while multiplication of specific heat of flue gas and fuel gas temperature changes represented the heat content of flue gas. The specific heat of water and flue gas was assumed as  $4.186 \text{ kJ/kg} \cdot ^\circ\text{C}$  and  $1.02 \text{ kJ/kg} \cdot ^\circ\text{C}$ , respectively. Capture efficiency of the lab-scale STHE system were calculated by the dividing the heat content of water to heat content of flue gas. As shown in Figure 5.14, the capture efficiency under water flow rates and different fuel conditions were plotted. Results indicated that capture efficiency of the lab-scale STHE system in the range of 17% to 32% during the co-combustion of PL and NG. For the cases

of NG combustion, the capture efficiency was relatively lower than co-combustion case. The possible reason is that the PL addition in combustion process may increase heat input which produce more particles in the flue gas that carry more heat energy. The capture efficiency was decreased by water flow rate increment due to the time of passing through the tube were decreased and less heat from flue gas can be captured by water. In order to have high capture efficiency of 27%-32%, the suggested water flow rate was 0.30 GPM.

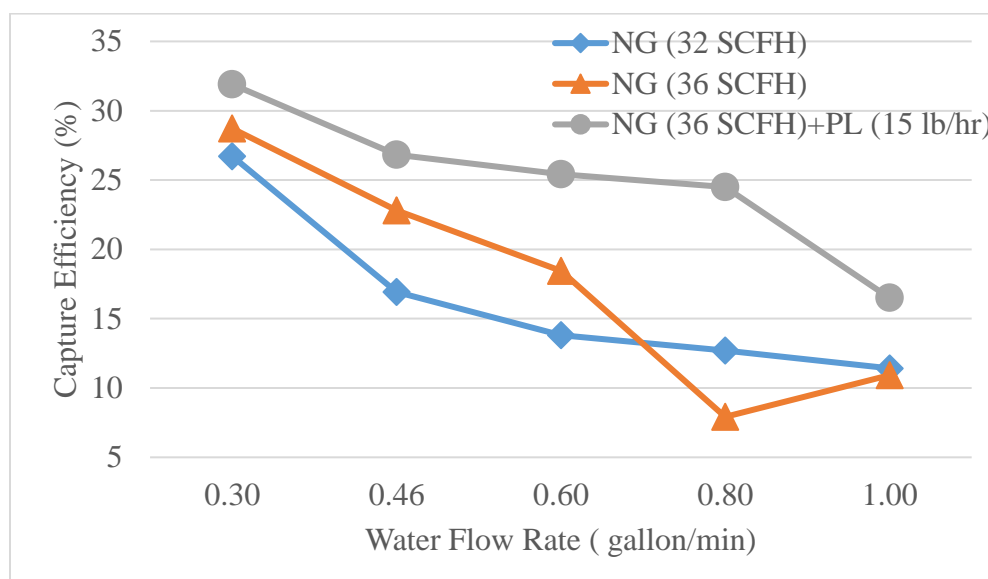


**Figure 5.14: Heat Capture Efficiency of the Lab-scale STHE System**

Heat exchanger outlet temperature indicated the instantaneous hot water temperature from the exit of the lab-scale STHE system. As shown in Figure 5.15, various heat exchanger outlet temperatures (from 82 °F to 127 °F) were sent to the five radiators in the mobile trailer house to simulate the space heating of the poultry houses. The temperature of hot water was gradually decreased by passing through the radiator 1 (about 10°F-29°F), radiator 3 (about 12°F-32°F) and radiator 5 (9°F-39°F). When the outlet temperature increased to 127 °F, temperature drop after radiator 5 was increased to 39 °F.

The higher outlet temperature from heat exchanger indicated that larger heat release from the radiators to the trailer and provide more efficient space heating.

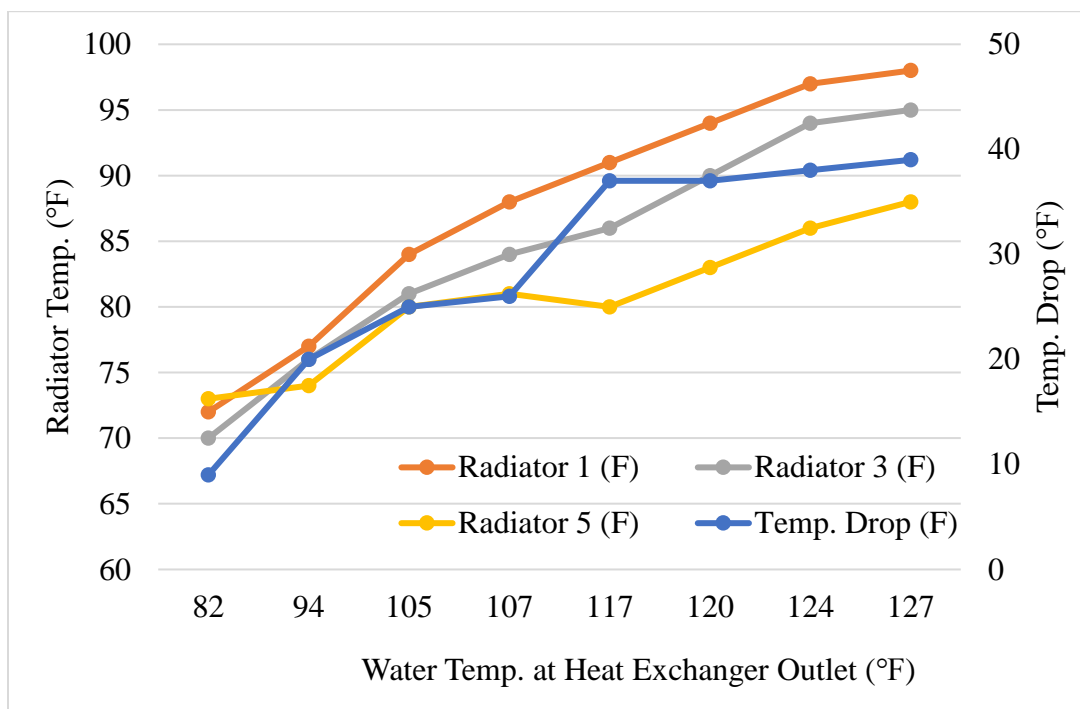


**Figure 5.15: Temperature of Heat Exchanger Outlets Vs. Radiator Outlets**

As shown in the Figure 5.16, the closed loop between the lab-scale STHE system and radiators in the mobile mini trailer was built to increase the outlet temperature at lab-scale STHE exit. Hot water pump was to circulate the water in the closed loop to increase the both inlet and outlet temperature of heat exchanger. Recent test results indicated that the maximum of outlet temperature (up to 146°F) of lab-scale STHE system with inlet temperature of 87°F at rate of 0.46-0.64 GPM while hot flue gas temperature of 621°C was decreased to 360.8°C. The trailer temperature increased from 43 °F to 80 °F (within 130 minutes) during the combustion process while the outside temperature is 34 °F.

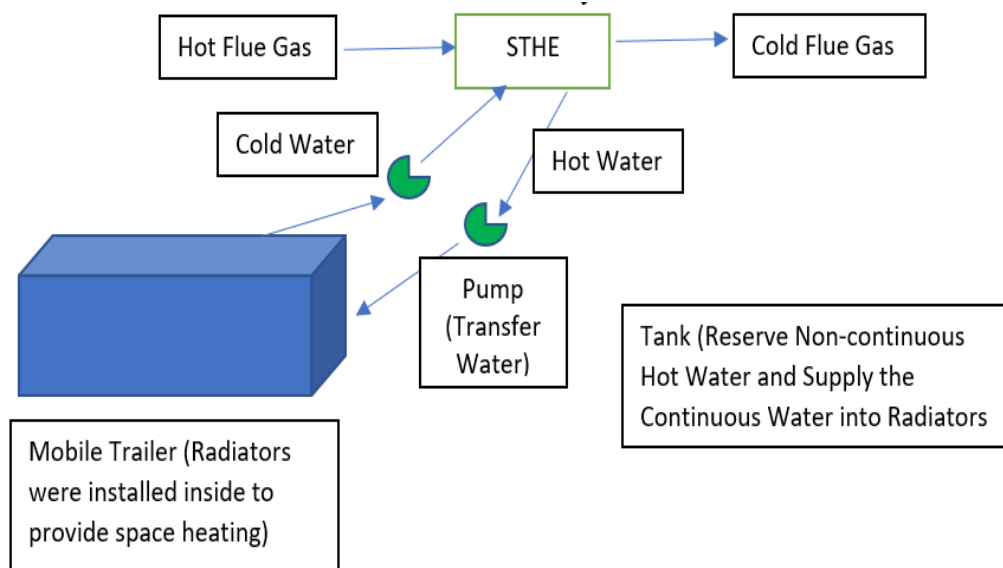


**Figure 5.16: Closed Loop of the Lab-scale Heating Module**

As shown in Figure 5.17, heat transfer performance of concurrent (Option A, direction of flue gas and water is same) and countercurrent (Option B, direction of flue gas and water is opposite) was also compared. Results indicated that concurrent have more efficient process to heat water (up to 146 °F) while countercurrent has lower hot heat water temperature (up to 126 °F).

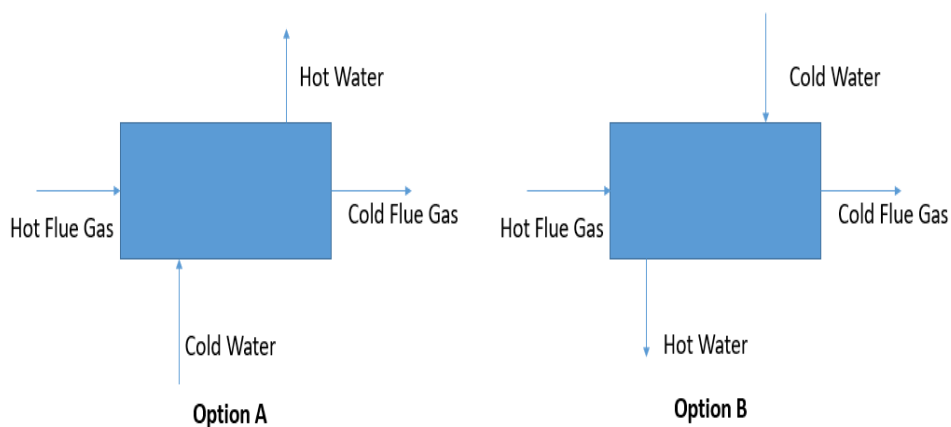


**Figure 5.17: Comparison of Concurrent and Countercurrent**

The hot flue gas from the combustion chamber was passed the cyclone and lab-scale STHE system and collected before exiting the chimney to measure the emission

levels. Table 5.1 provide the summary of emission results from the three different combustion processes. Results indicated that NO<sub>x</sub> and SO<sub>2</sub> emissions were decreased during the PL and NG co-combustion process. Poultry litter-rich condition at bottom of the chamber may increase CO and prohibit the NO<sub>x</sub> emission while Ca concentration in the PL may also react with SO<sub>2</sub> in the flue gas to decrease the SO<sub>2</sub> formation as well.

**Table 5.1: Emissions from Combustion Process**

Feeding Rate	CO (ppm)	NO <sub>x</sub> (ppm)	SO <sub>2</sub> (ppm)
NG (32 SCFH)	80-100	28-50	10-22
NG (36 SCFH)	126-240	32-60	15-30
NG (36 SCFH) + PL (15lb/hr)	300-480	10-35	8-20

**Note: SCFH=Standard Cubic Feet Per Hour, ppm=parts per million**

Table 5.2 indicated the energy production and associated emissions during the combustion process. Electricity output and hot water temperature increased by increasing the overall chamber temperature ranges. In case of increasing the chamber temperature, the emissions of NO<sub>x</sub> and SO<sub>2</sub> emissions were decreased while the CO emission was slightly increased. There should be more future studies to figure out the relationship between emissions and energy production process.

**Table 5.2 Summary of Energy Production and Associated Emissions**

Chamber Temp. (°C)	Flue Gas Temp. (°C)	Electricity (watt)	Hot Water (°F)	CO (ppm)	NO <sub>x</sub> (ppm)	SO <sub>2</sub> (ppm)
580.6- 902.1	536.5	108	107	312	74	3
657.2-911.2	575.8	242	117	10	10	9
692.6-960.4	623.2	458	125	4	19	14
668.7-985.6	643.4	478	136	14	43	16

The emission standards for the different type of materials and counties are varied. As shown in Table 5.3, German and U. S. Environmental Protection Agency (EPA)

standards for the case of municipal solid waste combustion are different. In the U.S., there is no limitation for the poultry litter combustion in small-scale combustion system yet and no emission standards for the small-scale biomass combustion system (150,000Btu/hr). As shown in Table 5.3, the emission limits for the CO, NO<sub>x</sub>, SO<sub>2</sub> and PM are 77-87 ppm, 141-257 ppm, 23-76 ppm and 18.3 mg/Nm<sup>3</sup>, respectively. The safety level of CO emission are 25-70 ppm (Licata et al., 1997). Emission results from poultry litter combustion in lab-scale biomass conversion system show that emission results may be able to meet the emission standards and ensure user's safety if the optimal operating conditions for the minimal emissions can be programmed by the automatic feedback system.

**Table 5.3 German and U.S. EPA Standards for Municipal Solid Wastes**

	Germany	U.S. EPA
CO	100 mg/Nm <sup>3</sup> (87 ppm)	89 mg/Nm <sup>3</sup> (77ppm)
NO <sub>x</sub>	400 mg/Nm <sup>3</sup> (257 ppm)	219 mg/Nm <sup>3</sup> (141 ppm)
SO <sub>2</sub>	200 mg/Nm <sup>3</sup> (76ppm)	61 mg/Nm <sup>3</sup> (23 ppm)
PM	30 mg/Nm <sup>3</sup>	18.3 mg/Nm <sup>3</sup>

In this study, the lab-scale STHE system were designed, fabricated and tested to convert residual flue gas into hot water during the co-combustion of poultry litter and natural gas. Results showed that the lab-scale STHE system can produce the hot water (up to 146 °F) in the closed loop heating module with concurrent approach during the co-combustion process. The trailer temperature increased from 43 °F to 80 °F (within 130 minutes) during the combustion process while the outside temperature is 34 °F. This study showed that the innovative lab-scale STHE prototype integrated the benefits of the twisted tube and segmental baffle to produce hot water that can be used to provide enough space heating of poultry houses by using on-farm waste (e.g. poultry litter).

## **Chapter 6. Conclusions, Recommendations and Future Works**

### **6.1 Conclusions and Concluding Remarks**

Poultry farmers award contracts from the poultry producers (e.g., Perdue, Mountaire, Tyson) to raise chickens and responsible to clean and process poultry litter during the farming process. However, the large production rate and excess land application of poultry litter causes eutrophication (e.g. nitrogen, phosphorus), particularly along the shores of the Chesapeake Bay, the largest estuary system in the United States. Excess land application may also cause odor problems for neighbors and water pollutions, ultimately affect both aquatic ecology and human health. These problems and challenges are creating an urgent need for the efficient, clean, environmentally friendly and sustainable alternative disposal approaches. Biomass to energy operations provide one approach to disposing of high concentrations of poultry litter and partially substituting the fossil fuels. An approach that is even more appealing given Governor Hogan's recently announced strict environmental regulations, to prohibit use of poultry litter on significant acreage in Maryland. Thus, the most important fuel properties, such as ultimate analysis elements, proximate analysis composition and higher heating value (HHV) are critical to determine and develop the alternative technologies for the energy conversion process of biomass fuels (i.e., poultry litter).

In this study, 48 poultry litter sample data were collected from different sources to analyze and characterize fuel properties. The C content of poultry litter samples was found to be in the range of 38.90%-67.93% while it has average values of N, S and Cl in 6.25%, 0.82% and 0.88%, respectively. These elements (e.g., N, S, and Cl) might have a potential to create adverse environmental problems (e.g., acid rain, climate change, ash deposition,

corrosion and fouling) and must to be considered in the development and design process of alternative disposal systems. Results showed the HHV of poultry litter samples varies from 6.78 to 27.90 MJ/kg and has an average of 14.08 MJ/kg. The moisture content is in the wide range of 5% and 43% because samples were collected from various farm locations along with different type of bed materials. Poultry litter also a relatively high ash value of 26.71% (mean), which may allow lower fusion temperature and create ash-related problems (e.g., agglomeration, fouling and slagging). High volatile matter (VM) content indicated that it is extremely reactive biomass fuel and easier to ignite even at relative low temperatures. Relatively higher moisture and VM content of poultry litter may also require an enough residence time in the combustion chamber to ensure complete combustion and lower emissions.

Then, HHV of poultry litter samples are plotted as a function of fixed carbon, VM, and ash components (in wt %, dry-basis) by using scatter plots to show how HHV results vary with different composition of proximate analysis data. HHV results were found to increase with the FC contents. In contrast, there is a clear trend in HHV results decreasing with the increase of ash contents while the correlation of VM and HHV is not obvious as liner relationship. Individual concentration of C, H and O were plotted against the corresponding HHV values to explore the appropriateness of the relationship between major elements and HHV values. It can be found that major elements of ultimate analysis have better linear dependence than the proximate analysis data. However, ultimate analysis suffered a drawback; it needs an elemental analysis as an input data, which needs expensive equipment and highly skilled analysts. Thus, proximate-based regression models were developed to predict HHV because it is relatively simple and cheap to perform in any

laboratory with limited resources. Fifteen new regression models were developed by using proximate analysis data of poultry litter samples. Results show that the simple multiple linear regression model (N1) compromise all proximate analysis components. Results also show that the polynomial terms for VM, as well as interaction effects of FC and ash, are necessary for the best-fit regression model (N15) to further lower estimation errors. Moreover, comparison results show that best-fit regression model has a higher  $R^2$  (91.62%) and lower estimation errors than the existing proximate-based models. Therefore, this new regression model can be an excellent tool for predicting the HHV of poultry litter and does not require any expensive equipment that measures HHV or elemental compositions.

In response to the fossil fuel depletion issue, high water consumption and adverse environmental issues found in current power plants, the Stirling engine-based biomass conversion (SEBC) system was designed, fabricated, and developed with integration of the 1 kW SE and an existing advanced lab-scale swirling fluidized bed combustor (SFBC) prototype. The effects of operating factors (e.g., EA, SA, PA, and mixing ratio) on electricity output, temperature profiles and emissions (e.g., CO, NO<sub>x</sub>, SO<sub>2</sub>) performance of SEBC system during the poultry litter and natural gas co-combustion process was investigated and evaluated with statistical methods. Results indicated that maximum power output reached about 905 Watts at head temperature of 584 °C and water flow rate of 13.1 L/min. The PA flow rate was found to have a significant effect on the temperature (P-value = 0.018), NO<sub>x</sub> (P-value = 0.006) and SO<sub>2</sub> (P-value = 0.041). Furthermore, the CO emissions (P-value = 0.008) was significantly affected by the SA flow rates. This study showed that the SEBC system is possible to convert poultry litter into useful energy (electricity) with relatively low emissions (NO<sub>x</sub> ranges from 31-140 ppm, SO<sub>2</sub> ranges from 1 to 50 ppm and,

CO emissions varies from 15-1048 ppm). In addition, PM emissions results showed less than MD permitting thresholds of 0.35 lb/MMBtu.

In order to collect more residual heat from the waste hot flue gas during poultry litter and natural co-combustion process, this study also focused on the improvement of heat transfer coefficients on the both shell and tube sides. Design, fabrication and evaluation of the lab-scale STHE prototype under various operating conditions were performed. The innovative lab-scale STHE prototype integrated the benefits of the twisted tubes and segmental baffle to improve heat transfer coefficients and capture more residual heat. Closed loop heating module was built by integration of the six radiators in the mobile mini trailer, hot water pump, lab-scale STHE system and connection pipes to mimic the space heating of poultry houses. Results showed that the lab-scale STHE system was able to produce the hot water (up to 146 °F) in the closed loop heating module with concurrent approach during the poultry litter and natural gas co-combustion process. In the meantime, the mobile mini trailer temperature was increased from 43 °F to 80 °F (within 130 minutes) while the outside temperature was 34°F. This study proved the possibility of generating hot water and providing enough space heating of poultry houses by using on-farm waste (i.e., poultry litter).

In summary, the poultry litter has a potential to use a biomass fuel and substitute fossil fuels in the energy production process. Lab-scale advanced SFBC along the Stirling engine and shell-tube heat exchanger (STHE) prototype may able to form the lab-scale biomass conversation system to process poultry litter into useful energy, include electricity and hot water with minimal emissions. Fly ash from combustion can also be utilized as construction and soil amendments. Therefore, energy generation from poultry litter by

using the lab-scale biomass conversion system may provide a sustainable and net-zero solution for the users (i.e., poultry farmers).

## **6.2 Recommendations & Future Works**

For future studies, the following are suggested:

- Future work should focus on identify the relationship between energy production (e.g., electricity, hot water) and emissions to optimize the small-scale biomass conversion system.
- Develop automatic feedback system to control air flow rates and fuel feeding rates based on emission and energy production.
- Collecting more poultry litter samples from various poultry farm within U.S. to identify the difference of fuel properties based on geological location.
- Conducting proximate analysis in the laboratory and collect experimental data that more accurate proximate-based HHV models can be developed and validated.
- Future research should collect more data on different biomass types that the different approach, such as artificial neuro networks (ANN) can be used to develop mathematical models to predict the HHV of biomass samples.
- A complete 3D and computational fluid dynamics (CFD) modeling should apply to model and simulate biomass combustion and co-combustion process
- Effect of Stirling engine heights on the engine head temperature and electricity output should be focused
- Accurate real time hot flue gas flow rates and compositions should be measured by liquid flow meter to calculate the heat transfer of flue gases and water

- Different fuel-N content fuels, combustion temperatures, fuel/air ratios should focus on the future study to perform modeling of NO<sub>x</sub> emission
- Particulate matter sampling equipment, cooling time, and methods can lead to significant different results of PM, and therefore the standards method are needed.
- Pressure drop and heat transfer coefficient of the lab-scale STHE system will be calculated to provide overall heat transfer performance of the lab-scale STHE system.

## References

- Abelha, P., Gulyurtlu, I., Boavida, D., Barros, J. S., Cabrita, I., Leahy, J., . . . & Leahy, M. (2003). Combustion of poultry litter in a fluidised bed combustor. *Fuel*, 82(6), 687-692.
- Agbor, E., Zhang, X., & Kumar, A. (2014). A review of biomass co-firing in North America. *Renewable and Sustainable Energy Reviews*, 40, 930-943.
- Akkaya, A.V. (2009). Proximate analysis based multiple regression models for higher heating value estimation of low rank coals. *Fuel Processing Technology*, 90, 165–170.
- Al-Naiema, I., Estillore, A. D., Mudunkotuwa, I. A., Grassian, V. H., & Stone, E. A. (2015). Impacts of co-firing biomass on emissions of particulate matter to the atmosphere. *Fuel*, 162, 111-120.
- Amann, M., Klimont, Z., & Wagner, F. (2013). Regional and global emissions of air pollutants: Recent trends and future scenarios. *Annual Review of Environment and Resources*, 38, 31-55.
- Asmantas, L. A., Nemira, M. A., & Trilikauskas, V. V. (1985). Coefficients of heat transfer and hydraulic drag of a twisted oval tube. *Heat transfer: Soviet Research*, 17(4), 103-109.
- Arashnia, I., Najafi, G., Ghobadian, B., Yusaf, T., Mamat, R., & Kettner, M. (2015). Development of micro-scale biomass-fuelled CHP system using Stirling engine. *Energy Procedia*, 75, 1108-1113.
- Armesto, L., Bahillo, A., Veijonen, K., Cabanillas, A., & Otero, J. (2002). Combustion behaviour of rice husk in a bubbling fluidised bed. *Biomass and Bioenergy*, 23(3), 171-179.

- Bahillo, A., Cabanillas, A., Gayan, P., Diego, L. D., & Adanez, J. (2003). Co-combustion of coal and biomass in FB boilers: Model validation with experimental results from CFB pilot plant. *46th Int. Energy Agency–Fluidized Bed Conversion (IEA–FBC)*.
- Balat, M. (2006). Biomass energy and biochemical conversion processing for fuels and chemicals. *Energy Sources, Part A: Recovery, Utilization and Environmental Effects*, 28(6), 517-525.
- Balat, M., & Bozbas, K. (2006). Wood as an energy source: potential trends, usage of wood, and energy politics. *Energy Sources, Part A: Recovery, Utilization and Environmental Effects*, 28(9), 837-844.
- Barelli, L., Bidini, G., Gallorini, F., & Ottaviano, A. (2012). Dynamic analysis of PEMFC-based CHP systems for domestic application. *Applied Energy*, 91(1), 13-28.
- Baskar, P., & Senthilkumar, A. (2016). Effects of oxygen enriched combustion on pollution and performance characteristics of a diesel engine. *Engineering Science and Technology, an International Journal*, 19(1), 438-443.
- Basu, P. (2010). *Biomass gasification and pyrolysis: Practical design and theory*. Academic press.
- Baxter, L. (2005). Biomass-coal co-combustion: Opportunity for affordable renewable energy. *Fuel*, 84(10), 1295-1302.
- Beer, J. M. (2000). Combustion technology developments in power generation in response to environmental challenges. *Progress in Energy and Combustion Science*, 26(4), 301-327.

- Berndes, G., Hoogwijk, M., & Van den Broek, R. (2003). The contribution of biomass in the future global energy supply: A review of 17 studies. *Biomass and Bioenergy*, 25(1), 1-28.
- Bhattacharya, S. C. (1998). State of the art of biomass combustion. *Energy Sources*, 20(2), 113-135.
- Bichkar, P., Dandgaval, O., Dalvi, P., Godase, R., & Dey, T. (2018). Study of shell and tube heat exchanger with the effect of types of baffles. *Procedia Manufacturing*, 20, 195-200.
- Biomass Energy Center. (2017), Fuel prices per kWh, updated July 11<sup>th</sup> 2017, Retrieved from <https://www.forestry.gov.uk/forestry/infd-9peg3u>
- Biswas, S., Majhi, S., Mohanty, P., Pant, K. K., & Sharma, D. K. (2014). Effect of different catalyst on the co-cracking of Jatropha oil, vacuum residue and high-density polyethylene. *Fuel*, 133, 96-105.
- Brassard, P., Palacios, J. H., Godbout, S., Bussi eres, D., Lagac e, R., Larouche, J. P. & Pelletier, F. (2014). Comparison of the gaseous and particulate matter emissions from the combustion of agricultural and forest biomasses. *Bioresource Technology*, 115, 300-306.
- Cao, Y., Zhou, H., Fan, J., Zhao, H., Zhou, T., Hack, P., . . . & Pan, W. P. (2008). Mercury emissions during cofiring of sub-bituminous coal and biomass (chicken waste, wood, coffee residue, and tobacco stalk) in a laboratory-scale fluidized bed combustor. *Environmental Science & Technology*, 42(24), 9378-9384.

- Cardozo, E., Erlich, C., Malmquist, A., & Alejo, L. (2014). Integration of a wood pellet burner and a Stirling engine to produce residential heat and power. *Applied Thermal Engineering*, 73(1), 671-680.
- Channiwala, S. A., & Parikh, P. P. (2002). A unified correlation for estimating HHV of solid, liquid and gaseous fuels. *Fuel*, 81(8), 1051-1063.
- Chastain, J. P., Camberato, J. J., & Skewes, P. (2001). Poultry manure production and nutrient content. *Chapter 3b in: Confined Animal Manure Managers Certification Program Manual B Poultry Version*, 2, 1-17.
- Chastain, J. P., Coloma-del Valle, A., & Moore, K. P. (2012). Using broiler litter as an energy source: Energy content and ash composition. *Applied Engineering in Agriculture*, 28(4), 513-522.
- Chen, G., Ezekiel, A., & Bardhan, T. K. (2013). Optimization of factor settings for pharmaceutical filling process by factorial design of mixed levels. *Industrial and Systems Engineering Review*, 1(2), 110-122.
- Coleman, D. E., & Montgomery, D. C. (1993). A systematic approach to planning for a designed industrial experiment. *Technometrics*, 35(1), 1-12.
- Cordero, T., Marquez, F., Rodriguez-Mirasol, J. & Rodriguez, J. J. (2001). Predicting heating values of lignocellulosics and carbonaceous materials from proximate analysis. *Fuel*, 80, 1567–1571.
- Corria, M. E., Cobas, V. M., & Lora, E. S. (2006). Perspectives of Stirling engines use for distributed generation in Brazil. *Energy Policy*, 34(18), 3402-3408.

- Coufal, C. D., Chavez, C., Niemeyer, P. R., & Carey, J. B. (2006). Measurement of broiler litter production rates and nutrient content using recycled litter. *Poultry Science*, 85(3), 398-403.
- Cotana, F., Coccia, V., Petrozzi, A., Cavalaglio, G., Gelosia, M., & Merico, M. C. (2014). Energy valorization of poultry manure in a thermal power plant: Experimental campaign. *Energy Procedia*, 45, 315–322.
- Damirchi, H., Najafi, G., Alizadehnia, S., Ghobadian, B., Yusaf, T., & Mamat, R. (2015). Design, fabrication and evaluation of gamma-type Stirling engine to produce electricity from biomass for the micro-CHP system. *Energy Procedia*, 75, 137-143.
- Damirchi, H., Najafi, G., Alizadehnia, S., Mamat, R., Azwadi, C. S. N., Azmi, W. H., & Noor, M. M. (2016). Micro combined heat and power to provide heat and electrical power using biomass and Gamma-type Stirling engine. *Applied Thermal Engineering*, 103, 1460-1469.
- Danielsen, S. O. (2009). *Investigation of a twisted-tube type shell-and-tube heat exchanger* (Master's thesis, Institutt for Energi-og Prosessteknikk, Trondheim, Norway, June 2009).
- Demirbas, A. (2004). Combustion characteristics of different biomass fuels. *Progress in Energy and Combustion Science*, 30(2), 219-230.
- Demirbas, A. (2005). Potential applications of renewable energy sources, biomass combustion problems in boiler power systems and combustion related environmental issues. *Progress in Energy and Combustion Science*, 31(2), 171-192.
- Demirbaş, A. (2006). Global renewable energy resources. *Energy Sources, Part A: Recovery, Utilization, and Environmental Effects*, 28(8), 779-792.

- Demirbas, A. (2009). Prediction of higher heating values for vegetable oils and animal fats from proximate analysis data. *Energy Sources, Part A: Recovery, Utilization, and Environmental Effects*, 31, 1264–1270.
- Demirbas, M. F., Balat, M., & Balat, H. (2009). Potential contribution of biomass to the sustainable energy development. *Energy Conversion and Management*, 50(7), 1746-1760.
- Deng, W., Yan, J., Li, X., Wang, F., Chi, Y. & Lu, S. (2009). Emission characteristics of dioxins, furans and polycyclic aromatic hydrocarbons during fluidized-bed combustion of sewage sludge. *Journal of Environmental Sciences*, 21(12), 1747-1752.
- De Paepe, M., D’Herdt, P., & Mertens, D. (2006). Micro-CHP systems for residential applications. *Energy Conversion and Management*, 47(18-19), 3435-3446.
- Dong, L., Liu, H., & Riffat, S. (2009). Development of small-scale and micro-scale biomass-fuelled CHP systems—A literature review. *Applied Thermal Engineering*, 29(11), 2119-2126.
- Duan, F., Chyang, C., Chin, Y., & Tso, J. (2013). Pollutant emission characteristics of rice husk combustion in a vortexing fluidized bed incinerator. *Journal of Environmental Sciences*, 25(2), 335-339.
- Duan, Z., Shen, F., Cao, X., & Zhang, J. (2016). Comprehensive effects of baffle configuration on the performance of heat exchanger with helical baffles. *Nuclear Engineering and Design*, 300, 349-357.
- Dubey, V. V. P., Verma, R. R., Verma, P. S., & Srivastava, A. K. (2014). Performance analysis of shell and tube type heat exchanger under the effect of varied operating condition. *IOSR Journal of Mechanical and Civil Engineering*, 11(3), 8-17.

- Dzyubenko, B. V. (1983). Drag in a heat exchanger with a twisted flow. *Journal of Engineering Physics and Thermophysics*, 44(3), 237-241.
- Eiamsa-Ard, S., Kaewkohkiat, Y., Thianpong, C., & Promvongse, P. (2008). Combustion behavior in a dual-staging vortex rice husk combustor with snail entry. *International Communications in Heat and Mass Transfer*, 35(9), 1134-1140.
- Evlev, V. M., Kalinin, E. K., Danilov, I. I., Dziubenko, B. V., & Dreitser, G. A. (1982). Heat transfer in the turbulent swirling flow in a channel of complex shape. *Heat Transfer*, 3, 171-176.
- Fenimore, C. P. (1971). Formation of nitric oxide in premixed hydrocarbon flames. *Symposium (International) on Combustion*, 13(1), 373-380.
- Font-Palma, C. (2012). Characterisation, kinetics and modelling of gasification of poultry manure and litter: An overview. *Energy Conversion and Management*, 53(1), 92-98.
- Fournel, S., Marcos, B., Godbout, S., & Heitz, M. (2015). Predicting gaseous emissions from small-scale combustion of agricultural biomass fuels. *Bioresource Technology*, 179, 165-172.
- Fox, E. C., Krishnan, R. P., Daw, C. S., & Jones, J. E. (1986). A review of fluidized-bed combustion technology in the United States. *Energy*, 11(11-12), 1183-1200.
- Friedl, A., Padouvas, E., Rotter, H., & Varmuza, K. (2005). Prediction of heating values of biomass fuel from elemental composition. *Analytica Chimica Acta*, 544(1-2), 191-198.
- Froese, R. E., Shonnard, D. R., Miller, C. A., Koers, K. P., & Johnson, D. M. (2010). An evaluation of greenhouse gas mitigation options for coal-fired power plants in the US Great Lakes States. *Biomass and Bioenergy*, 34(3), 251-262.

- García, D., González, M. A., Prieto, J. I., Herrero, S., López, S., Mesonero, I., & Villasante, C. (2014). Characterization of the power and efficiency of Stirling engine subsystems. *Applied Energy*, *121*, 51-63.
- García, R., Pizarro, C., Lavín, A. G., Bueno, J. L. (2014). Spanish biofuels heating value estimation. Part II: Proximate analysis data. *Fuel*, *117*, 1139–1147.
- Gardiner, W. C. (2000). *Gas-phase combustion chemistry*. W. C. Gardiner (Ed.). New York, NY: Springer.
- Ghugare, S. B., Tiwary, S., Elangovan, V., Tambe, S. S. (2014). Prediction of higher heating value of solid biomass fuels using artificial intelligence formalisms. *Bioenergy Research*, *7*, 681–692.
- Glarborg, P., Kubel, D., Dam-Johansen, K., Chiang, H. M., & Bozzelli, J. W. (1996). Impact of SO<sub>2</sub> and NO on CO oxidation under post-flame conditions, *International Journal of Chemical Kinetics*, *28*, (10), 773-790.
- Glarborg, P., Jensen, A. D., & Johnsson, J. E. (2003). Fuel nitrogen conversion in solid fuel fired systems. *Progress in Energy and Combustion Science*, *29*(2), 89-113.
- Henihan, A. M., Leahy, M. J., Leahy, J. J., Cummins, E., & Kelleher, B. P. (2003). Emissions modeling of fluidised bed co-combustion of poultry litter and peat. *Bioresource Technology*, *87*(3), 289-294.
- Houshfar, E. (2012). *Experimental and numerical studies on two-stage combustion of biomass* (Doctoral Thesis). Retrieved from <https://brage.bibsys.no/xmlui/handle/11250/234646>

- Hu, Y., Naito, S., Kobayashi, N., & Hasatani, M. (2000). CO<sub>2</sub>, NO<sub>x</sub> and SO<sub>2</sub> emissions from the combustion of coal with high oxygen concentration gases. *Fuel*, 79(15), 1925-1932.
- Jenkins, B., Baxter, L. L., & Miles, T. R. (1998). Combustion properties of biomass. *Fuel Processing Technology*, 54(1), 17-46.
- Jia, L., & Anthony, E. J. (2011). Combustion of poultry-derived fuel in a coal-fired pilot-scale circulating fluidized bed combustor. *Fuel Processing Technology*, 92(11), 2138-2144.
- Johnsson, J. E. (1994). Formation and reduction of nitrogen oxides in fluidized-bed combustion. *Fuel*, 73(9), 1398-1415.
- Kabir, M. R., & Kumar, A. (2012). Comparison of the energy and environmental performances of nine biomass/coal co-firing pathways. *Bioresource Technology*, 124, 394-405.
- Kazagic, A., & Smajevic, I. (2009). Synergy effects of co-firing wooden biomass with Bosnian coal. *Energy*, 34(5), 699-707.
- Kelleher, B. P., Leahy, J. J., Henihan, A. M., O'dwyer, T. F., Sutton, D., & Leahy, M. J. (2002). Advances in poultry litter disposal technology—a review. *Bioresource Technology*, 83(1), 27-36.
- Khan, A. A., De Jong, W., Jansens, P. J., & Spliethoff, H. (2009). Biomass combustion in fluidized bed boilers: Potential problems and remedies. *Fuel Processing Technology*, 90(1), 21-50.
- Koh, M. P., & Hoi, W. K. (2003). Sustainable biomass production for energy in Malaysia. *Biomass and Bioenergy*, 25(5), 517-529.

- Koppejan, J., & Van Loo, S. (Eds.). (2012). *The handbook of biomass combustion and co-firing*. Abingdon, United Kingdom: Routledge.
- Kuprianov, V. I., Kaewklum, R., & Chakritthakul, S. (2011). Effects of operating conditions and fuel properties on emission performance and combustion efficiency of a swirling fluidized-bed combustor fired with a biomass fuel. *Energy*, 36(4), 2038-2048.
- Küçükbayrak, S., Dürüs, B., Meriçboyu, A.E. & Kadioğlu, E. (1991). Estimation of calorific values of Turkish lignites. *Fuel*, 70, 979–981.
- Laryea-Goldsmith, R. (2010). *Concurrent combustion of biomass and municipal solid waste* (PhD Thesis). Retrieved from <http://ethos.bl.uk/OrderDetails.do?uin=uk.bl.ethos.535416>
- Leckner, B., & Karlsson, M. (1993). Gaseous emissions from circulating fluidized bed combustion of wood. *Biomass and Bioenergy*, 4(5), 379-389.
- Leckner, B. (1998). Fluidized bed combustion: Mixing and pollutant limitation. *Progress in Energy and Combustion Science*, 24(1), 31-61.
- Levlev, V. M., Dzyubenko, B. V., Dreitser, G. A., & Vilemas, Y. V. (1982). In-line and cross-flow helical tube heat exchangers. *International Journal of Heat and Mass Transfer*, 25(3), 317-323.
- Li, S., Wu, A., Deng, S., & Pan, W. P. (2008). Effect of co-combustion of chicken litter and coal on emissions in a laboratory-scale fluidized bed combustor. *Fuel Processing Technology*, 89(1), 7-12.

- Li, X., Zhu, D., Yin, Y., Liu, S., & Mo, X. (2018). Experimental study on heat transfer and pressure drop of twisted oval tube bundle in cross flow. *Experimental Thermal and Fluid Science*, 99, 251-258.
- Li, Z., Ren, F., Chen, Z., Chen, Z., & Wang, J. (2010). Influence of declivitous secondary air on combustion characteristics of a down-fired 300-MW utility boiler. *Fuel*, 89(2), 410-416.
- Liang, F. Y., Ryvak, M., Sayeed, S., & Zhao, N. (2012). The role of natural gas as a primary fuel in the near future, including comparisons of acquisition, transmission and waste handling costs of as with competitive alternatives. *Chemistry Central Journal*, 6(1), S4.
- Licata, A., Hartenstein, H. U., & Terracciano, L. (1997). *Comparison of US EPA and European emission standards for combustion and incineration technologies* (No. CONF-970440-). Solid Waste Association of North America, Silver Spring, MD (United States); Air and Waste Management Association, Pittsburgh, PA (United States); Integrated Waste Services Association, Washington, DC (United States); National Renewable Energy Lab., Golden, CO (United States); American Society of Mechanical Engineers, Yonkers, NY (United States). Solid Waste Processing Div.; Environmental Protection Agency, Research Triangle Park, NC (United States). Air Pollution Technology Branch.
- Loeffler, D., & Anderson, N. (2014). Emissions tradeoffs associated with cofiring forest biomass with coal: A case study in Colorado, USA. *Applied Energy*, 113, 67-77.
- Lombardi, S., Bizon, K., Marra, F. S., & Continillo, G. (2015). Effect of coupling parameters on the performance of fluidized bed combustor-Stirling Engine for a Micro CHP System. *Energy Procedia*, 75, 834-839.

- Lynch, D., Henihan, A. M., Kwapinski, W., Zhang, L., & Leahy, J. J. (2013a). Ash agglomeration and deposition during combustion of poultry litter in a bubbling fluidized-bed combustor. *Energy & Fuels*, 27(8), 4684-4694.
- Lynch, D., Henihan, A. M., Bowen, B., Lynch, D., McDonnell, K., Kwapinski, W., & Leahy, J. J. (2013b). Utilisation of poultry litter as an energy feedstock. *Biomass and Bioenergy*, 49, 197-204.
- Maghanki, M. M., Ghobadian, B., Najafi, G., & Galogah, R. J. (2013). Micro combined heat and power (MCHP) technologies and applications. *Renewable and Sustainable Energy Reviews*, 28, 510-524.
- Mahmoud, A., Shuhaimi, M., & Samed, M. A. (2009). A combined process integration and fuel switching strategy for emissions reduction in chemical process plants. *Energy*, 34(2), 190-195.
- Mahmoudi, S., Baeyens, J., & Seville, J. P. K. (2010). NO<sub>x</sub> formation and selective noncatalytic reduction (SNCR) in a fluidized bed combustor of biomass, *Biomass and Bioenergy*, 34(9), 1393-1409.
- Majumder, A. K., Jain, R., Banerjee, P., & Barnwal, J. P. (2008). Development of a new proximate analysis based correlation to predict calorific value of coal. *Fuel*, 87(13), 3077-3081.
- Malone, G. W., Sims, T., & Gedamu, N. (1992). Quantity and quality of poultry manure produced under current management programs. Final report to the Delaware Department of Natural Resources and Environmental Control and Delmarva Poultry Industry, Inc., University of Delaware. *Research and Education Center, Georgetown, Delaware*.

- Martín, D. S., & del Mar Rubio-Varas, M. (2017). Freshwater for cooling needs: A long-run approach to the nuclear water footprint in Spain. *Ecological Economics*, 140, 146-156.
- Masiá, A. T., Buhre, B. J. P., Gupta, R. P., & Wall, T. F. (2007). Characterising ash of biomass and waste. *Fuel Processing Technology*, 88(11-12), 1071-1081.
- Master, B.I., Chunangad, K.S. & Pushpanathan, V., 2003. Fouling mitigation using helixchanger heat exchangers. *Proceedings of the ECI Conference on Heat Exchanger Fouling and Cleaning: Fundamentals and Applications*, Santa Fe, NM, May 18–22, 17–322.
- Master, B.I., et al., 2006. Most frequently used heat exchangers from pioneering research to worldwide applications. *Heat Transfer Engineering*, 27, 4–11.
- McKendry, P. (2002a). Energy production from biomass (part 1): Overview of biomass. *Bioresource Technology*, 83(1), 37-46.
- McKendry, P. (2002b). Energy production from biomass (part2): Conversion technologies. *Bioresource Technology*, 83(1), 47–54.
- McIlveen-Wright, D. R., Huang, Y., Rezvani, S., Mondol, J. D., Redpath, D., Anderson, M., . . . & Williams, B. C. (2011). A techno-economic assessment of the reduction of carbon dioxide emissions through the use of biomass co-combustion. *Fuel*, 90(1), 11-18.
- Mehrabian, M. A., & Hemmat, M. (2001). The overall heat transfer characteristics of a double pipe heat exchanger: Comparison of experimental data with predictions of standard correlations. *WIT Transactions on Modelling and Simulation*, 30, 12.

- Miccio, F. (2013). On the integration between fluidized bed and Stirling engine for micro-generation. *Applied Thermal Engineering*, 52(1), 46-53.
- Miles, T. R., Miles Jr, T. R., Baxter, L. L., Bryers, R. W., Jenkins, B. M., & Oden, L. L. (1995). *Alkali deposits found in biomass power plants: A preliminary investigation of their extent and nature. Volume 1* (No. NREL/TP-433-8142-Vol. 1; SAND-96-8225-Vol. 1). National Renewable Energy Lab., Golden, CO (United States); Miles (Thomas R.), Portland, OR (United States); Sandia National Labs., Livermore, CA (United States); Foster Wheeler Development Corp., Livingston, NJ (United States); California Univ., Davis, CA (United States); Bureau of Mines, Albany, OR (United States). Albany Research Center.
- Miller, J. A., & Bowman, C. T. (1989). Mechanism and modeling of nitrogen chemistry in combustion. *Progress in Energy and Combustion Science*, 15(4), 287-338.
- Mittal, M. L., Sharma, C., & Singh, R. (2012). Estimates of emissions from coal fired thermal power plants in India. *2012 International Emission Inventory Conference*, 13-16, Tampa, Florida.
- Montgomery, D. C. (2017). *Design and analysis of experiments*. John Wiley & Sons.
- Montgomery, D. C., & Runger, G. C. (2010). *Applied statistics and probability for engineers*. John Wiley & Sons.
- Moka, V. K. (2012). *Estimation of calorific value of biomass from its elementary components by regression analysis* (Doctoral dissertation).
- Munir, S., Nimmo, W., & Gibbs, B. M. (2011). The effect of air staged, co-combustion of pulverised coal and biomass blends on NO<sub>x</sub> emissions and combustion efficiency. *Fuel*, 90(1), 126-135.

- Natural Resource, Agriculture, and Engineering Service (NRAES) (1999). Poultry waste management handbook. *Publ. No. NRAES-132. Cooperative Extension, 152.*
- Ng, J. H., Khor, J. H., Wong, K. Y., Rajoo, S., & Chong, C. T. (2015). Statistical analysis of engine system-level factors for palm biodiesel fuelled diesel engine responses. *Energy Procedia, 75*, 99-104.
- Nhuchhen, D.R.; Afzal, M.T. (2017). HHV predicting correlations for torrefied biomass using proximate and ultimate analyses. *Bioengineering, 4*, 7.
- Nhuchhen, D. R., & Salam, P. A. (2012). Estimation of higher heating value of biomass from proximate analysis: A new approach. *Fuel, 99*, 55-63.
- Nhuchhen, D. R. (2016). Prediction of carbon, hydrogen, and oxygen compositions of raw and torrefied biomass using proximate analysis. *Fuel, 180*, 348-356.
- Nikolaisen, L., Nielsen, C., Larsen, M. G., Nielsen, V., Zielke, U., Kristensen, J. K., & Holm-Christensen, B. (1998). Straw for energy production. Technology-Environment-Economy. *Copenhagen Center for Biomass Technology/Danish Energy Agency.*
- Nussbaumer, T., & Hustad, J. E. (1997). Overview of biomass combustion. *Developments in Thermochemical Biomass Conversion*, Netherlands: Springer.
- Nussbaumer, T. (2003). Combustion and co-combustion of biomass: Fundamentals, technologies, and primary measures for emission reduction. *Energy & Fuels, 17*(6), 1510-1521.
- Ozturk, S., & Eyriboyun, M. (2010). NOx formation in combustion of natural gases used in Turkey under different conditions. *Journal of Thermal Science and Technology, 30*(2), 95-102.

- Özyuğuran, A., & Yaman, S. (2017). Prediction of calorific value of biomass from proximate analysis. *Energy Procedia*, *107*, 130-136.
- Palma, C. F., & Martin, A. D. (2013). Inorganic constituents formed during small-scale gasification of poultry litter: A model-based study. *Fuel Processing Technology*, *116*, 300-307.
- Paltsev, S., Jacoby, H. D., Reilly, J. M., Ejaz, Q. J., Morris, J., O'Sullivan, F., . . . & Kragha, O. (2011). The future of US natural gas production, use, and trade. *Energy Policy*, *39*(9), 5309-5321.
- Parikh, J., Channiwala, S. A., & Ghosal, G. K. (2005). A correlation for calculating HHV from proximate analysis of solid fuels. *Fuel*, *84*(5), 487-494.
- Patel, B., & Gami, B. (2012). Biomass characterization and its use as solid fuel for combustion. *Iranica Journal of Energy & Environment*, *3*(2), 123-128.
- Patel, M., Zhang, X., & Kumar, A. (2016). Techno-economic and life cycle assessment on lignocellulosic biomass thermochemical conversion technologies: A review. *Renewable and Sustainable Energy Reviews*, *53*, 1486-1499.
- Parikh, J., Channiwala, S. A., & Ghosal, G. K. (2005). A correlation for calculating HHV from proximate analysis of solid fuels. *Fuel*, *84*, 487-494.
- Patterson, P. H., Lorenz, E. S., Weaver Jr, W. D., & Schwartz, J. H. (1998). Litter production and nutrients from commercial broiler chickens. *Journal of Applied Poultry Research*, *7* (3), 247-252.
- Perera, P., & Bandara, W. (2010). Potential of using poultry litter as a feedstock for energy production.

- Permchart, W., & Kouprianov, V. I. (2004). Emission performance and combustion efficiency of a conical fluidized-bed combustor firing various biomass fuels. *Bioresource Technology*, *92*(1), 83-91.
- Piao, G., Aono, S., Kondoh, M., Yamazaki, R., & Mori, S. (2000). Combustion test of refuse derived fuel in a fluidized bed. *Waste Management*, *20*(5), 443-447.
- Proskurina, S., Sikkema, R., Heinimö, J., & Vakkilainen, E. (2016). Five years left—How are the EU member states contributing to the 20% target for EU's renewable energy consumption; the role of woody biomass. *Biomass and Bioenergy*, *95*, 64-77.
- Qian, X., & Lee, S. W. (2014). The design and analysis of energy efficient building envelopes for the commercial buildings by mixed-level factorial design and statistical methods. *Middle Atlantic Section Proceedings*.
- Quiroga, G., Castrillón, L., Fernández-Nava, Y., & Marañón, E. (2010). Physico-chemical analysis and calorific values of poultry manure. *Waste Management*, *30*, 880–884.
- Ramzy, E., Shaharin, A., & Bambang, A. (2013). Prediction of heating values of oil palm fronds from ultimate analysis. *Journal of Applied Sciences*, *13*(3), 491-496.
- Roesler, J. F., Yetter, R. A. & Dryer, F. L. (1995). Kinetic interactions of CO, NO<sub>x</sub>, and HCl emissions in post combustion gases, *Combustion and Flame*, *100*(3), 495-504.
- Saidur, R., Abdelaziz, E. A., Demirbas, A., Hossain, M. S., & Mekhilef, S. (2011). A review on biomass as a fuel for boilers. *Renewable and Sustainable Energy Reviews*, *15*(5), 2262-2289.
- Salahuddin, U., Bilal, M., & Ejaz, H. (2015). A review of the advancements made in helical baffles used in shell and tube heat exchangers. *International Communications in Heat and Mass Transfer*, *67*, 104-108.

- Salzmann, R. & T. Nussbaumer (2001). Fuel staging for NO<sub>x</sub> reduction in biomass combustion: experiments and modeling, *Energy & Fuels*, 15(3), 575-582.
- Sami, M., Annamalai, K., & Wooldridge, M. (2001). Co-firing of coal and biomass fuel blends. *Progress in Energy and Combustion Science*, 27(2), 171-214.
- Sasaki, N., Knorr, W., Foster, D. R., Etoh, H., Ninomiya, H., Chay, S., . . . & Sun, S. (2009). Woody biomass and bioenergy potentials in Southeast Asia between 1990 and 2020. *Applied Energy*, 86, S140-S150.
- Savolainen, K. (2003). Co-firing of biomass in coal-fired utility boilers. *Applied Energy*, 74(3), 369-381.
- Sebastián, F., Royo, J., & Gómez, M. (2011). Cofiring versus biomass-fired power plants: GHG (Greenhouse Gases) emissions savings comparison by means of LCA (Life Cycle Assessment) methodology. *Energy*, 36(4), 2029-2037.
- Seltman, H. J. (2014). Experimental design and analysis. Retrieved from <http://www.stat.cmu.edu/~hseltman/309/Book/Book.pdf>
- Shen, J., Zhu, S., Liu, X., Zhang, H., & Tan, J. (2010). The prediction of elemental composition of biomass based on proximate analysis. *Energy Conversion and Management*, 51(5), 983-987.
- Sheng, C., & Azevedo, J. L. T. (2005). Estimating the higher heating value of biomass fuels from basic analysis data. *Biomass and Bioenergy*, 28(5), 499-507.
- Si, Q., Xia, Q., Liang, L. H., & Li, D. X. (1995). Investigation of heat transfer and flow resistance on twisted tube heat exchanger. *Journal of Chemical Industry and Engineering (China)*, 46(5), 601-608.

- Skeer, J., & Wang, Y. (2006). Carbon charges and natural gas use in China. *Energy Policy*, 34(15), 2251-2262.
- Suksankraisorn, K., Patumsawad, S., Vallikul, P., Fungtammasan, B., & Accary, A. (2004). Co-combustion of municipal solid waste and Thai lignite in a fluidized bed. *Energy Conversion and Management*, 45(6), 947-962.
- Sun, P., Hui, S. E., Gao, Z., Zhou, Q., Tan, H., Zhao, Q., & Xu, T. (2013). Experimental investigation on the combustion and heat transfer characteristics of wide size biomass co-firing in 0.2 MW circulating fluidized bed. *Applied Thermal Engineering*, 52(2), 284-292.
- Swaminathan, R. (2013). Cost Effective, Low Capacity, Biomass Fired Power Plant. *Energy and Power*, 3(1), 1-6.
- Tan, X. H., Zhu, D. S., Zhou, G. Y., & Zeng, L. D. (2012). Experimental and numerical study of convective heat transfer and fluid flow in twisted oval tubes. *International Journal of Heat and Mass Transfer*, 55(17-18), 4701-4710.
- Tan, X. H., Zhu, D. S., Zhou, G. Y., & Zeng, L. D. (2013). Heat transfer and pressure drop performance of twisted oval tube heat exchanger. *Applied Thermal Engineering*, 50(1), 374-383.
- Tan, X. H., Zhu, D. S., Zhou, G. Y., & Yang, L. (2013). 3D numerical simulation on the shell side heat transfer and pressure drop performances of twisted oval tube heat exchanger. *International Journal of Heat and Mass Transfer*, 65, 244-253.
- Tariq, A. S., & Purvis, M. R. I. (1996). NO<sub>x</sub> emissions and thermal efficiencies of small-scale biomass-fuelled combustion plant with reference to process industries in a developing country. *International Journal of Energy Research*, 20(1), 41-55.

- Thantharate, V., & Zodpe, D. B. (2013). Experimental and numerical comparison of heat transfer performance of twisted tube and plain tube heat exchangers. *International Journal of Scientific and Engineering Research*, 4(7), 1107-1113.
- Thombare, D. G., & Verma, S. K. (2008). Technological development in the Stirling cycle engines. *Renewable and Sustainable Energy Reviews*, 12(1), 1-38.
- Tillman, D. A., Duong, D., & Miller, B. (2009). Chlorine in solid fuels fired in pulverized fuel boilers-sources, forms, reactions, and consequences: A literature review. *Energy & Fuels*, 23(7), 3379-3391.
- Topal, H., & Amirabedin, E. (2012). Determination of some important emissions of poultry waste co-combustion. *Scientific Journal of Riga Technical University. Environmental and Climate Technologies*, 8(1), 12-17.
- Tripathi, M., Sahu, J. N., & Ganesan, P. (2016). Effect of process parameters on production of biochar from biomass waste through pyrolysis: A review. *Renewable and Sustainable Energy Reviews*, 55, 467-481.
- U.S. Energy Information Administration (EIA) (2014), *Annual Energy Outlook, 2014*, Retrieved from [https://19january2017snapshot.epa.gov/energy/about-us-electricity-system-and-its-impact-environment\\_.html](https://19january2017snapshot.epa.gov/energy/about-us-electricity-system-and-its-impact-environment_.html)
- U.S. Energy Information Administration (EIA) (2016a), *International Energy Outlook 2016*, Retrieved from <https://www.eia.gov/outlooks/ieo/electricity.cfm>
- U.S. Energy Information Administration (EIA) (2016b), *Electricity in the U.S.*, Retrieved from [https://www.eia.gov/energyexplained/index.cfm?page=electricity\\_in\\_the\\_united\\_states](https://www.eia.gov/energyexplained/index.cfm?page=electricity_in_the_united_states)

- U.S. Environmental Protection Agency (EPA) (2014). *Sources of Greenhouse Gas Emissions*, Retrieved from <https://www.epa.gov/ghgemissions/sources-greenhouse-gas-emissions>
- U. S. Environmental Protection Agency (2016), Clean Power Plan for Existing Plants, Retrieved from <http://www.epa.gov/cleanpowerplan/clean-power-plan-existing-power-plants>
- Van den Broek, R., Faaij, A., & van Wijk, A. (1996). Biomass combustion for power generation. *Biomass and Bioenergy*, *11*(4), 271-281.
- Vargas-Moreno, J. M., Callejón-Ferre, A. J., Pérez-Alonso, J., & Velázquez-Martí, B. (2012). A review of the mathematical models for predicting the heating value of biomass materials. *Renewable and Sustainable Energy Reviews*, *16*(5), 3065-3083.
- Varol, M., Atimtay, A. T., Olgun, H., & Atakül, H. (2014a). Emission characteristics of co-combustion of a low calorie and high sulfur–lignite coal and woodchips in a circulating fluidized bed combustor: Part 1. Effect of excess air ratio. *Fuel*, *117*, 792-800.
- Varol, M., Atimtay, A. T., & Olgun, H. (2014b). Emission characteristics of co-combustion of a low calorie and high-sulfur-lignite coal and woodchips in a circulating fluidized bed combustor: Part 2. Effect of secondary air and its location. *Fuel*, *130*, 1-9.
- Vassilev, S. V., Baxter, D., Andersen, L. K., & Vassileva, C. G. (2010). An overview of the chemical composition of biomass. *Fuel*, *89*(5), 913-933.
- Verma, M., Loha, C., Sinha, A. N. & Chatterjee, P. K. (2017). Drying of biomass for utilizing in a co-firing with coal and its impact on environment – A review. *Renewable and Sustainable Energy Reviews*, *71*, 723-741.

- Villeneuve, J., Palacios, J. H., Savoie, P. & Godbout, S. (2012). A critical review of emission standards and regulations regarding biomass combustion in small scale units (< 3MW). *Bioresource Technology*, *111*, 1–11.
- Wang, X., Hu, Z., Deng, S., Xiong, Y., & Tan, H. (2014). Effect of biomass/coal co-firing and air staging on NO<sub>x</sub> emission and combustion efficiency in a drop tube furnace. *Energy Procedia*, *61*, 2331-2334.
- Wang, X., Tan, H., Niu, Y., Pourkashanian, M., Ma, L., Chen, E., ... Xu, T. (2011). Experimental investigation on biomass co-firing in a 300MW pulverized coal-fired utility furnace in China. *Proceedings of the Combustion Institute*, *33*(2), 2725-2733.
- Wei, X., Schnell, U., Han, X., & Hein, K. R. (2004). Interactions of CO, HCl, and SO<sub>x</sub> in pulverised coal flames. *Fuel*, *83*(9), 1227-1233.
- Werther, J., Saenger, M., Hartge, E. U., Ogada, T., & Siagi, Z. (2000). Combustion of agricultural residues. *Progress in Energy and Combustion Science*, *26*(1), 1-27.
- Whitely, N., Ozao, R., Artiaga, R., Cao, Y., & Pan, W. P. (2006). Multi-utilization of chicken litter as biomass source. Part I. Combustion. *Energy & Fuels*, *20*(6), 2660-2665.
- World Energy Statistics (2018), *Global Energy Statistical Year Book 2018, Total Energy Consumption*, Retrieved from <https://yearbook.enerdata.net/total-energy/world-consumption-statistics.html>
- Wünning, J. A., & Wünning, J. G. (1997). Flameless oxidation to reduce thermal NO-formation. *Progress in Energy and Combustion Science*, *23*(1), 81-94.

- Xie, J. J., Yang, X. M., Zhang, L., Ding, T. L., Song, W. L., & Lin, W. G. (2007). Emissions of SO<sub>2</sub>, NO and N<sub>2</sub>O in a circulating fluidized bed combustor during co-firing coal and biomass. *Journal of Environmental Sciences*, *19*(1), 109-116.
- Yang, S., Zhang, L., & Xu, H. (2011). Experimental study on convective heat transfer and flow resistance characteristics of water flow in twisted elliptical tubes. *Applied Thermal Engineering*, *31*(14-15), 2981-2991.
- Yang, W., Zhu, Y., Cheng, W., Sang, H., Yang, H., & Chen, H. (2017). Characteristics of particulate matter emitted from agricultural biomass combustion. *Energy & Fuels*, *31*(7), 7493-7501.
- Yang, X., & Dziegielewski, B. (2007). Water use by thermoelectric power plants in the United States. *JAWRA Journal of the American Water Resources Association*, *43*(1), 160-169.
- Yin, C. Y. (2011). Prediction of higher heating values of biomass from proximate and ultimate analyses. *Fuel*, *90*(3), 1128-1132.
- Zhang, J. F., Li, B., Huang, W. J., Lei, Y. G., He, Y. L., & Tao, W. Q. (2009). Experimental performance comparison of shell-side heat transfer for shell-and-tube heat exchangers with middle-overlapped helical baffles and segmental baffles. *Chemical Engineering Science*, *64*(8), 1643-1653.
- Zhang, X., Myhrvold, N. P., & Caldeira, K. (2014). Key factors for assessing climate benefits of natural gas versus coal electricity generation. *Environmental Research Letters*, *9*(11), 114022.

- Zhu, S., & Lee, S. W. (2005). Co-combustion performance of poultry wastes and natural gas in the advanced Swirling Fluidized Bed Combustor (SFBC). *Waste Management*, 25(5), 511-518.
- Zhu, S., Lee, S., Hargrove, S. K., & Chen, G. (2007). Prediction of combustion efficiency of chicken litter using an artificial neural network approach. *Fuel*, 86(5), 877-886.
- Zhou, Z. J., Zhou, N., Chen, Y. J., Zhou, J., Liu, J., & Cen, K. (2010). Experimental research on the combustion and NO<sub>x</sub> generation characteristics of low volatile coal. *Proceedings of the Chinese Society of Electrical Engineering*, 30, 55-61.